

8-1-2016

Store operated calcium entry in glomerular mesangial cells and diabetic nephropathy

Sarika Chaudhari

University of North Texas Health Science Center at Fort Worth, sarika.chaudhari@live.unthsc.edu

Follow this and additional works at: <http://digitalcommons.hsc.unt.edu/theses>



Part of the [Medical Sciences Commons](#)

Recommended Citation

Chaudhari, S. , "Store operated calcium entry in glomerular mesangial cells and diabetic nephropathy" Fort Worth, Tx: University of North Texas Health Science Center; (2016).
<http://digitalcommons.hsc.unt.edu/theses/922>

This Dissertation is brought to you for free and open access by UNTHSC Scholarly Repository. It has been accepted for inclusion in Theses and Dissertations by an authorized administrator of UNTHSC Scholarly Repository. For more information, please contact Tom.Lyons@unthsc.edu.

Chaudhari, Sarika. Store Operated Calcium Entry in Glomerular Mesangial Cells and Diabetic Nephropathy. Doctor of Philosophy (Integrative Physiology), July 2016, 184 pp., 3 tables, 28 figures, bibliography, 365 titles.

Glomerular mesangial cells (MCs) are the major source of extracellular matrix (ECM). One of the early pathological changes in diabetic nephropathy (DN) is accumulation of ECM in glomeruli. Multifunctional store-operated Ca^{2+} entry (SOCE) regulates MC function. However, whether and how SOCE in MCs contributes to pathophysiology of DN remains unknown. The aim of the study was to investigate association of SOCE in MCs with ECM protein expression and the underlying mechanism using both in vitro and in vivo systems.

Study I was to determine the effect of diabetes on SOCE. In cultured human MCs, we found that prolonged high glucose (HG) treatment (7 days) significantly increased SOCE and membrane currents through store-operated channels (SOC). These responses were abolished by SOC inhibitors. Consistently, prolonged HG treatment also increased the abundance of SOC proteins STIM1 and Orai1. HG also increased STIM1, but not Orai1 mRNA expression. Furthermore, both STIM1 and Orai1 proteins were also increased in the glomeruli/renal cortices of diabetic rats.

Study II determined the influence of SOCE in MCs on ECM protein expression. We found that activation of SOC by thapsigargin reduced the abundance of fibronectin and collagen IV while inhibitors of SOC had opposite effects. Knockdown of Orai1 in human MCs increased fibronectin abundance. The HG induced increase in fibronectin

was attenuated by SOCE. Using a nanoparticle siRNA delivery system, specific knockdown of Orai1 in MCs in mice increased glomerular fibronectin and collagen IV protein content and mesangial expansion.

Study III determined the mechanism for inhibition of ECM protein expression by SOCE. We found that activation of SOC attenuated TGF β 1 mediated phosphorylation and translocation of Smad3, a known fibrotic pathway in MCs. However, there was no change in the production or secretion of TGF β 1 by MCs. Orai1 knockdown in MCs in mice increased the activation of Smad3.

Taken together, our results indicate that SOCE in MCs may be increased in the late stage of diabetes, which suppresses ECM protein expression by inhibiting TGF β 1-smad3 pathway.

STORE OPERATED CALCIUM ENTRY IN GLOMERULAR MESANGIAL
CELLS AND DIABETIC NEPHROPATHY

DISSERTATION

Presented to the Graduate Council of the
Graduate School of Biomedical Sciences

University of North Texas

Health Science Center at Fort Worth

For the Degree of

DOCTOR OF PHILOSOPHY

By

Sarika Chaudhari, M.B.B.S., M.D.

Fort Worth, Texas

July, 2016

ACKNOWLEDGMENTS

I would like to express my deepest gratitude and respect to my mentor Dr. Rong Ma. I thank him for giving me the opportunity to work in his lab and also for his guidance, patience and support that I received from him during my time as his student. His enthusiasm for research and science kept me engaged with my research project. This dissertation would not have been possible without his encouragement. My heartfelt thanks goes to my committee members Dr. Tom Cunningham, Dr Robert Mallet, Dr Joseph Yuan, and Dr Ladislav Dory for their kind support, valuable time and vital suggestions at every juncture of my project and during the compilation of this dissertation. I thank my colleagues from Dr. Ma's lab, Dr Yanxia Wang, Dr Yanfeng Ding and Min Ding for their help and technical expertise during my stay in the lab.

Special thanks are due to the funding support that included a R01 grant from the National Institutes of Health and a Grant-in-Aid from American Heart Association Southwestern Affiliate, both, with Dr Ma as principal investigator and a grant from National Natural Science Foundation of China to Peiwen Wu. I received a Doctoral Student Bridge Grant from UNTHSC and Grant - in - Aid Research Grant from Sigma Xi Research Society, which I am very grateful for and which facilitated the work in this dissertation as well.

I am forever grateful to my wonderful family, my parents, late Mr Devidas and Mrs Sulabha, my mother-in-law, Mrs Nalini, my husband and my greatest support, Kiran Chaudhari and my beautiful kids Shourya and Adheet. I could not have achieved so much without their unconditional love and faith in me. They were, are and always will be my biggest strength and weakness.

Articles resulting from this dissertation:

Chaudhari S, Wu P, Wang Y, Ding Y, Yuan J, Begg M, Ma R. High glucose and diabetes enhanced store operated Ca^{2+} entry and increased expression of its signaling proteins in mesangial cells. *Am J Physiol Renal Physiol*. 2014; 306(9):F1069-80

Wu P, Wang Y, Davis ME, Zuckerman JE, **Chaudhari S**, Begg M, Ma R. Store-operated Ca^{2+} channel in glomerular mesangial cells negatively regulates extracellular matrix protein expression. *J Am Soc Nephrol*. 2015 Nov; 26(11):2691-702.

Chaudhari S, Ma R. Store-operated calcium entry and diabetic complications. *Exp Biol Med* (Maywood) 2016 Feb; 241(4):343-52.

Chaudhari S, Li W, Wang Y, Jiang H, Ma R. Store Operated Calcium Entry Suppressed $\text{TGF}\beta 1$ -Smad3 Signaling Pathway in Glomerular Mesangial Cells. To be submitted to *Am J Physiol Renal Physiol*.

Other published works

Wang Y, Ding M, **Chaudhari S**, Yanfeng Ding, Joseph Yuan, Dorota Stankowska, Shaoqing He, Raghu Krishnamoorthy, Joseph T. Cunningham, Rong Ma. Nuclear factor κB mediates suppression of canonical transient receptor potential 6 expression by reactive oxygen species and protein kinase C in kidney cells. *J Biol Chem*. 2013; 288(18):12852-12865.

Wang Y, **Chaudhari S**, Ren Y, Ma R. Impairment of HNF4 α Binding to stim1 Promoter Contributes to High Glucose-induced Upregulation of STIM1 Expression in Glomerular Mesangial Cells. *Am J Physiol Renal Physiol*. 2015 May 15; 308(10):F1135-45.

Ma R, **Chaudhari S** and Li W. Canonical Transient Receptor Potential 6 Channel: A New Target of Reactive Oxygen Species in Renal Physiology and Pathology. *Antioxid Redox Signal*. 2016 Mar 18. [Epub ahead of print]

TABLE OF CONTENTS

	Page
LIST OF TABLES	viii
LIST OF ILLUSTRATIONS	ix
CHAPTER	
I. INTRODUCTION	1
Background	1
Specific Aims	10
Figures	12
Abbreviations	24
References	26
II. HIGH GLUCOSE AND DIABETES ENHANCED STORE-OPERATED Ca^{2+} ENTRY AND INCREASED EXPRESSION OF ITS SIGNALING PROTEINS IN MESANGIAL CELLS.....	46
Abstract	47
Keywords	47
Introduction	48
Materials and Methods	49
Results	54

Discussion	59
Acknowledgements and Grants	62
Figures	64
Abbreviations	83
References	84
III. STORE-OPERATED Ca^{2+} CHANNELS IN MESANGIAL CELLS INHIBIT MATRIX PROTEIN EXPRESSION	95
Abstract	96
Keywords	96
Introduction	97
Materials and Methods	98
Results	101
Discussion	104
Acknowledgements and Grants	107
Figures	108
Abbreviations	120
References	121
IV. STORE OPERATED CALCIUM ENTRY SUPPRESSED TGF β 1-SMAD3 SIGNALING PATHWAY IN GLOMERULAR MESANGIAL CELLS.....	128
Abstract	129
Keywords	129
Introduction	130
Materials and Methods	131

Results	136
Discussion	139
Acknowledgements and Grants	143
Figures	145
Abbreviations	163
References	165

V. SUMMARY, GENERAL DISCUSSION AND FUTURE DIRECTIONS

Summary and General Discussion	173
Future Directions	176
Figure	179
Abbreviations	181
References	182

APPENDIX

Store-Operated Ca ²⁺ Channels in Mesangial Cells Inhibit Matrix Protein Expression. (Published Manuscript)	184
--	-----

LIST OF TABLES

CHAPTER II

Table 1. Primers used for real-time PCR63

Table 2. Diabetic parameters in LFD and HFD rats63

CHAPTER IV

Table 1. siRNAs used for transient transfection144

Figure 4. STIM1 protein abundance in presence of high glucose in human mesangial cells	72
Figure 5. Orai1 protein abundance in presence of high glucose in human mesangial cells	74
Figure 6. STIM1 protein abundance in the glomeruli/renal cortices from control and diabetic rat kidneys	77
Figure 7. Orai1 protein abundance in the glomeruli/renal cortices from control and diabetic rats	79
Figure 8. Influence of high glucose on STIM1, STIM2, and Orai1 mRNA expressions in in human mesangial cells	81

CHAPTER III

Figure 1. Regulation of extracellular matrix protein expression by pharmacological activation/inhibition of store-operated calcium channel in human mesangial cells	108
Figure 2. Effect of knockdown of Orai1 on extracellular matrix protein expression in human mesangial cells	110
Figure 3. Downregulation of high glucose-stimulated extracellular matrix protein expression by store-operated calcium entry in human mesangial cells	112
Figure 4. Distribution of nanoparticles with siRNA against Orai1 in mesangial cells in mouse kidney	114
Figure 5. Effect of in vivo knockdown of Orai1 in mesangial cells on extracellular matrix protein expression in mice glomeruli	117

CHAPTER IV

Figure 1. Effect of store-operated calcium entry on TGF β 1 secretion or production in human mesangial cells	145
Figure 2. Downregulation of TGF β 1-induced phosphorylated Smad3 protein expression after pharmacological activation of store-operated calcium entry in human mesangial cells.....	147
Figure 3. TGF β 1-induced phosphorylated Smad3 expression after knockdown of Orai1 in human mesangial cells	149
Figure 4. TGF β 1-induced phosphorylated Smad3 expression after overexpression of Orai1 in human mesangial cells	151
Figure 5. TGF β 1-stimulated translocation of Smad3 to the nucleus after activation of store-operated calcium entry	154
Figure 6. Distribution of nanoparticle-siRNA delivery system for Orai1 siRNA in mesangial cells in mouse kidney	157
Figure 7. Effect of knockdown of Orai1 in mesangial cells on activation of Smad3 in mice glomeruli	159
Figure 8. Diagram demonstrating the pathway involved in regulation of TGF β 1-Smad3 signaling by Orai1-mediated store-operated calcium entry in mesangial cells	161

CHAPTER V

Figure 1. Diagram depicting the compensatory store operated calcium entry pathway in the mesangial cells in diabetic nephropathy	179
---	-----

CHAPTER 1

INTRODUCTION

Background

Glomerular Mesangial Cell Physiology

Glomerulus, the filtering site of nephron, constitutes a network of capillaries surrounded by Bowman's capsule. (Figure 1A) The filtering membrane across which plasma is filtered consists of fenestrated endothelial cells of capillaries, followed by glomerular basement membrane and slit pores of specialized epithelial cells of capsule called podocytes (1). Glomerular mesangial cells (MCs), a special form of microvascular pericytes (2), are another important type of cells along with endothelial cells and podocytes. MCs generate and are embedded in their own extracellular matrix (ECM) forming the mesangium which is interspersed between the glomerular capillary loops and is in direct contact with the endothelial cells (3,4) (Figure 1B). MCs form the support network for the capillary tuft and maintain the architecture of glomerulus (5). Local accumulation of macromolecules that reach mesangial space is prevented partly by phagocytosis and degradation by these cells (2). MCs and their matrix function in close harmony with podocytes and endothelial cells as one functional unit (6). Alterations in one cell type can produce changes in the others. With the advent and ease of cell

culture techniques it has become possible to dissect out the role of individual member of this unit.

The smooth muscle like contractile property of MCs in response to various vasoactive stimuli like angiotensin II (AngII), endothelin (ET) is important for fine tuning of the glomerular filtration rate (GFR) independent of afferent and efferent arterioles (2,6,7). This contraction is dependent on the influx of Ca^{2+} from the extracellular space. MCs also exhibit receptors for and secretion of various growth factors and cytokines (6,8). Some of these like transforming growth factor β 1 (TGF β 1), platelet derived growth factor (PDGF) and fibroblast growth factor (FGF) can act in paracrine as well as autocrine manner (8,9). For example, in response to stretch MCs generate soluble factors such as TGF β 1 (10), vessel epithelial growth factor (VEGF) (11), and connective tissue growth factor (12), and high glucose stimulates MCs to secrete TGF β 1 (13). These growth factors and cytokines in turn activate multiple intracellular signaling pathways like protein kinase C, mitogen-activated protein kinase/extracellular signal-regulated kinase, p38, c-Jun N-terminal kinase, and phosphatidylinositol-3 kinase/Akt (14-16) , and consequently, regulate cell growth, contractility, gene transcription and protein synthesis.

Another major function of MCs is production of mesangial matrix or ECM which is a highly dynamic and tightly regulated structure. ECM is made up of various constituents like type IV collagen (only the α 1 and α 2 chains); type V collagen; laminin (A, B1, and B2), considerable amounts of fibronectin, heparan sulfate and chondroitin sulfate proteoglycans, entactin, and nidogen, minor amounts of the proteoglycans decorin and biglycan (4,17). Mesangial matrix components can influence matrix-cell signaling in response to stimuli like mechanical stretch (18). They can also impact MC growth and proliferation both directly and indirectly, the latter by binding to different growth factors and regulating their activation and release. For example,

activation of matrix metalloproteinases releases TGF β 1 from its binding protein to act on MCs. The composition and volume of mesangial matrix can be markedly altered during diseases like diabetic nephropathy (DN)(4,17,19,20).

MC function and Ca²⁺ signaling

The function of MCs is regulated by intracellular Ca²⁺ signaling. Extensive ongoing research in the field indicates that Ca²⁺ entering the cell via specific Ca²⁺ channels has a precise targeted pathway activation and outcome (21-23). A number of different Ca²⁺ channels are now known to regulate MC function including voltage-operated calcium channels (VOCC), receptor-operated channels (ROC), and store-operated channels (SOC) (Figure 2). VOCC are activated when the plasma membrane is depolarized by any factor. Using fura-2 fluorescence, Yu et al. first characterized these channels in cultured rat MCs. These channels are known to influence MC growth and can be blocked by nifedipine, a selective VOCC inhibitor (24). Further electrophysiological experiments by Matsunaga et al (25). using patch clamp technique suggested the presence of ROC for PDGF in rat MCs. It was later demonstrated that various vasoactive and mitogenic agents like PDGF, insulin, AngII, and ET exert their effects via these channels to regulate MC growth and contraction (26-28). These ligands bind to their receptors activating G protein-coupled cell signaling cascade that leads to generation of diacylglycerol (DAG) and inositol triphosphate (IP₃). DAG reacts with ROC to influence Ca²⁺ entry through these channels.

Mene et al. for the first time in 1994, observed a novel Ca²⁺ entry mechanism in human MCs that occurred after depletion of intracellular Ca²⁺ stores. This Ca²⁺ entry response was also found in rat and mouse MCs (27,29,30). The internal Ca²⁺ store depletion-activated Ca²⁺ channel which

was previously known calcium release activated calcium channels is known as SOC. The Ca^{2+} entry through SOC is known as store operated calcium entry (SOCE). Circulating or locally produced hormones/cytokines/growth factors that activate either G protein coupled receptors or receptor tyrosine kinases can open SOC through activation of the phospholipase C/ IP_3 pathway (31). Electrophysiological studies in cells with depleted endoplasmic reticulum (ER) stores have shown membrane currents with diverse properties, indicating that different classes of cells express distinct SOC(32). The biophysical properties of SOCs in cultured human MCs were first characterized by Li et al. (33) and Ma et al. (34) using techniques like Ca^{2+} imaging and electrophysiology. These channels are described as non-specific cation permeable channels with very low single-channel conductance of 1-2.1 pS. In absence of divalent cations they are very permeable to monovalent cations (34). Experimentally, SOC can be activated using sarcoplasmic/endoplasmic reticulum Ca^{2+} ATPase (SERCA) inhibitors like thapsigargin (TG) and cyclopiazonic acid (CPA) or IP_3 that activates IP_3 receptors in the ER membrane (35).

Molecular components of SOC

Although SOC has been recognized almost three decades ago, the definite molecular identity of the channel was not known until recently. High throughput RNA interference screening recognized two protein families, stromal interaction molecule (STIM) (36,37) and Orai (38-40), as essential components of SOCE. There are two isoforms for STIM, STIM1 and STIM2. Both are structurally very similar varying only at extreme N and C termini (41,42). STIM1 is a single-pass transmembrane protein located predominantly in the ER membrane and some in the plasma membrane (PM) (42,43). In the ER, it functions as a Ca^{2+} sensor to sense ER luminal Ca^{2+} concentration (36,44). The N terminal Ca^{2+} sensing domain is a tight cluster of

short α helices comprising two EF-hand domains and a sterile α motif (SAM) domain while cytoplasmic C-terminal region contains more extensive α helical regions long enough to couple with PM Orai channels (36,45) (Figure 3A). Orai family of proteins constitute the tetramembrane-spanning proteins Orai1, Orai2, and Orai3, with both the N- and C- termini located on the cytosolic side of the PM (Figure 3B). Orai proteins are pore-forming unit of SOC located at the plasma membrane (38,46). Each protein has conserved acidic residues that are crucial for forming the highly Ca^{2+} -selective filter and channel pore regions (39,46,47) At resting state, STIM1 is widely distributed through the ER membrane. However, upon store depletion, STIM1 protein rapidly oligomerizes and aggregates to form puncta and subsequently moves into PM junctional regions (36,48), where it directly associates and subsequently activates C-terminal cytoplasmic coiled-coil region of Orai1 leading to Ca^{2+} entry into the cytosol (49,50) (Figure 4).

Prior to the discovery of Orai1 and STIM1, several isoforms of canonical transient receptor potential (TRPC) proteins were proposed as the molecular components. They are still considered to be involved in SOCE by interacting with STIM1 and/or Orai1 (51-54). In cultured human MCs Ma and coworkers have provided evidence for STIM1 as a prerequisite for SOCE and role of TRPC1, TRPC4 as possible SOC units (55).

SOCE and its diverse role

SOCE was initially considered as a major mechanism of Ca^{2+} entry in non-excitabile cells, such as immune cells, platelets, and endothelial cells serving functions like maintenance of intracellular Ca^{2+} levels, exocytosis, cell proliferation, apoptosis and activation of gene transcription (56,57). Later, this Ca^{2+} entry pathway was also found in many excitable cells, such

as neurons (58), cardiac myocytes (59), skeletal muscle cells (60) and vascular smooth muscle cells (61). It is now widely accepted that SOCE is a ubiquitous Ca^{2+} signaling pathway that regulates diverse cellular functions in a variety of tissues and organ systems (34,62-68). SOC function is distinct in different tissues and cell types (69,70). In general, the SOC-associated signaling pathway promotes protein synthesis and cell growth (69), for instance, contributing to cardiac hypertrophy (68,71). However, a recent study revealed that the SOC-mediated Ca^{2+} influx suppressed cell growth in mouse embryonic fibroblasts and rat uterine leiomyoma cells through inhibition of Akt1 (72). Thus, the effect of SOC on protein production might be cell type specific and/or cell context dependent. Therefore, it is not surprising that dysfunction of SOC can lead to a series of disorders, such as immunodeficiency, myopathy, and vascular diseases (62,68,70-78).

Diabetes and SOCE

Dysregulation of Ca^{2+} homeostasis and Ca^{2+} signaling is well known in diabetes (79-82). Over the past decade, accumulating evidence has demonstrated that many diabetic complications involve alterations of SOCE and its signaling pathways (83-85). Since diabetes and its complications are becoming epidemic worldwide and there is no curative therapy currently available for diabetic complications, continued exploration of the basic pathophysiology of diabetic complications and of new therapeutic approaches is in need. SOCE is involved in the regulation of pathological events occurring in multiple organ systems in a diverse manner. Prolonged exposure of human umbilical vein endothelial cells (4 days) to high glucose medium resulted in a significant increase in apoptosis, which was associated with increased SOC activity (86). Daskoulidou et al. provided evidence that high glucose enhanced SOCE in vascular

endothelial cells and this enhancement was due to increased abundance of Orai1-3 and STIM1-2 proteins. They further showed that the mRNA expression levels of Orai1-3 and STIM1-2 were significantly increased in the abdominal aortae of STZ-diabetic mice and Akita diabetic mice (84). On the contrary, SOCE was substantially reduced in retinal microvascular smooth muscle and aortic smooth muscle cells from STZ diabetic rats (87,88). Importantly, the contractile response of the vessel was significantly reduced in the diabetic rats compared to that in control rats (88). Mita et al. (89) demonstrated similar results in Goto-Kakizaki rats, type 2 diabetic animals. On the other hand, the saphenous veins from patients with type 2 diabetes showed exaggerated CPA-induced SOCE and contraction compared to the vessels from subjects without diabetes (83). The discrepancies in the effect of SOCE on vascular smooth muscle cells in these animal and human studies may be due to differences in the species, severity of diabetes or the segments of vessels involved. In platelets from type 2 diabetic patients earlier studies revealed that SOCE stimulated by thrombin, TG or ionomycin was significantly greater than in those from healthy controls and later was attributed to increased expression of STIM1 and Orai1 (90-92). Pang et al. (93) demonstrated significantly decreased SOCE stimulated by AngII or TG in cultured neonatal rat ventricular myocytes with short-term hyperglycemia (20 h) accompanied by blunted Ca^{2+} dependent hypertrophic response and nuclear translocation of nuclear factor of activated T-cells.

Diabetes and SOCE in MCs

Diabetic nephropathy, one of the most common complications of diabetes mellitus, is a major cause of end stage renal disease (ESRD) (94,95). Early features of DN include glomerular hypertrophy with thickening of the glomerular basement membrane and expansion of glomerular

mesangium, which eventually develop into glomerulosclerosis and renal insufficiency (96-100). Glomerular MCs are the major contributor to these structural changes in diabetic kidney (17,101,102). MC function is controlled by intracellular Ca^{2+} signaling which involves several types of Ca^{2+} channels, including SOC (103). Furthermore, studies demonstrated that SOC participated in hormone-stimulated Ca^{2+} responses in MCs (27,104-106).

Alterations of SOC function in MCs under conditions of diabetes have been extensively studied in both in vitro and in vivo settings. In the earlier studies conducted in cultured rat and human MCs, Mene et al. demonstrated that arginine vasopressin- and AngII-induced SOCE was attenuated by high glucose treatment (30 mM for 5 days) (106,107). However, both vasopressin and AngII not only activate SOC, but activate ROC as well (108,109). Therefore, the attenuation of the Ca^{2+} response by high glucose in that study might be due to impairment of ROC. Nutt and coworkers examined the effects of high glucose on ET-1- (activates both SOC and ROC) and TG- (selectively activates SOC)-induced Ca^{2+} response in cultured rat MCs. They revealed that high glucose treatment at 30 mM for 5–7 days significantly reduced ET1-induced Ca^{2+} entry, but had no effect on TG induced Ca^{2+} response (27). Their study suggests that in a time period of 5 days, high glucose treatment did not impair SOCE, but significantly inhibited the Ca^{2+} entry through ROC.

(Chaudhari et al., EBM, 2015: pg344) (110).

Apparently, the diabetes/high glucose effect on SOCE in MCs is complex and may be dependent on the species (human vs. rat/mouse) and the stage of diabetes/duration of high glucose treatment.

DN and ECM

Diabetic nephropathy, associated with initial hyperfiltration and microalbuminuria, is followed over years by gradual decline in GFR with moderate to severe proteinuria, finally reaching a stage of renal insufficiency and ESRD (111-113). The gradual impairment of the kidney is caused by structural alterations which at the beginning consist of a gradual and progressive accumulation of ECM in the mesangium and glomerular basement membrane (96,114,115). While defects in the glomerular basement membrane are mainly associated with the proteinuria, gradual impingement of growing mesangium in the surrounding capillary network is accountable for declining GFR over years (116). The correlation of extent of matrix expansion with declining glomerular function provides evidence for this patho-clinical finding (115,117,118). Expansion of mesangial matrix in early stage of diabetes has been partly attributed to the glomerular hypertension in the absence of systemic hypertension causing stretching of MCs and release of growth factors and cytokines (96,119).

Hyperglycemia is the major stimulus to renal cells to produce cytokines and growth factors that are responsible for accumulation of ECM (99,119-123). ECM expansion can be due to either increased content of proteins normally present in the mesangium or deposition of new proteins that normally are not present in this tissue or both. The major ECM proteins that are increased in diabetic kidney are collagen IV and fibronectin, and in very late stages of DN, collagen I and II (114). In addition to hyperglycemia, reactive oxygen species, Ang II, advanced glycation end products and growth factors also stimulate production of ECM proteins in MCs as well as in other renal cells in diabetes. Among those pathogenic factors, TGF β is a central mediator for renal injury in diabetic kidney (124-129) (Figure 5).

TGF β -Smad pathway

Transforming growth factor β is the prototype cytokine of TGF β superfamily and is known to stimulate production of ECM proteins contributing to renal fibrosis (130,131). There are three isoforms of TGF β namely, TGF β 1, TGF β 2 and TGF β 3. TGF β 1 is the most common and best characterized isoform and a critical player for ECM expression in MCs in diabetes (13,132-134). The main downstream signaling pathway of TGF β is the Smad pathway, particularly Smad3 signaling (135-138) (Figure 6). The receptors for TGF β , type II and type I are serine-threonine kinases. Binding of TGF β 1 to its type II receptor transphosphorylates the GS domain of type I receptor and activates its kinase activity, resulting in phosphorylation of intracellular substrates Smad2 and Smad3. Both Smad2 and 3 are combined with Smad4 and subsequently translocate into the nucleus where they regulate gene transcription(13,139). Activation of Smad3 by TGF β 1 promotes expression of ECM proteins (137,138) while the role of Smad2 is obscure. Although the Smad signaling is the main pathway for TGF β 1 effects in diabetes, TGF β 1 also activates other pathways like TAK1 (TGF β associated kinase 1) Erk (extracellular signal regulated kinases), p38, MAPK (mitogen activated protein kinase) and Akt/mTOR (mammalian target of rapamycin). All of those pathways interact with each other and with the Smad pathway (140-144).

Specific aims of this study

Glomerular MCs are the major source of ECM proteins. Expansion of glomerular mesangium is one of the early pathological changes in DN. This structural impairment, if not treated, will progress to irreversible kidney damage and renal insufficiency, and eventually to ESRD. TGF β 1-Smad3 pathway plays a critical role in ECM expansion and development of DN.

The function of MCs depends on various intracellular Ca^{2+} signaling pathways. We have demonstrated previously that SOCE exists in MCs. Dysregulation of SOCE was demonstrated in various cells in diabetes. However, whether and how SOCE in MCs contributes to pathophysiology of DN remains unknown. The following three specific aims were designed, using both in vitro and in vivo systems, to address the hypothesis that SOCE is altered in MCs in diabetes and that it regulates the ECM protein expression in MCs likely through its interaction with the TGF β 1-Smad3 pathway.

Specific aim I: To determine the effect of high glucose/diabetes on SOCE and further characterize the molecular mechanisms for the change in SOCE in mesangial cells.

Specific aim II: To define the effect of SOCE in mesangial cells on the extracellular matrix proteins expression.

Specific aim III: To determine if TGF β 1-Smad3 pathway mediates the effect of SOCE on ECM proteins in mesangial cells.

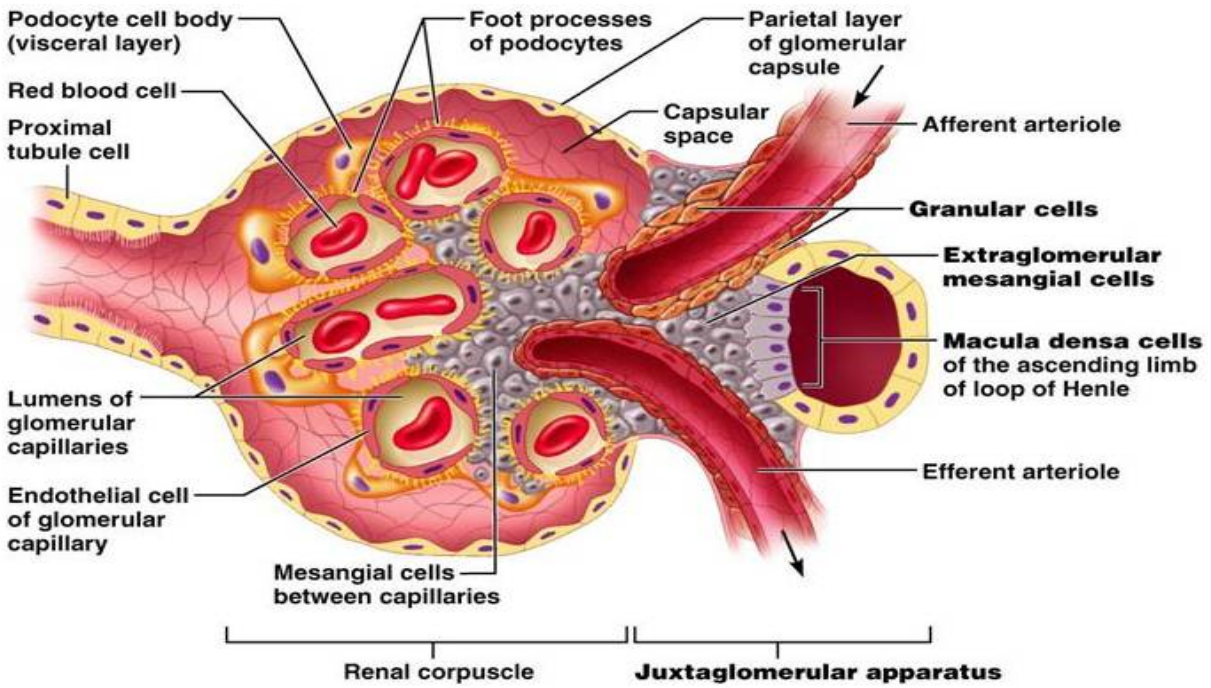
These three specific aims are included in this dissertation as Chapters II, III, and IV, respectively in the form of manuscripts. Each chapter consists of introduction, material and methods, results and discussion sections described therein. Chapter V presents an overall conclusion integrating the outcomes of the specific aims, along with discussion of study limitations and future directions.

Figure 1. Structure of normal renal glomerulus.

A. Section through normal glomerulus. Afferent arteriole and efferent arteriole carries blood to and from the glomerulus. Afferent arteriole divides to form the glomerular capillary network surrounded by Bowman's capsule. Glomerular MCs are interspersed between the capillary loops and are distinct from the extra-glomerular MCs present between and surrounding the afferent and efferent arterioles. Blood is filtered from the capillary lumen through the layer of endothelial cells, glomerular basement membrane and slit pores of podocytes to the capsular space. (Modified from Marieb et al. 2007(145)) **B.** Schematic diagram, showing three dimensional arrangement of glomerular cells. Endothelial cells of the capillaries are separated from the slit pores of podocytes by basement membrane, while MCs are in direct contact with the endothelial cells. (Modified from Kumar et al., Robbins Basic Pathology 8th edition © Elsevier)

Figure 1.

A



B

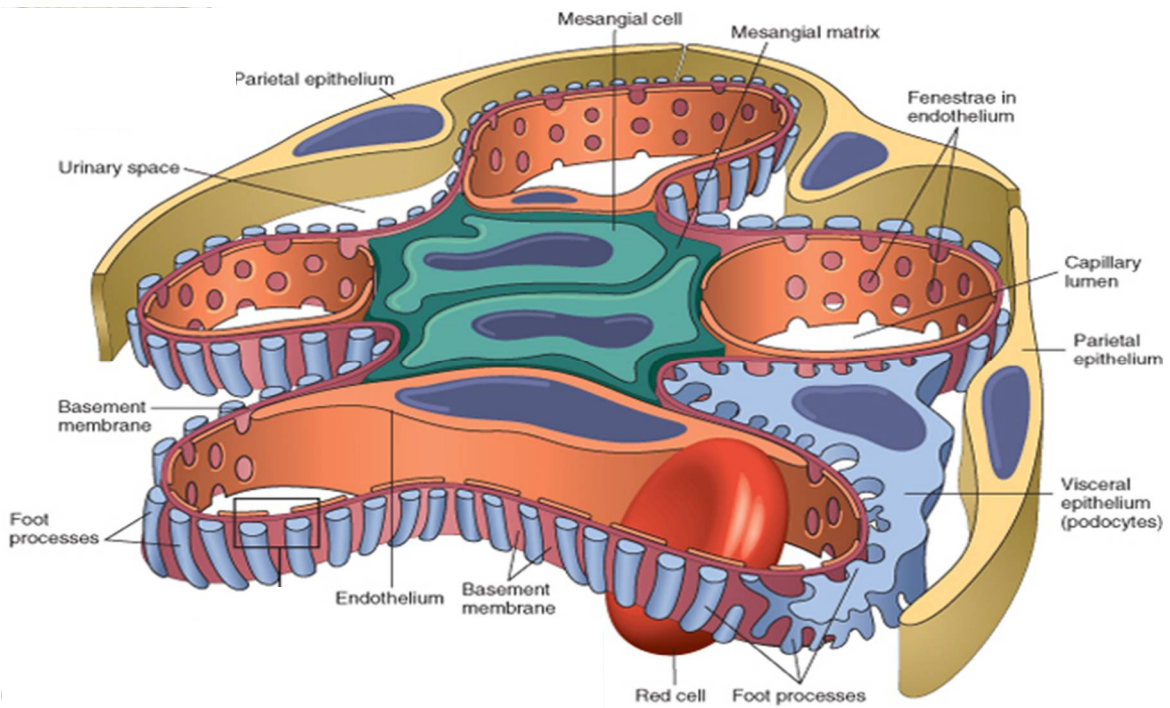


Figure 2. Major Ca²⁺ entry pathways in MCs.

Agonist binding to G-protein coupled receptor or tyrosine kinase receptors activates phospholipase C that forms DAG and IP₃ from phosphatidylinositol 4,5 bisphosphate. Membrane depolarization and DAG activates VOC and ROC, respectively. IP₃ binds to its receptor on the ER membrane and releases Ca²⁺. This store depletion is sensed by STIM1 protein on the ER membrane, which in turn activates Orai1 and allows Ca²⁺ to enter the cell. This Ca²⁺ entry secondary to internal Ca²⁺ store depletion is termed SOCE. Compounds which block SERCA pump such as TG and CPA on the ER membrane or IP₃ that releases Ca²⁺ from ER can be used to activate SOCE. (Dashed arrow indicates inhibition.)

Figure 2.

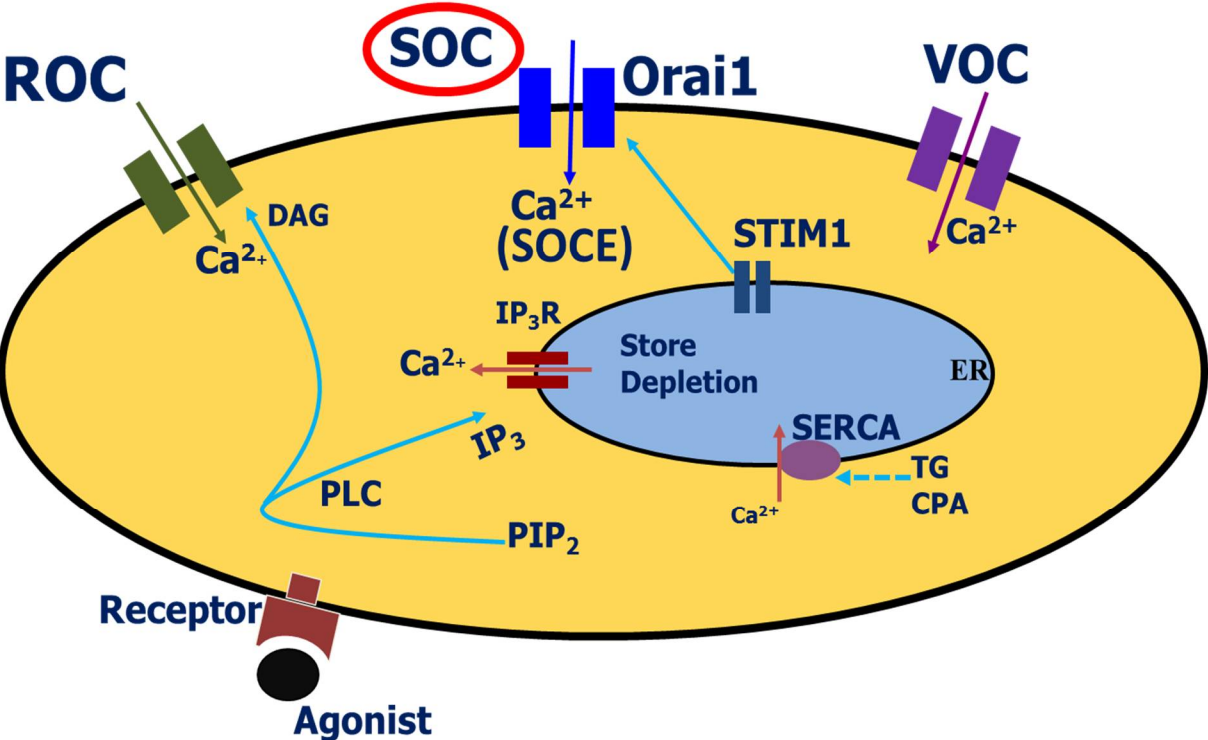
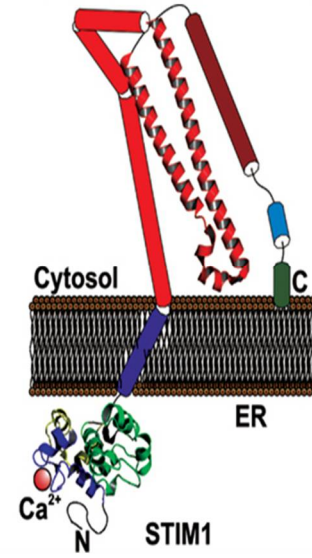
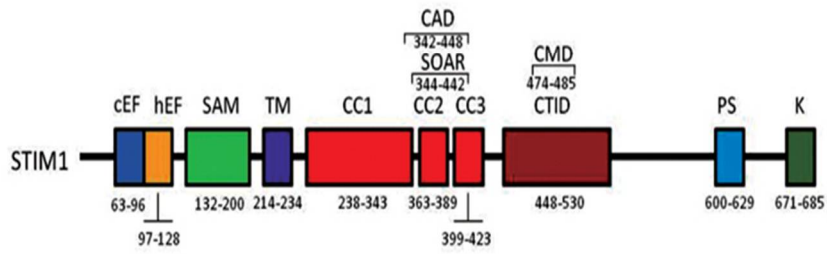


Figure 3. Molecular structure of STIM1 and Orai1

A. Architecture of STIM1 (left). The ER luminal N-terminal region includes a Ca^{2+} binding canonical EF-hand motif (cEF), a hidden EF-hand (hEF) motif, and a sterile α -motif (SAM). STIM1 has a single transmembrane domain TM. The cytosolic C-terminal region includes three coiled-coil (CC) regions (CC1, CC2, and CC3), which contain the SOAR (STIM–Orai activating region) or CAD (CRAC activation domain). Downstream of CC3 there is a C-terminal inhibitory domain (CTID), which overlaps the CRAC modulatory domain. The C-terminal region also contains a Pro/Ser-rich domain (PS) and a Lys-rich domain (K). The right panel is a cartoon depicting a possible crystal structure of STIM1 monomer in the coalescent state. **B.** Architecture of Orai1 (left). Both N and C terminals are on cytosolic side. The N terminal region contains an arginin-rich region, (R) and a proline-rich region, (P) (present in Orai1 α , not in Orai1 β), an arginine-lysine-rich region, (RK), four transmembrane domains (TM); and a coiled-coil domain (CC). On right is the cartoon depicting Orai1 α monomer crystal structure in the resting state. (Modified from Rosado et al., 2015.(146))

Figure 3.

A



B

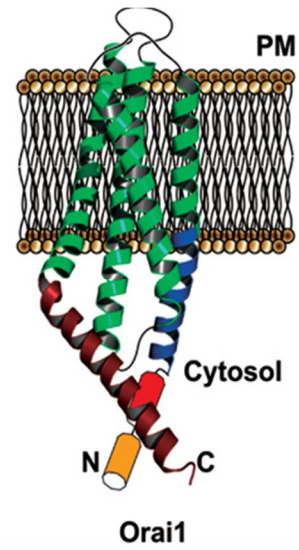
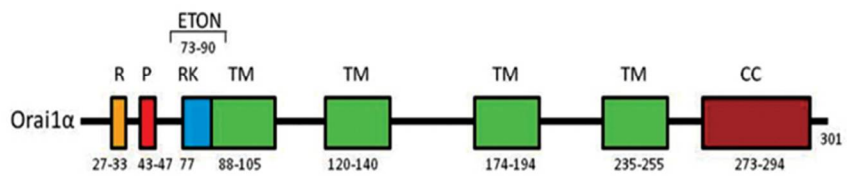


Figure 4. Molecular coupling between STIM1 and Orai1 within ER-PM junctions.

In conditions of repleted Ca^{2+} STIM1 is diffusely distributed along the ER membrane. Depletion of ER luminal Ca^{2+} causes Ca^{2+} dissociation from the STIM1 N-terminal cEF-hand, leading to aggregation of STIM1 which accumulates in pre-existing ER-PM junctions. Diffusible Orai1 tetramers in the PM are trapped in junctions by interaction with STIM1 and conformationally gate the opening of Orai1 channels. Extracellular Ca^{2+} then enters the cytosol leading to store-operated Ca^{2+} entry.

Figure 4.

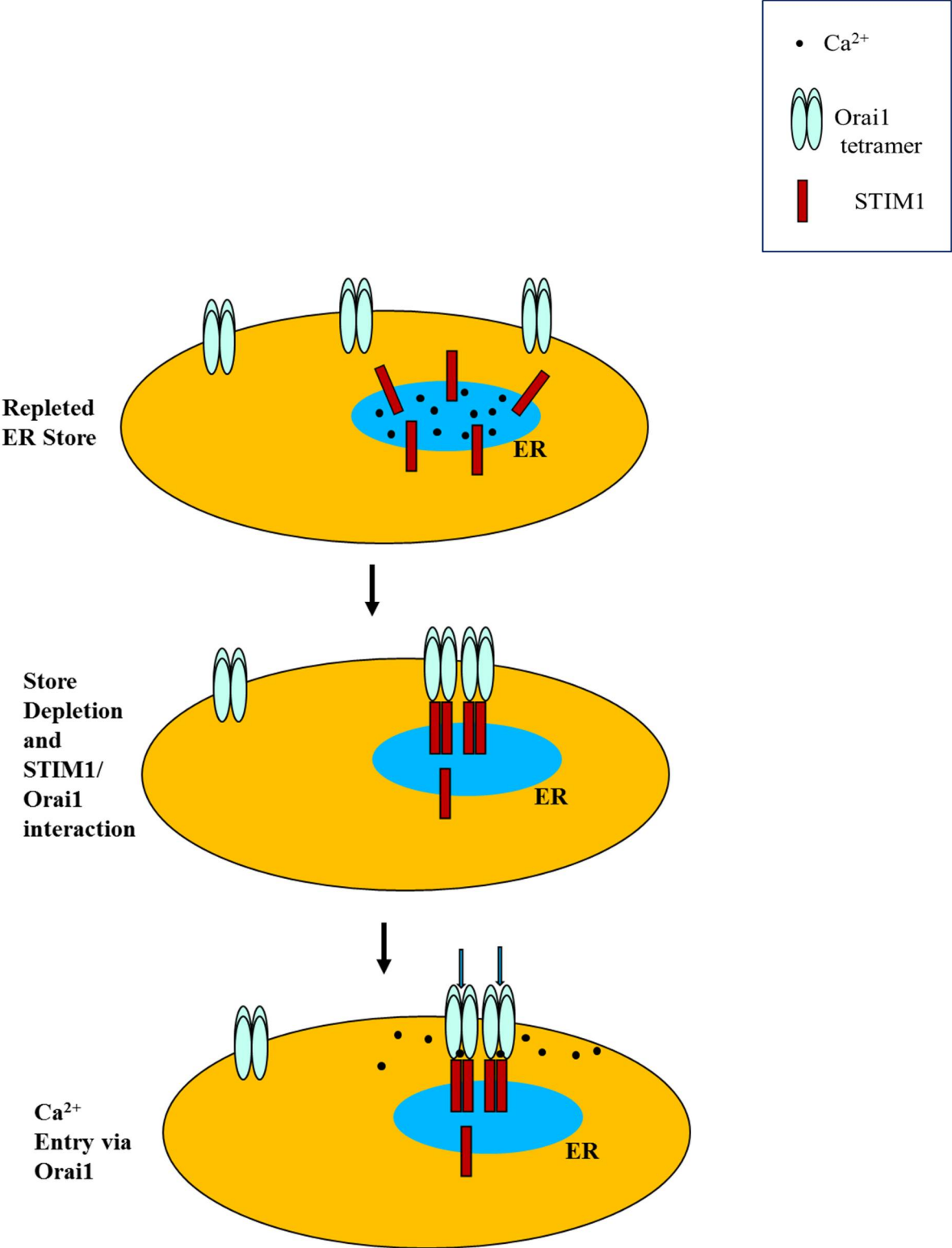


Figure 5. Intracellular pathways stimulated by hyperglycemia in diabetes. High glucose activates intracellular signaling pathways that in turn activates or interact with other pathways leading to activation of cytokines and transcriptional factors and ultimately regulates gene expression and fate of the cell. (Modified from Kanwar et al., 2008. (96))

Figure 5.

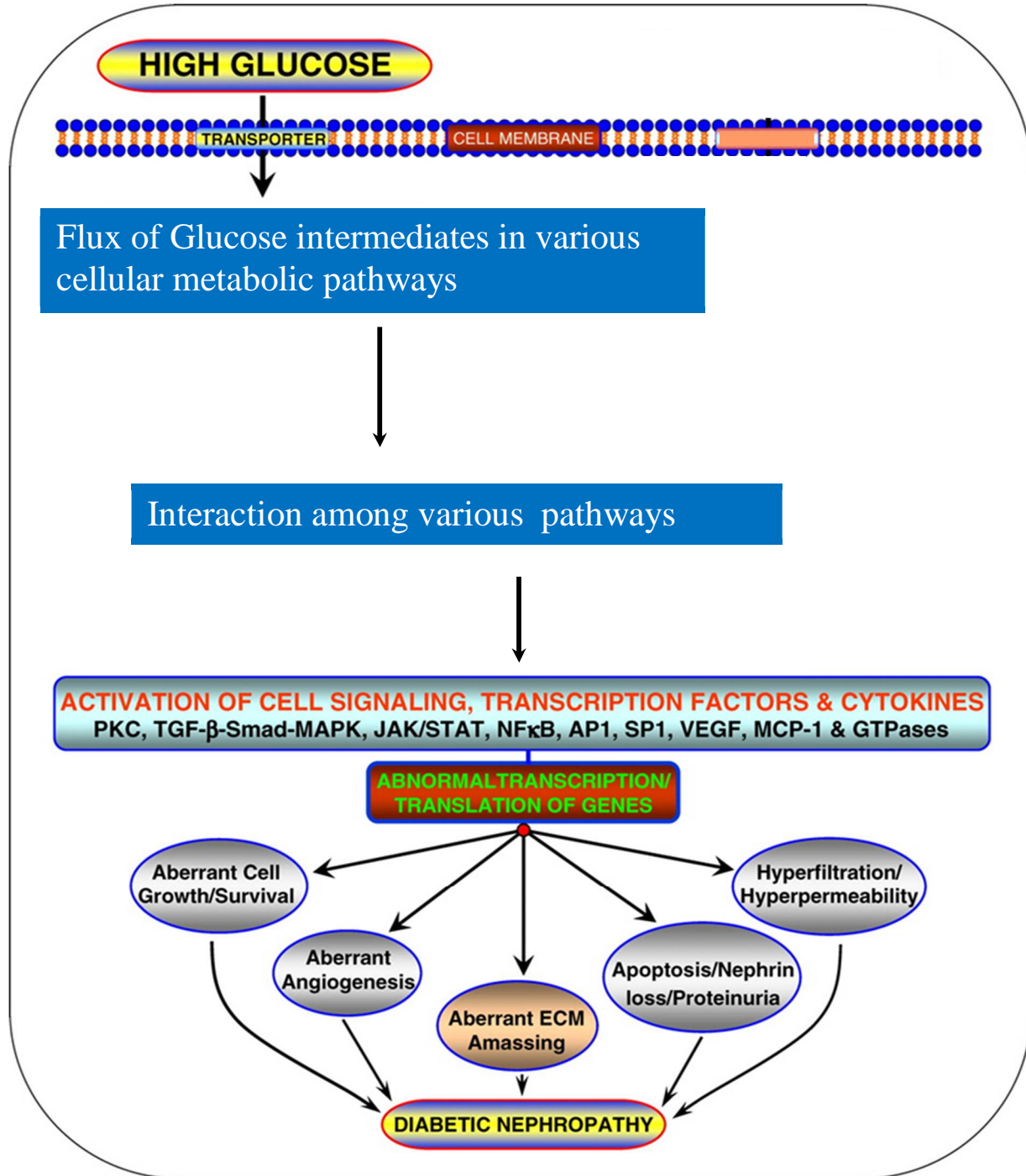
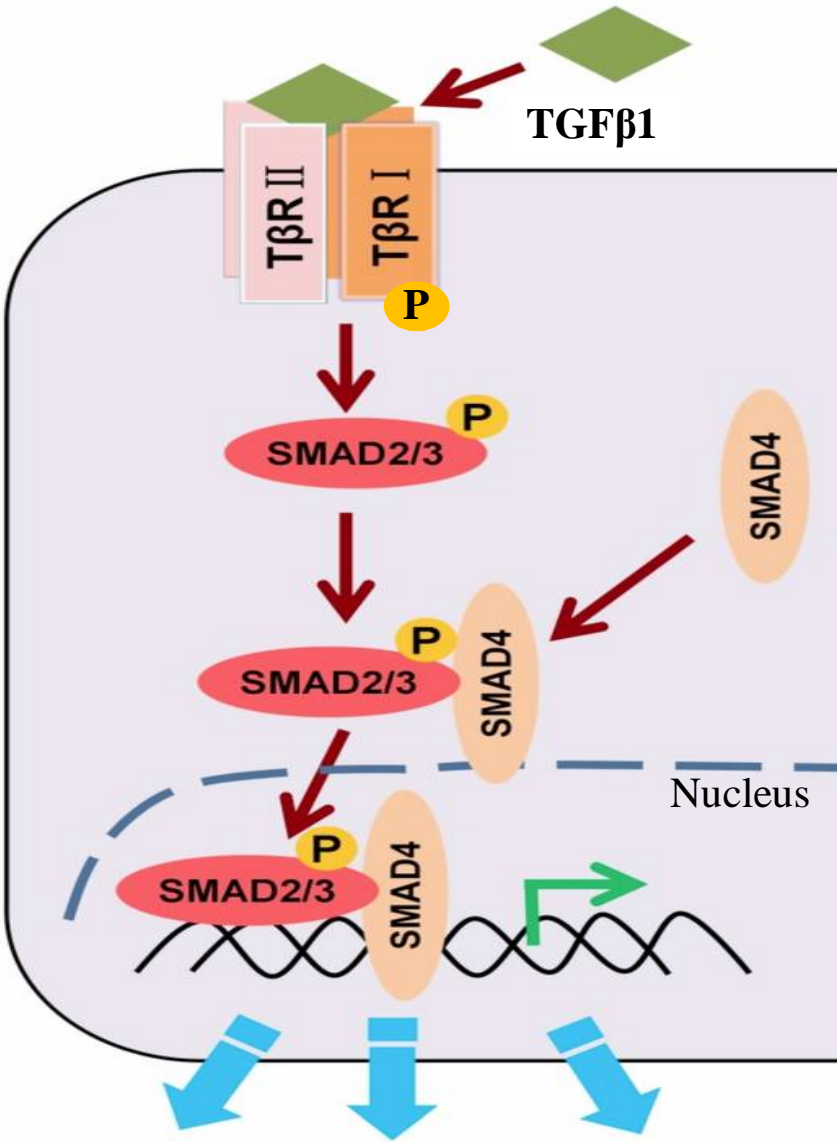


Figure 6. TGFβ1-Smad3 pathway activation.

Binding of TGFβ1 to its receptors leads to activation of receptor operated Smads, Smad2 and Smad3 by phosphorylation. Activated Smad2/3 subsequently translocates into the nucleus along with common Smad, Smad4 and regulates transcription of various genes, including those for ECM proteins. (Modified from Xie et al., 2014.(147))

Figure 6.



Regulation of Gene Transcription

Abbreviations

Ang II: angiotensin II

CPA: cyclopiazonic acid

DAG: diacylglycerol

DN: Diabetic nephropathy

ECM: extracellular matrix

ER: endoplasmic reticulum

Erk: extracellular signal regulated kinases

ESRD: end stage renal disease

ET: endothelin

GFR: glomerular filtration rate

IP₃: inositol triphosphate

MAPK: mitogen activated protein kinase

MCs: mesangial cells

mTOR: mammalian target of rapamycin

PDGF: platelet derived growth factor

PM: plasma membrane

ROC: receptor-operated channels

SERCA: sarcoplasmic/endoplasmic reticulum Ca²⁺ ATPase

SOC: store-operated channels

SOCE: store operated calcium entry

STIM: stromal interaction molecule

TAK1: TGFβ associated kinase 1

TG: thapsigargin

TGFβ: transforming growth factor beta

TRPC: canonical transient receptor potential

VEGF: vessel epithelial growth factor

VOCC: voltage-operated channels

References:

- (1) Tryggvason K, Wartiovaara J. How does the kidney filter plasma? *Physiology* (Bethesda) 2005 Apr;20:96-101.
- (2) Schlondorff D. The glomerular mesangial cell: an expanding role for a specialized pericyte. *FASEB J* 1987 Oct;1(4):272-281.
- (3) Mene P, Simonson MS, Dunn MJ. Physiology of the mesangial cell. *Physiol Rev* 1989 Oct;69(4):1347-1424.
- (4) Couchman JR, Beavan LA, McCarthy KJ. Glomerular matrix: synthesis, turnover and role in mesangial expansion. *Kidney Int* 1994;45(2):328-335.
- (5) Kriz W, Elger M, Mundel P, Lemley KV. Structure-stabilizing forces in the glomerular tuft. *J Am Soc Nephrol* 1995 Apr;5(10):1731-1739.
- (6) Schlondorff D, Banas B. The mesangial cell revisited: no cell is an island. *J Am Soc Nephrol* 2009 Jun;20(6):1179-1187.
- (7) Blantz RC, Gabbai FB, Tucker BJ, Yamamoto T, Wilson CB. Role of mesangial cell in glomerular response to volume and angiotensin II. *Am J Physiol* 1993 Jan;264(1 Pt 2):F158-65.
- (8) Sterzel RB, Schulze-Lohoff E, Marx M. Cytokines and mesangial cells. *Kidney International Supplement* 1993(39).
- (9) Kaname S, Uchida S, Ogata E, Kurokawa K. Autocrine secretion of transforming growth factor- β in cultured rat mesangial cells. *Kidney Int* 1992;42(6):1319-1327.

- (10) Riser BL, Cortes P, Heilig C, Grondin J, Ladson-Wofford S, Patterson D, et al. Cyclic stretching force selectively up-regulates transforming growth factor-beta isoforms in cultured rat mesangial cells. *Am J Pathol* 1996 Jun;148(6):1915-1923.
- (11) Gruden G, Thomas S, Burt D, Zhou W, Chusney G, Gnudi L, et al. Interaction of angiotensin II and mechanical stretch on vascular endothelial growth factor production by human mesangial cells. *J Am Soc Nephrol* 1999 Apr;10(4):730-737.
- (12) Riser BL, Denichilo M, Cortes P, Baker C, Grondin JM, Yee J, et al. Regulation of connective tissue growth factor activity in cultured rat mesangial cells and its expression in experimental diabetic glomerulosclerosis. *J Am Soc Nephrol* 2000 Jan;11(1):25-38.
- (13) Hoffman BB, Sharma K, Zhu Y, Ziyadeh FN. Transcriptional activation of transforming growth factor- β 1 in mesangial cell culture by high glucose concentration. *Kidney Int* 1998;54(4):1107-1116.
- (14) Ingram AJ, Ly H, Thai K, Kang M, Scholey JW. Activation of mesangial cell signaling cascades in response to mechanical strain. *Kidney Int* 1999;55(2):476-485.
- (15) Ingram AJ, James L, Ly H, Thai K, Scholey JW. Stretch activation of jun N-terminal kinase/stress-activated protein kinase in mesangial cells. *Kidney Int* 2000;58(4):1431-1439.
- (16) Krepinsky JC, Li Y, Chang Y, Liu L, Peng F, Wu D, et al. Akt mediates mechanical strain-induced collagen production by mesangial cells. *J Am Soc Nephrol* 2005 Jun;16(6):1661-1672.
- (17) Abboud HE. Mesangial cell biology. *Exp Cell Res* 2012;318(9):979-985.

- (18) Bieritz B, Spessotto P, Colombatti A, Jahn A, Prols F, Hartner A. Role of α_8 integrin in mesangial cell adhesion, migration, and proliferation. *Kidney Int* 2003;64(1):119-127.
- (19) Kashgarian M, Sterzel RB. The pathobiology of the mesangium. *Kidney Int* 1992;41(3):524-529.
- (20) Scindia YM, Deshmukh US, Bagavant H. Mesangial pathology in glomerular disease: targets for therapeutic intervention. *Adv Drug Deliv Rev* 2010;62(14):1337-1343.
- (21) Berridge MJ, Dupont G. Spatial and temporal signalling by calcium. *Curr Opin Cell Biol* 1994;6(2):267-274.
- (22) Berridge MJ, Lipp P, Bootman MD. The versatility and universality of calcium signalling. *Nature reviews Molecular cell biology* 2000;1(1):11-21.
- (23) Dolmetsch RE, Lewis RS, Goodnow CC, Healy JJ. Differential activation of transcription factors induced by Ca^{2+} response amplitude and duration. 1997.
- (24) Yu YM, Lermioglu F, Hassid A. Modulation of Ca^{2+} by agents affecting voltage-sensitive Ca^{2+} channels in mesangial cells. *Am J Physiol* 1989 Dec;257(6 Pt 2):F1094-9.
- (25) Matsunaga H, Ling BN, Eaton DC. Ca^{2+} -permeable channel associated with platelet-derived growth factor receptor in mesangial cells. *Am J Physiol* 1994 Aug;267(2 Pt 1):C456-65.
- (26) Ling BN, Matsunaga H, Ma H, Eaton DC. Role of growth factors in mesangial cell ion channel regulation. *Kidney Int* 1995;48(4):1158-1166.

- (27) Nutt LK, O'Neil RG. Effect of elevated glucose on endothelin-induced store-operated and non-store-operated calcium influx in renal mesangial cells. *J Am Soc Nephrol* 2000 Jul;11(7):1225-1235.
- (28) Saleh H, Schlatter E, Lang D, Pauels H, Heidenreich S. Regulation of mesangial cell apoptosis and proliferation by intracellular Ca^{2+} signals. *Kidney Int* 2000;58(5):1876-1884.
- (29) Mene P, Teti A, Pugliese F, Cinotti GA. Calcium release-activated calcium influx in cultured human mesangial cells. *Kidney Int* 1994;46(1):122-128.
- (30) Wang X, Pluznick JL, Wei P, Padanilam BJ, Sansom SC. TRPC4 forms store-operated Ca^{2+} channels in mouse mesangial cells. *Am J Physiol Cell Physiol* 2004 Aug;287(2):C357-64.
- (31) Broad LM, Braun FJ, Lievremont JP, Bird GS, Kurosaki T, Putney JW, Jr. Role of the phospholipase C-inositol 1,4,5-trisphosphate pathway in calcium release-activated calcium current and capacitative calcium entry. *J Biol Chem* 2001 May 11;276(19):15945-15952.
- (32) Parekh AB, Putney JW. Store-operated calcium channels. *Physiol Rev* 2005;85(2):757-810.
- (33) Li WP, Tsiokas L, Sansom SC, Ma R. Epidermal growth factor activates store-operated Ca^{2+} channels through an inositol 1,4,5-trisphosphate-independent pathway in human glomerular mesangial cells. *J Biol Chem* 2004 Feb 6;279(6):4570-4577.
- (34) Ma R, Smith S, Child A, Carmines PK, Sansom SC. Store-operated Ca^{2+} channels in human glomerular mesangial cells. *Am J Physiol Renal Physiol* 2000 Jun;278(6):F954-61.

- (35) Putney JW. Recent breakthroughs in the molecular mechanism of capacitative calcium entry (with thoughts on how we got here). *Cell Calcium* 2007;42(2):103-110.
- (36) Liou J, Kim ML, Heo WD, Jones JT, Myers JW, Ferrell JE, Jr, et al. STIM is a Ca²⁺ sensor essential for Ca²⁺-store-depletion-triggered Ca²⁺ influx. *Curr Biol* 2005 Jul 12;15(13):1235-1241.
- (37) Roos J, DiGregorio PJ, Yeromin AV, Ohlsen K, Lioudyno M, Zhang S, et al. STIM1, an essential and conserved component of store-operated Ca²⁺ channel function. *J Cell Biol* 2005 May 9;169(3):435-445.
- (38) Feske S, Gwack Y, Prakriya M, Srikanth S, Puppel S, Tanasa B, et al. A mutation in Orai1 causes immune deficiency by abrogating CRAC channel function. *Nature* 2006;441(7090):179-185.
- (39) Vig M, Peinelt C, Beck A, Koomoa DL, Rabah D, Koblan-Huberson M, et al. CRACM1 is a plasma membrane protein essential for store-operated Ca²⁺ entry. *Science* 2006 May 26;312(5777):1220-1223.
- (40) Zhang SL, Yeromin AV, Zhang XH, Yu Y, Safrina O, Penna A, et al. Genome-wide RNAi screen of Ca²⁺ influx identifies genes that regulate Ca²⁺ release-activated Ca²⁺ channel activity. *Proceedings of the National Academy of Sciences* 2006;103(24):9357-9362.
- (41) Soboloff J, Spassova MA, Tang XD, Hewavitharana T, Xu W, Gill DL. Orai1 and STIM reconstitute store-operated calcium channel function. *J Biol Chem* 2006;281(30):20661-20665.

- (42) Hewavitharana T, Deng X, Wang Y, Ritchie MF, Girish GV, Soboloff J, et al. Location and function of STIM1 in the activation of Ca²⁺ entry signals. *J Biol Chem* 2008;283(38):26252-26262.
- (43) Spassova MA, Soboloff J, He LP, Xu W, Dziadek MA, Gill DL. STIM1 has a plasma membrane role in the activation of store-operated Ca²⁺ channels. *Proc Natl Acad Sci U S A* 2006 Mar 14;103(11):4040-4045.
- (44) Cahalan MD. STIMulating store-operated Ca²⁺ entry. *Nat Cell Biol* 2009;11(6):669-677.
- (45) Wang Y, Deng X, Mancarella S, Hendron E, Eguchi S, Soboloff J, et al. The calcium store sensor, STIM1, reciprocally controls Orai and CaV1.2 channels. *Science* 2010 Oct 1;330(6000):105-109.
- (46) Prakriya M, Feske S, Gwack Y, Srikanth S, Rao A, Hogan PG. Orai1 is an essential pore subunit of the CRAC channel. *Nature* 2006;443(7108):230-233.
- (47) Yeromin AV, Zhang SL, Jiang W, Yu Y, Safrina O, Cahalan MD. Molecular identification of the CRAC channel by altered ion selectivity in a mutant of Orai. *Nature* 2006;443(7108):226-229.
- (48) Wu MM, Buchanan J, Luik RM, Lewis RS. Ca²⁺ store depletion causes STIM1 to accumulate in ER regions closely associated with the plasma membrane. *J Cell Biol* 2006 Sep 11;174(6):803-813.
- (49) Deng X, Wang Y, Zhou Y, Soboloff J, Gill DL. STIM and Orai: dynamic intermembrane coupling to control cellular calcium signals. *J Biol Chem* 2009 Aug 21;284(34):22501-22505.

- (50) Wang Y, Deng X, Gill DL. Calcium signaling by STIM and Orai: intimate coupling details revealed. *Sci Signal* 2010 Nov 16;3(148):pe42.
- (51) Horinouchi T, Higashi T, Higa T, Terada K, Mai Y, Aoyagi H, et al. Different binding property of STIM1 and its novel splice variant STIM1L to Orai1, TRPC3, and TRPC6 channels. *Biochem Biophys Res Commun* 2012;428(2):252-258.
- (52) Kim MS, Zeng W, Yuan JP, Shin DM, Worley PF, Muallem S. Native Store-operated Ca²⁺ Influx Requires the Channel Function of Orai1 and TRPC1. *J Biol Chem* 2009 Apr 10;284(15):9733-9741.
- (53) Liao Y, Erxleben C, Abramowitz J, Flockerzi V, Zhu MX, Armstrong DL, et al. Functional interactions among Orai1, TRPCs, and STIM1 suggest a STIM-regulated heteromeric Orai/TRPC model for SOCE/Icrac channels. *Proc Natl Acad Sci U S A* 2008 Feb 26;105(8):2895-2900.
- (54) Worley PF, Zeng W, Huang GN, Yuan JP, Kim JY, Lee MG, et al. TRPC channels as STIM1-regulated store-operated channels. *Cell Calcium* 2007;42(2):205-211.
- (55) Sours-Brothers S, Ding M, Graham S, Ma R. Interaction between TRPC1/TRPC4 assembly and STIM1 contributes to store-operated Ca²⁺ entry in mesangial cells. *Exp Biol Med* (Maywood) 2009 Jun;234(6):673-682.
- (56) Parekh AB, Putney JW, Jr. Store-operated calcium channels. *Physiol Rev* 2005 Apr;85(2):757-810.

- (57) Targos B, Baranska J, Pomorski P. Store-operated calcium entry in physiology and pathology of mammalian cells. *Acta Biochim Pol* 2005;52(2):397-409.
- (58) Gruszczynska-Biegala J, Pomorski P, Wisniewska MB, Kuznicki J. Differential roles for STIM1 and STIM2 in store-operated calcium entry in rat neurons. *PloS one* 2011;6(4):e19285.
- (59) Uehara A, Yasukochi M, Imanaga I, Nishi M, Takeshima H. Store-operated Ca^{2+} entry uncoupled with ryanodine receptor and junctional membrane complex in heart muscle cells. *Cell Calcium* 2002;31(2):89-96.
- (60) Pan Z, Brotto M, Ma J. Store-operated Ca^{2+} entry in muscle physiology and diseases. *BMB Rep* 2014 Feb;47(2):69-79.
- (61) Leung F, Yung L, Yao X, Laher I, Huang Y. Store-operated calcium entry in vascular smooth muscle. *Br J Pharmacol* 2008;153(5):846-857.
- (62) Feske S. Calcium signalling in lymphocyte activation and disease. *Nature Reviews Immunology* 2007;7(9):690-702.
- (63) Darbellay B, Arnaudeau S, Konig S, Jousset H, Bader C, Demaurex N, et al. STIM1- and Orai1-dependent store-operated calcium entry regulates human myoblast differentiation. *J Biol Chem* 2009 Feb 20;284(8):5370-5380.
- (64) Lyfenko AD, Dirksen RT. Differential dependence of store-operated and excitation-coupled Ca^{2+} entry in skeletal muscle on STIM1 and Orai1. *J Physiol* 2008 Oct 15;586(Pt 20):4815-4824.

- (65) Abdullaev IF, Bisailon JM, Potier M, Gonzalez JC, Motiani RK, Trebak M. Stim1 and Orai1 mediate CRAC currents and store-operated calcium entry important for endothelial cell proliferation. *Circ Res* 2008 Nov 21;103(11):1289-1299.
- (66) Bisailon JM, Motiani RK, Gonzalez-Cobos JC, Potier M, Halligan KE, Alzawahra WF, et al. Essential role for STIM1/Orai1-mediated calcium influx in PDGF-induced smooth muscle migration. *Am J Physiol Cell Physiol* 2010 May;298(5):C993-1005.
- (67) Potier M, Gonzalez JC, Motiani RK, Abdullaev IF, Bisailon JM, Singer HA, et al. Evidence for STIM1- and Orai1-dependent store-operated calcium influx through ICRAC in vascular smooth muscle cells: role in proliferation and migration. *FASEB J* 2009 Aug;23(8):2425-2437.
- (68) Voelkers M, Salz M, Herzog N, Frank D, Dolatabadi N, Frey N, et al. Orai1 and Stim1 regulate normal and hypertrophic growth in cardiomyocytes. *J Mol Cell Cardiol* 2010;48(6):1329-1334.
- (69) Lis A, Peinelt C, Beck A, Parvez S, Monteilh-Zoller M, Fleig A, et al. CRACM1, CRACM2, and CRACM3 are store-operated Ca²⁺ channels with distinct functional properties. *Current Biology* 2007;17(9):794-800.
- (70) Ogawa A, Firth AL, Smith KA, Maliakal MV, Yuan JX. PDGF enhances store-operated Ca²⁺ entry by upregulating STIM1/Orai1 via activation of Akt/mTOR in human pulmonary arterial smooth muscle cells. *Am J Physiol Cell Physiol* 2012 Jan 15;302(2):C405-11.
- (71) Agrotis A, Koulis C. STIM1: a new therapeutic target in occlusive vascular disease? *Cardiovasc Res* 2009;81(4):627-628.

- (72) Peng H, Liu J, Sun Q, Chen R, Wang Y, Duan J, et al. mTORC1 enhancement of STIM1-mediated store-operated Ca²⁺ entry constrains tuberous sclerosis complex-related tumor development. *Oncogene* 2012.
- (73) Feske S, Picard C, Fischer A. Immunodeficiency due to mutations in ORAI1 and STIM1. *Clinical Immunology* 2010;135(2):169-182.
- (74) Feske S. ORAI1 and STIM1 deficiency in human and mice: roles of store-operated Ca²⁺ entry in the immune system and beyond. *Immunol Rev* 2009;231(1):189-209.
- (75) Picard C, McCarl C, Papolos A, Khalil S, Lüthy K, Hivroz C, et al. STIM1 mutation associated with a syndrome of immunodeficiency and autoimmunity. *N Engl J Med* 2009;360(19):1971-1980.
- (76) Duke AM, Hopkins PM, Calaghan SC, Halsall JP, Steele DS. Store-operated Ca²⁺ entry in malignant hyperthermia-susceptible human skeletal muscle. *J Biol Chem* 2010 Aug 13;285(33):25645-25653.
- (77) Zhao X, Weisleder N, Thornton A, Oppong Y, Campbell R, Ma J, et al. Compromised store-operated Ca²⁺ entry in aged skeletal muscle. *Aging cell* 2008;7(4):561-568.
- (78) McCarl C, Picard C, Khalil S, Kawasaki T, Röther J, Papolos A, et al. ORAI1 deficiency and lack of store-operated Ca²⁺ entry cause immunodeficiency, myopathy, and ectodermal dysplasia. *J Allergy Clin Immunol* 2009;124(6):1311-1318. e7.
- (79) Guerrero-Hernandez A, Verkhratsky A. Calcium signalling in diabetes. *Cell Calcium* 2014;56(5):297-301.

- (80) Arruda AP, Hotamisligil GS. Calcium homeostasis and organelle function in the pathogenesis of obesity and diabetes. *Cell metabolism* 2015;22(3):381-397.
- (81) Mene P, Pugliese G, Pricci F, Di Mario U, Cinotti G, Pugliese F. High glucose inhibits cytosolic calcium signaling in cultured rat mesangial cells. *Kidney Int* 1993;43(3):585-591.
- (82) Kostyuk E, Svichar N, Shishkin V, Kostyuk P. Role of mitochondrial dysfunction in calcium signalling alterations in dorsal root ganglion neurons of mice with experimentally-induced diabetes. *Neuroscience* 1999;90(2):535-541.
- (83) Chung AW, Au Yeung K, Chum E, Okon EB, van Breemen C. Diabetes modulates capacitative calcium entry and expression of transient receptor potential canonical channels in human saphenous vein. *Eur J Pharmacol* 2009 Jun 24;613(1-3):114-118.
- (84) Daskoulidou N, Zeng B, Berglund LM, Jiang H, Chen GL, Kotova O, et al. High glucose enhances store-operated calcium entry by upregulating ORAI/STIM via calcineurin-NFAT signalling. *J Mol Med (Berl)* 2014 Dec 5.
- (85) Ding H, Triggle CR. Endothelial dysfunction in diabetes: multiple targets for treatment. *Pflugers Arch* 2010 May;459(6):977-994.
- (86) Tamareille S, Mignen O, Capiod T, Rucker-Martin C, Feuvray D. High glucose-induced apoptosis through store-operated calcium entry and calcineurin in human umbilical vein endothelial cells. *Cell Calcium* 2006 Jan;39(1):47-55.

- (87) Curtis T, Major E, Trimble E, Scholfield C. Diabetes-induced activation of protein kinase C inhibits store-operated Ca² uptake in rat retinal microvascular smooth muscle. *Diabetologia* 2003;46(9):1252-1259.
- (88) Ma L, Zhu B, Chen X, Liu J, Guan Y, Ren J. Abnormalities of sarcoplasmic reticulum Ca²⁺ mobilization in aortic smooth muscle cells from streptozotocin-induced diabetic rats. *Clin Exp Pharmacol Physiol* 2008 May;35(5-6):568-573.
- (89) Mita M, Ito K, Taira K, Nakagawa J, Walsh MP, Shoji M. Attenuation of store-operated Ca²⁺ entry and enhanced expression of TRPC channels in caudal artery smooth muscle from Type 2 diabetic Goto-Kakizaki rats. *Clin Exp Pharmacol Physiol* 2010 Jul;37(7):670-678.
- (90) Redondo PC, Jardin I, Hernandez-Cruz JM, Pariente JA, Salido GM, Rosado JA. Hydrogen peroxide and peroxynitrite enhance Ca²⁺ mobilization and aggregation in platelets from type 2 diabetic patients. *Biochem Biophys Res Commun* 2005 Aug 5;333(3):794-802.
- (91) Saavedra FR, Redondo PC, Hernández-Cruz JM, Salido GM, Pariente JA, Rosado JA. Store-operated Ca² entry and tyrosine kinase pp60^{src} hyperactivity are modulated by hyperglycemia in platelets from patients with non insulin-dependent diabetes mellitus. *Arch Biochem Biophys* 2004;432(2):261-268.
- (92) Zbidi H, Lopez JJ, Amor NB, Bartegi A, Salido GM, Rosado JA. Enhanced expression of STIM1/Orai1 and TRPC3 in platelets from patients with type 2 diabetes mellitus. *Blood Cells Mol Dis* 2009 Sep-Oct;43(2):211-213.

- (93) Pang Y, Hunton DL, Bounelis P, Marchase RB. Hyperglycemia inhibits capacitative calcium entry and hypertrophy in neonatal cardiomyocytes. *Diabetes* 2002 Dec;51(12):3461-3467.
- (94) Collins AJ, Foley RN, Herzog C, Chavers BM, Gilbertson D, Ishani A, et al. Excerpts from the US Renal Data System 2009 Annual Data Report. *Am J Kidney Dis* 2010 Jan;55(1 Suppl 1):S1-420, A6-7.
- (95) Foley RN, Collins AJ. End-stage renal disease in the United States: an update from the United States Renal Data System. *J Am Soc Nephrol* 2007 Oct;18(10):2644-2648.
- (96) Kanwar YS, Wada J, Sun L, Xie P, Wallner EI, Chen S, et al. Diabetic nephropathy: mechanisms of renal disease progression. *Exp Biol Med* 2008;233(1):4-11.
- (97) Simonson M. Phenotypic transitions and fibrosis in diabetic nephropathy. *Kidney Int* 2007;71(9):846-854.
- (98) Mason RM, Wahab NA. Extracellular matrix metabolism in diabetic nephropathy. *Journal of the American Society of Nephrology* 2003;14(5):1358-1373.
- (99) Kanwar YS, Akagi S, Sun L, Nayak B, Xie P, Wada J, et al. Cell biology of diabetic kidney disease. *Nephron Exp Nephrol* 2005;101(3):e100-10.
- (100) Ziyadeh FN. Mediators of diabetic renal disease: the case for *tgf-Beta* as the major mediator. *J Am Soc Nephrol* 2004 Jan;15 Suppl 1:S55-7.

- (101) Gooch JL, Gorin Y, Zhang B, Abboud HE. Involvement of calcineurin in transforming growth factor- β -mediated regulation of extracellular matrix accumulation. *J Biol Chem* 2004;279(15):15561-15570.
- (102) Gorin Y, Block K, Hernandez J, Bhandari B, Wagner B, Barnes JL, et al. Nox4 NAD (P) H oxidase mediates hypertrophy and fibronectin expression in the diabetic kidney. *J Biol Chem* 2005;280(47):39616-39626.
- (103) Ma R, Pluznick JL, Sansom SC. Ion channels in mesangial cells: function, malfunction, or fiction. *Physiology* 2005;20(2):102-111.
- (104) Ma R, Sansom SC. Epidermal growth factor activates store-operated calcium channels in human glomerular mesangial cells. *J Am Soc Nephrol* 2001 Jan;12(1):47-53.
- (105) Mene P, Pugliese F, Cinotti GA. Regulation of capacitative calcium influx in cultured human mesangial cells: roles of protein kinase C and calmodulin. *J Am Soc Nephrol* 1996 Jul;7(7):983-990.
- (106) Mene P, Pugliese G, Pricci F, Di Mario U, Cinotti GA, Pugliese F. High glucose level inhibits capacitative Ca²⁺ influx in cultured rat mesangial cells by a protein kinase C-dependent mechanism. *Diabetologia* 1997 May;40(5):521-527.
- (107) Mene P, Pascale C, Teti A, Bernardini S, Cinotti GA, Pugliese F. Effects of advanced glycation end products on cytosolic Ca²⁺ signaling of cultured human mesangial cells. *J Am Soc Nephrol* 1999 Jul;10(7):1478-1486.

- (108) Ding Y, Winters A, Ding M, Graham S, Akopova I, Muallem S, et al. Reactive oxygen species-mediated TRPC6 protein activation in vascular myocytes, a mechanism for vasoconstrictor-regulated vascular tone. *J Biol Chem* 2011 Sep 9;286(36):31799-31809.
- (109) Saleh S, Albert A, Peppiatt C, Large W. Angiotensin II activates two cation conductances with distinct TRPC1 and TRPC6 channel properties in rabbit mesenteric artery myocytes. *J Physiol (Lond)* 2006;577(2):479-495.
- (110) Chaudhari S, Ma R. Store-operated calcium entry and diabetic complications. *Exp Biol Med (Maywood)* 2016 Feb;241(4):343-352.
- (111) Collins AJ, Foley RN, Chavers B, Gilbertson D, Herzog C, Ishani A, et al. US Renal Data System 2013 Annual Data Report. *Am J Kidney Dis* 2014 Jan;63(1 Suppl):A7.
- (112) Keane WF, Brenner BM, De Zeeuw D, Grunfeld J, Mcgill J, Mitch WE, et al. The risk of developing end-stage renal disease in patients with type 2 diabetes and nephropathy: the RENAAL study. *Kidney Int* 2003;63(4):1499-1507.
- (113) Nathan DM. Long-term complications of diabetes mellitus. *N Engl J Med* 1993;328(23):1676-1685.
- (114) Mason RM, Wahab NA. Extracellular matrix metabolism in diabetic nephropathy. *Journal of the American Society of Nephrology* 2003;14(5):1358-1373.
- (115) Dalla Vestra M, Saller A, Bortoloso E, Mauer M, Fioretto P. Structural involvement in type 1 and type 2 diabetic nephropathy. *Diabetes Metab* 2000 Jul;26 Suppl 4:8-14.

- (116) Steffes MW, Østerby R, Chavers B, Mauer SM. Mesangial expansion as a central mechanism for loss of kidney function in diabetic patients. *Diabetes* 1989;38(9):1077-1081.
- (117) Østerby R, Tapia J, Nyberg G, Tencer J, Willner J, Rippe B, et al. Renal structures in type 2 diabetic patients with elevated albumin excretion rate. *APMIS* 2001;109(11):751-761.
- (118) Østerby R, Hartmann A, Nyengaard JR, Bangstad H. Development of renal structural lesions in type-1 diabetic patients with microalbuminuria. *Virchows Archiv* 2002;440(1):94-101.
- (119) Schena FP, Gesualdo L. Pathogenetic mechanisms of diabetic nephropathy. *Journal of the American Society of Nephrology* 2005;16(3 suppl 1):S30-S33.
- (120) Abrass CK. Diabetic nephropathy. Mechanisms of mesangial matrix expansion. *West J Med* 1995 Apr;162(4):318-321.
- (121) Brownlee M. The pathobiology of diabetic complications a unifying mechanism. *Diabetes* 2005;54(6):1615-1625.
- (122) Gruden G, Perin PC, Camussi G. Insight on the pathogenesis of diabetic nephropathy from the study of podocyte and mesangial cell biology. *Current diabetes reviews* 2005;1(1):27-40.
- (123) Remuzzi G, Benigni A, Remuzzi A. Mechanisms of progression and regression of renal lesions of chronic nephropathies and diabetes. *J Clin Invest* 2006;116(2):288-296.
- (124) Di Paolo S, Gesualdo L, Ranieri E, Grandaliano G, Schena FP. High glucose concentration induces the overexpression of transforming growth factor-beta through the activation of a

platelet-derived growth factor loop in human mesangial cells. *Am J Pathol* 1996 Dec;149(6):2095-2106.

(125) Wolf G, Ziyadeh FN. The role of angiotensin II in diabetic nephropathy: emphasis on nonhemodynamic mechanisms. *American journal of kidney diseases* 1997;29(1):153-163.

(126) Weston BS, Wahab NA, Mason RM. CTGF mediates TGF-beta-induced fibronectin matrix deposition by upregulating active alpha5beta1 integrin in human mesangial cells. *J Am Soc Nephrol* 2003 Mar;14(3):601-610.

(127) Riser BL, Denichilo M, Cortes P, Baker C, Grondin JM, Yee J, et al. Regulation of connective tissue growth factor activity in cultured rat mesangial cells and its expression in experimental diabetic glomerulosclerosis. *J Am Soc Nephrol* 2000 Jan;11(1):25-38.

(128) Iglesias-de la Cruz, M Carmen, Ruiz-Torres P, Alcamí J, Díez-Marqués L, Ortega-Velázquez R, Chen S, et al. Hydrogen peroxide increases extracellular matrix mRNA through TGF- β 1 in human mesangial cells. *Kidney Int* 2001;59(1):87-95.

(129) Forbes JM, Thallas V, Thomas MC, Founds HW, Burns WC, Jerums G, et al. The breakdown of preexisting advanced glycation end products is associated with reduced renal fibrosis in experimental diabetes. *FASEB J* 2003 Sep;17(12):1762-1764.

(130) Lan HY. Diverse roles of TGF-beta/Smads in renal fibrosis and inflammation. *Int J Biol Sci* 2011;7(7):1056-1067.

(131) Leask A, Abraham DJ. TGF-beta signaling and the fibrotic response. *FASEB J* 2004 May;18(7):816-827.

- (132) Li JH, Huang XR, Zhu H, Johnson R, Lan HY. Role of TGF- β signaling in extracellular matrix production under high glucose conditions. *Kidney Int* 2003;63(6):2010-2019.
- (133) Schnaper HW, Hayashida T, Hubchak SC, Poncelet AC. TGF- β signal transduction and mesangial cell fibrogenesis. *Am J Physiol Renal Physiol* 2003 Feb;284(2):F243-52.
- (134) Yu L, Border WA, Huang Y, Noble NA. TGF- β isoforms in renal fibrogenesis. *Kidney Int* 2003;64(3):844-856.
- (135) Bae E, Kim S, Hong S, Liu F, Ooshima A. Smad3 linker phosphorylation attenuates Smad3 transcriptional activity and TGF- β 1/Smad3-induced epithelial–mesenchymal transition in renal epithelial cells. *Biochem Biophys Res Commun* 2012;427(3):593-599.
- (136) Fujimoto M, Maezawa Y, Yokote K, Joh K, Kobayashi K, Kawamura H, et al. Mice lacking Smad3 are protected against streptozotocin-induced diabetic glomerulopathy. *Biochem Biophys Res Commun* 2003;305(4):1002-1007.
- (137) Runyan CE, Schnaper HW, Poncelet AC. Smad3 and PKC δ mediate TGF- β 1-induced collagen I expression in human mesangial cells. *Am J Physiol Renal Physiol* 2003 Sep;285(3):F413-22.
- (138) Isono M, Chen S, Hong SW, Iglesias-de la Cruz, M Carmen, Ziyadeh FN. Smad pathway is activated in the diabetic mouse kidney and Smad3 mediates TGF- β -induced fibronectin in mesangial cells. *Biochem Biophys Res Commun* 2002;296(5):1356-1365.

- (139) Feng X, Derynck R. Specificity and versatility in TGF- β signaling through Smads. *Annu Rev Cell Dev Biol* 2005;21:659-693.
- (140) Derynck R, Zhang YE. Smad-dependent and Smad-independent pathways in TGF- β family signalling. *Nature* 2003;425(6958):577-584.
- (141) Mu Y, Gudey SK, Landström M. Non-Smad signaling pathways. *Cell Tissue Res* 2012;347(1):11-20.
- (142) Massague J, Chen YG. Controlling TGF-beta signaling. *Genes Dev* 2000 Mar 15;14(6):627-644.
- (143) Hayashida T, Decaestecker M, Schnaper HW. Cross-talk between ERK MAP kinase and Smad signaling pathways enhances TGF-beta-dependent responses in human mesangial cells. *FASEB J* 2003 Aug;17(11):1576-1578.
- (144) Runyan CE, Schnaper HW, Poncelet AC. The phosphatidylinositol 3-kinase/Akt pathway enhances Smad3-stimulated mesangial cell collagen I expression in response to transforming growth factor-beta1. *J Biol Chem* 2004 Jan 23;279(4):2632-2639.
- (145) Marieb EN. *Human Anatomy & Physiology*. : Benjamin-Cummings Publishing Company; 1989.
- (146) Rosado JA, Diez R, Smani T, Jardín I. STIM and Orai1 Variants in Store-Operated Calcium Entry. *Frontiers in pharmacology* 2015;6.

(147) Xie F, Zhang Z, van Dam H, Zhang L, Zhou F. Regulation of TGF- β superfamily signaling by SMAD mono-ubiquitination. *Cells* 2014;3(4):981-993.

CHAPTER II

HIGH GLUCOSE AND DIABETES ENHANCED STORE-OPERATED Ca^{2+} ENTRY AND INCREASED EXPRESSION OF ITS SIGNALING PROTEINS IN MESANGIAL CELLS

Sarika Chaudhari, Peiwen Wu, Yanxia Wang, Yanfeng Ding, Joseph Yuan, Malcolm Begg, and
Rong Ma

American Journal of physiology, Renal Physiology. 2014 May;306(9): F1069-F1080

doi: 10.1152/ajprenal.00463.2013

Abstract

The present study was conducted to determine whether and how store-operated Ca^{2+} entry (SOCE) in glomerular mesangial cells (MCs) was altered by high glucose (HG) and diabetes. Human MCs (HMCs) were treated with either normal glucose or HG for different time periods. Cyclopiazonic acid-induced SOCE was significantly greater in the MCs with 7 day HG treatment and the response was completely abolished by GSK-7975A, a selective inhibitor of store-operated Ca^{2+} channel. Similarly, the inositol 1,4,5-trisphosphate-induced store-operated Ca^{2+} currents were significantly enhanced in the MCs treated with HG for 7 days and the enhanced response was abolished by both GSK-7975A and La^{3+} . In contrast, receptor-operated Ca^{2+} entry in MCs was significantly reduced by HG treatment. Western blot showed that HG increased the expression levels of STIM1 and Orai1 in cultured MCs. A significant HG effect occurred at a concentration as low as 10 mM, but required a minimum of 7 days. The HG effect in cultured MCs was recapitulated in renal glomeruli/cortex of both type I and II diabetic rats. Furthermore, quantitative real time RT-PCR revealed that a 6 day HG treatment significantly increased mRNA expression level of STIM1. However, the expressions of STIM2 and Orai1 transcripts were not affected by HG. Taken together, these results suggest that HG/diabetes enhanced SOCE in MCs by increasing STIM1/Orai1 protein expressions. HG upregulates STIM1 by promoting its transcription, but increases Orai1 protein through a post-transcriptional mechanism.

Keywords: Store-operated Ca^{2+} entry; STIM1; Orai1; mesangial cells; high glucose; diabetic nephropathy

Introduction

The ubiquitous store-operated Ca^{2+} entry (SOCE), the Ca^{2+} entry through store-operated Ca^{2+} channel (SOC) driven by depletion of endoplasmic reticulum (ER) Ca^{2+} is critical to the primary Ca^{2+} signaling pathway in a variety of cell types (59). This Ca^{2+} entry pathway plays an essential role in a wide variety of physiological functions including exocytosis, enzymatic activity, gene transcription, cell proliferation, and apoptosis (59). Although SOCE was originally described over two decades ago (64), its molecular mediators were unknown until recently. By high through-put RNAi screening, two protein families, STIM (45; 67) and Orai (22; 78; 87), were identified as required components of SOCE. STIM1 is a single-pass transmembrane protein located primarily in the ER membrane and functions as an ER Ca^{2+} sensor to sense the ER luminal Ca^{2+} concentration. Orai1 is a small plasma membrane protein and is believed to be the pore-forming unit of SOC. Upon depletion of ER Ca^{2+} , STIM1 aggregates and translocates to ER-plasma membrane junctions, where it physically associates and subsequently activates Orai1 and causes Ca^{2+} entry into the cytosol (12; 80).

It is well known that Ca^{2+} signals regulate function of renal microvasculature (10; 16; 18-21; 26). Glomerular mesangial cells (MCs) sit between glomerular capillary loops, a special part of renal microvasculature, and maintains the structural architecture of the capillary networks. These cells play important roles in mesangial matrix homeostasis, regulation of glomerular filtration rate and phagocytosis of apoptotic cells in glomerulus (1; 68; 74). MC dysfunction is closely associated with several glomerular diseases, such as diabetic nephropathy (37; 39; 69). Like many other cell types, MC function is largely regulated by intracellular Ca^{2+} signals and the MC Ca^{2+} homeostasis is, at a large extent, attributed to Ca^{2+} channels in the plasma membrane (47; 74). Over past decades, we and others have demonstrated that SOCE mediates MC Ca^{2+} responses to

a variety of circulating and locally produced hormones, such as angiotensin II (Ang II), endothelin 1, and epidermal growth factor (9; 43; 48; 55; 58). We further demonstrated that STIM1 was required for activation of SOCE in human MCs (HMCs) (73). However, the association of SOCE in MCs with diabetic nephropathy remains unknown. The aim of the present study was to determine what and how diabetes affects SOCE in MCs using cultured MCs in combination of animal models of diabetes.

Materials and Methods

MC culture. HMCs belong to CloneticsTM renal MC system and were purchased from Lonza (Walkersville, MD). MCs in a 75 cm² flask were cultured in normal glucose (5.6 mM, NG) DMEM medium (Gibco, Carlsbad, CA) supplemented with 25 mM HEPES, 4 mM glutamine, 1.0 mM sodium pyruvate, 0.1 mM nonessential amino acids, 100 U/ml penicillin, 100 µg/ml streptomycin and 20% FBS. When MCs reached ~90% confluence, the cells were split into 60-mm cell culture plates for various treatments as specified in figure legends. For NG treatment, 20 mM α -mannitol was added to the media for an osmotic control. For HG treatment, the concentration of D-glucose was 25 mM. Cells were growth-arrested with 0.5% FBS media during treatments. Culture media was replaced with fresh media every other day. Only subpassage 4-9 MCs were used in the present study.

Transient transfection of HMCs. In Figure 5 E & F, siRNA against human Orail or scramble control siRNA were transiently transfected into HMCs using Lipofectamine and Plus reagent (Invitrogen-BRL, Carlsbad, CA) following the protocols provided by the manufacturer. Cells were harvested for western blot 72 hours after transfection.

Western blot. The whole cell lysates, glomerular extracts or renal cortical extracts were fractionated by 10% SDS-PAGE, transferred to PVDF membranes, and probed with primary STIM1, Orai1, actin, and tubulin antibodies. Bound antibodies were visualized with Super Signal West Femto or Pico Luminol/Enhancer Solution (Thermo Scientific, Rockford, IL). The specific protein bands were visualized and captured using an AlphaEase FC Imaging System (Alpha Innotech, San Leandro, CA). The IDV of each band was measured by drawing a rectangle outlining the band using AlphaEase FC software with auto background subtraction. If a protein had double bands, a total IDV by summation of each band IDV was used. The expression levels of STIM1 and Orai1 proteins were quantified by normalization of the IDVs of those protein bands to that of actin bands on the same blot.

Quantitative real time RT-PCR. The total RNA was isolated from cultured HMCs using PerfectPure RNA cultured cell kit (5 Prime, Inc., Hamburg, Germany) following the manufacturer's protocol. All primers used in the present study were listed in Table 1. The primers were synthesized by IDT (Coralville, Iowa). A total of 1.0 μ g RNA in a final volume of 20 μ l was used for RT reactions using iScript cDNA synthesis kit (BioRad, Hercules, CA) following the manufacturer's reaction protocol. A total of 0.2 μ g RT product and 100 nM primer was used for real time PCR which was performed using iQ SYBR green supermix (BioRad, Hercules, CA) in a final volume of 20 μ l. The PCR mix was denatured at 95°C for 10 min, followed by 45 cycles of melting at 95°C for 15 s, annealing at 57°C for 10s and elongation at 72°C for 15 s. After amplification, a melting curve analysis from 65°C to 95°C with a heating rate of 0.02°C /s with a continuous fluorescence acquisition was made. The assay was run on a C1000™ Thermal Cycler (BioRad, Hercules, CA). The average C_t (threshold cycle) of fluorescence unit was used to analyze the mRNA levels. The STIM1, STIM2, and Orai1 mRNA

levels were normalized by their corresponding β -actin mRNA levels. Quantification was calculated as follows: mRNA levels = $2^{\Delta C_t}$, where $\Delta C_t = C_{t, \text{STIM1}}$ or $C_{t, \text{STIM2}}$ or $C_{t, \text{orai1}} - C_{t, \text{actin}}$.

Fura-2 fluorescence ratiometry. Measurement of $[Ca^{2+}]_i$ in MCs was performed using fura-2 fluorescence ratiometry as described in (81). Briefly, MCs, grown on a coverslip (22×22 mm), were loaded with 2 μ M acetoxymethyl ester of fura-2 (fura-2/AM) plus 0.018 g/dl Pluronic F-127 (Invitrogen, Grand Island, NY) for 50 min at room temperature followed by additional 20 min incubation in fura-2 free physiological saline solution. The coverslip was then placed in a perfusion chamber (Warner, Model RC-2OH) mounted on the stage of a Nikon Diaphot inverted microscope. Fura-2 fluorescence was monitored at 340 and 380 nm excitation wavelengths and at 510 nm emission wavelength using NIS Elements ARTM software (Nikon Instruments Inc., Melville, NY) at room temperature. $[Ca^{2+}]_i$ was calculated using the software following the manufacturer's instructions. Calibrations were performed at the end of each experiment, and conditions of high $[Ca^{2+}]_i$ were achieved by addition of 5 μ M ionomycin, whereas conditions of low $[Ca^{2+}]_i$ were obtained by addition of 5 mM EGTA.

Electrophysiology. The conventional whole-cell voltage clamp configuration was performed in single human MC cells at room temperature with a Warner PC-505B amplifier (Warner Instrument Corp., Hamden, CT) and Clampex 9.2 (Axon Instrument, Foster City, CA). Glass pipettes (plain, Fisher Scientific) with resistances of 3-5 M Ω were prepared with a pipette puller and polisher (PP-830 and MF-830, respectively, Narishige, Tokyo, Japan). When the whole-cell configuration was achieved, cell capacitance and series resistance were immediately compensated. The whole cell currents were continuously recorded at a holding potential of -80 mV until the end of each experiment (~10-15 min). Current traces were filtered at 1 kHz and analyzed off-line with Clamfit 9.2 (Axon Instrument, Foster City, CA). The compositions of the

pipette solution were (in mM): 140 Cs-aspartate, 6 MgCl₂, 10 BAPTA, 10 EGTA, and 10 HEPES. IP₃ (10 μM) was included in the solution for depleting internal Ca²⁺ stores (33; 44). There were two type of bathing solutions: Ca²⁺ solution and divalent free solution (DVF). The compositions of Ca²⁺ solution were (in mM): 130 NaCl, 5 KCl, 10 CaCl₂, 1 MgCl₂, and 10 HEPES, and the compositions of DVF solution were (in mM): 150 NaCl, 10 Na₂EDTA, and 10 HEPES.

Animals. The study protocol was approved by the University of North Texas Health Science Center Institutional Animal Care and Use Committee. Two rat models of diabetes were used in this study. 1) streptozotocin (STZ)-type I diabetes model: a total of 12 male Sprague-Dawley rats at an age of 8 weeks were purchased from Harlan (Indianapolis, IN). Diabetes (7 rats) was induced by intraperitoneal injection of STZ at 65 mg/kg body weight in sodium citrate buffer (0.01 M, pH 4.5) as we described previously (26; 46). An equivalent amount of sodium citrate buffer alone was used as a vehicle control (5 rats). Blood glucose levels were monitored 24 h later and periodically thereafter (LifeScan One Touch glucometer, Johnson & Johnson, Milpitas, CA) by rat-tailed blood sampling. STZ-injected rats with sustained elevation of blood glucose above 300 mg/dl were designated as diabetic rats. Four STZ-injected diabetic rats were sacrificed at 2 weeks after injection and the remaining 3 were sacrificed at 4 weeks after injection. 2) High fat diet (HFD) plus STZ (HFD/STZ)-type II diabetes model (11; 24; 65; 75): A total of 10 male Sprague-Dawley rats at an age of 6 weeks were evenly and randomly distributed to two groups, one group fed with low fat diet (LFD) which served as controls, and the other group fed with HFD. In LFD, fat, protein, carbohydrates and ethanol represent 10%, 20%, 67% and 1.8% of the total calories while in HFD, fat, protein, carbohydrates and ethanol represent 44%, 20%, 34%, and 1% of the total calories (Research Diets, Brunswick, NJ). In the group of HFD, after 5 weeks

of HFD, the rats were given STZ at 35 mg/kg via the tail vein. Fifteen weeks later when these HFD/STZ rats manifested overt type II diabetic phenotypes (Table 2), all LFD and HFD/STZ rats were sacrificed for biochemical assays.

Isolation of renal cortex and glomeruli, and extracting cortical and glomerular proteins.

The protocol of isolating glomeruli was described in (57) with modifications. Briefly, rats were euthanized and both kidneys were quickly removed. Renal cortex was separated from the other region of kidney using a sharp blade and the cortical tissue was minced using two sharp blades. For STZ-injected rats, glomeruli were isolated by differential sieving of minced renal cortex. Finely chopped kidney cortex in Hank's balanced salt solution (pH 7.4) was pressed through sequentially smaller metal sieves and collected on a final sieve of 63- μ m pore size (mini-sieve set, Scienceware, Pequannock, NJ). Glomeruli were pelleted by centrifugation at 500 g for 10 min at 4°C (Eppendorf, 5810R). We have previously shown that the purity of the glomerulus preparation was ~99% (26). Both cortical tissues and glomeruli were sonicated in a lysis buffer followed by centrifugation at 20817 g for 15 min at 4°C. The supernatants were collected for Western blot.

Materials. Cyclopiazonic acid (CPA) was purchased from Alomone labs (Har Hotzvim Hi-Tech Park, Jerusalem). GSK-7975A was kindly donated by GSK (Stevenage, UK). The rabbit polyclonal anti-STIM1 antibody was purchased from ProteinTech (Chicago, IL). Orai1 antibody was purchased from Abcam (for rat tissues) (Cambridge, MA) and Sigma (for HMCs) (Sigma, ST. Louis, MO). All other chemicals and antibodies were purchased from Sigma-Aldrich (Sigma, ST. Louis, MO) unless indicated in other places.

Statistical Analysis. Data were reported as means \pm SE. The one-way ANOVA plus Student-Newman-Keuls post-hoc analysis and Student unpaired t-test were used to analyze the

differences among multiple groups and between two groups, respectively. $P < 0.05$ was considered statistically significant. Statistical analysis was performed using SigmaStat (Jandel Scientific, San Rafael, CA).

Results

SOCE in HMCs was enhanced by prolonged HG treatment

In HMCs cultured in NG and HG with different time periods, we measured fura-2 fluorescence-indicated Ca^{2+} entry response using a classical “ Ca^{2+} add-back” protocol described in our previous publications (15; 16; 26; 27). CPA was used to activate SOCE. As shown in Figure 1, a Ca^{2+} entry response was observed upon re-addition of 2 mM Ca^{2+} to a Ca^{2+} free bathing solution in both NG and HG cultured MCs. There was no difference in the CPA-induced SOCE between NG and HG treatments for the time periods of 1 day and 3 days (Figure 1 A, B and E). However, this Ca^{2+} entry response was significantly greater in the cells with 7- and 14 day-HG treatments compared to NG treatment for the same time periods (Figure 1 C-E). The augmented response to 7 day HG treatment was completely abolished by GSK-7975A, a selective SOC inhibitor which directly acts on the pore region of SOC (2; 13; 25; 66), verifying the Ca^{2+} entry being mediated by SOC, i.e. SOCE (Figure 1D). Furthermore, in the absence of CPA, readdition of 2 mM Ca^{2+} also produced Ca^{2+} entry in both NG and HG 7 day-treated HMCs (Figure 1F). However, the tonic Ca^{2+} entry responses were much weaker compared to the responses in the presence of CPA (Figure 1 F & C) and did not have a significant difference between NG and HG treatments (Figure 1G). These results suggest that a prolonged HG treatment enhanced SOCE, but did not alter tonic Ca^{2+} entry.

SOC activity in HMCs was promoted by prolonged HG treatment

SOCE is mediated by SOC in the plasma membrane. Since chronic treatment with HG increased SOCE in MCs, we would expect a stimulatory effect on SOC by HG. As expected, whole cell patch clamp experiments showed that the store-operated Ca^{2+} currents were significantly augmented by HG treatment for 7 days, but not for 1 day (Figure 2 A-E). Because SOC is more conductive to monovalent cations over divalent cations (4; 5; 34; 62), we also measured DVF currents in the cells with NG and HG treatments. As shown in Figure 2 A-D and F, the DVF currents were much more robust compared to Ca^{2+} currents, a characteristic of SOC. Consistent with Ca^{2+} current response, the DVF currents were significantly augmented by 7 day, but not 1 day HG treatment (Figure 2A-D and F). Both the Ca^{2+} and DVF current responses to the prolonged HG treatment were significantly inhibited by GSK-7975A (10 μM), but not by DMSO, a vehicle control (Figure 2G). Furthermore, a low concentration of La^{3+} can selectively block SOC (7; 8; 49; 77). We examined how much currents were reduced by La^{3+} (2 μM) as an indication of SOC activity in NG- and HG-treated MCs. As shown in Figure 2H, the La^{3+} -sensitive decrease in DVF current was significantly greater in MCs with 7 day-HG treatment compared to NG treatment for the same time period. There was no significant difference in the La^{3+} response between NG and HG treatments for 1 day.

HG reduced receptor-operated Ca^{2+} entry (ROCE) in HMCs.

In addition to SOC, we and others have demonstrated that receptor operated Ca^{2+} channel (ROC) or canonical transient receptor potential channels (TRPC) also participate in Ca^{2+} signaling in MCs (16; 47; 58; 72). To be distinguished from SOC, ROC is defined as the channel activated by G-protein coupled receptor signaling pathway through a mechanism bypassing the IP_3 -induced internal Ca^{2+} store depletion. It has been debated for ~20 years whether HG-impaired Ca^{2+}

response in MCs was mediated by SOC or ROC (23; 26; 27; 52; 58; 71). To dissect SOCE from receptor-operated Ca^{2+} entry (ROCE) in response to HG treatment, we performed additional Ca^{2+} imaging study in which HMCs with NG or HG treatment for 7 days were incubated with CPA (25 μM) for ~7 min to deplete the internal Ca^{2+} stores (activation of SOC). As described above, SOCE was estimated by the elevation of $[\text{Ca}^{2+}]_i$ upon switching the bathing solution from Ca^{2+} free to 2 mM Ca^{2+} solution. This was followed by addition of Ang II (1 μM) into the bathing solution in the presence of CPA. Since the intracellular Ca^{2+} stores had been depleted by CPA, the additional increase in $[\text{Ca}^{2+}]_i$ by Ang II would be attributed to ROCE. As shown in Figure 3, although SOCE was significantly greater in the MCs with 7 day HG treatment (consistent with Figure 1), ROCE was significantly reduced. The contribution of ROCE to the additional response by Ang II was verified by an inhibitory effect of SKF96365 (an inhibitor of ROC) on the response (Figure 3 C&D). This Ang II-stimulated, SOCE independent Ca^{2+} response was also significantly attenuated by blocking voltage-gated Ca^{2+} channels with diltiazem (31; 49) (Figure 3 C&D). Activation of voltage-gated Ca^{2+} channel has been proposed as one mechanism for ROC-dependent Ca^{2+} response because of membrane depolarization by Na^+ influx through ROC (70; 83). In summary, these results are consistent with the notion that the Ang II-induced Ca^{2+} entry after CPA treatment was mediated by ROC.

HG increased STIM1 protein expression in cultured HMCs

STIM1 has been demonstrated as a key component of SOCE by gating SOC (45; 67). Our previous study has also shown that STIM1 was required for activation of SOCE in HMCs (73). Since HG-promoted SOCE in MCs was a chronic effect (Figs. 1&2), we thought that an increase in abundance of one or more key proteins in the SOCE pathway, such as STIM1, contributed to the HG effect. Thereby, western blots were performed to determine HG effect on STIM1 protein

expression in cultured HMCs. As shown in Figure 4, the expression level of STIM1 was remarkably increased by HG treatment. In agreement with the results from functional studies (Figs. 1 & 2), the HG effect on STIM1 expression was also a chronic process and a minimum of 7 days was required for a significant increase (Figure 4 A & C). We also examined STIM1 response to different concentrations of glucose and showed that a concentration of 10 mM was sufficient to significantly increase STIM1 protein expression (Figure 4 B and D). Although there was a trend of increase in STIM1 protein expression with increases in concentrations of glucose, no significant difference in STIM1 expression levels was observed among different concentrations of glucose in a range of 10 mM to 30 mM (Figure 4 B and D).

HG increased Orai1 protein expression in cultured HMCs

Orai1 is the pore-forming protein of SOC (12; 12; 80). To determine if HG-stimulated SOCE involved upregulation of Orai1 protein expression, western blot was performed in cultured HMCs. Orai1 protein was indicated by the two bands at sizes of ~37 kDa and ~43 kDa (Figure 5 A & B), which was verified by knockdown of Orai1 using siRNA (Figure 5 E & F). Similar to STIM1 response, HG significantly increased Orai1 protein level after ~7 day treatment (Figure 5 A & C) and a concentration of 10 mM was high enough to induce a significant increase (Figure 5 B & D).

To determine if Orai1 contributed to the enhanced SOCE, we examined the effect of knocking down Orai1 using siRNA on the HG-enhanced Ca^{2+} response. As shown in Figure 5G, HG treatment for 7 days significantly increased SOCE and this enhanced response was abolished by Orai1-siRNA, but not by a scramble siRNA.

Diabetes increased abundance of STIM1 and Orai1 proteins in glomeruli and renal cortex.

The *in vitro* effects of HG on expressions of the two key SOCE proteins in cultured MCs were further examined in intact animals. Several rat models of diabetes were used to detect diabetic effect on STIM1 and Orai1 protein expression in glomeruli/cortex, where MCs are located. In STZ type I diabetic rats, the model we have used before (26), the amount of STIM1 protein was dramatically increased in glomeruli from the rats with 4 weeks after STZ injection. Although the glomerular STIM1 protein in the rats with 2 weeks of STZ showed a tendency to increase, this response did not reach a significant level compared to non-diabetic control glomeruli (Figure 6 A & B). The upregulation of STIM1 protein by diabetes was further verified in the renal cortex of the rats with high fat diet followed by STZ treatment (Figure 6 C & D) which is a well established non-genetic type II diabetes model (11; 24; 65; 75). As shown in Table 2, these HFD/STZ rats manifested overt type II diabetic phenotypes characterized with albuminuria, hyperlipidemia, hyperglycemia and hyperinsulinemia.

In agreement with the STIM1 response to diabetes, Orai1 protein expression was also increased in the glomeruli from the rats with 4 weeks of STZ treatment and in the renal cortex of rats with high fat diet followed by STZ injection (Figure 7).

mRNA expression level of STIM1, but not Orai1 was increased by HG in HMCs.

To determine whether the diabetes/HG-associated upregulation of STIM1 and Orai1 in MCs occurred at the transcriptional or post-transcriptional level, we conducted quantitative real time RT-PCR. Total RNA was isolated from MCs treated with 5.6 mM and 25 mM glucose for 1, 3, and 6 days. As shown in Figure 8A, HG treatment for 6 days significantly increased the mRNA expression level of STIM1. The HG effect was specific because STIM2, which is another member of the STIM family and shares protein domain organization and biochemical features

with STIM1 (85), did not change by HG treatment (Figure 8B). Different from STIM1 response, Orai1 mRNA expression level did not increase at all by HG in a time range from 1 day to 6 day treatment (Figure 8C). These data suggest that HG and hyperglycemia in diabetes increased STIM1 protein expression by a positive regulation of STIM1 gene expression, but increased Orai1 protein expression through a post-transcriptional mechanism.

Discussion

HG effect on SOCE in MCs has been debated over 20 years. In an earlier study by Mene, et al., arginine vasopressin-induced Ca^{2+} influx was significantly reduced in rat MCs treated with HG (30 mM) for 5 days (52). Because this vasoconstrictor can release Ca^{2+} from the endoplasmic reticulum via the classical Gq-coupled receptor pathway, the authors speculated that the impaired Ca^{2+} response was due to a suppressed SOCE. However, their further data showing that the HG effect was mediated by protein kinase C, a mechanism bypassing the internal Ca^{2+} store depletion, contradicted with the SOCE mechanism. Several studies from other groups did not support SOCE responsible for HG-induced impairment of Ca^{2+} response (23; 58). For instance, Nutt and O'Neil in a later study demonstrated that it was ROC, but not SOC that was responsible for a reduced Ca^{2+} response to endothelin 1 in rat MCs treated with HG for 5-7 days (58). Their findings are consistent with our recent reports that HG reduced abundance of TRPC6 (26; 27), which is a well known ROC (14). The present study provided Ca^{2+} imaging and electrophysiological evidence that HG enhanced SOCE in HMCs. This conclusion was further supported by biochemical data which showed a significant increase in the expression level of STIM1 and Orai1 proteins, two key components of SOCE pathway (3; 32; 42; 45; 61; 63). Importantly, there is a good time correlation between increases in the two protein expression and

enhancement of SOCE in response to HG, suggesting a STIM1/Orai1 dependent mechanism for HG-promoted SOCE in MCs.

Like in many other studies (23; 52; 53; 58), HG-induced impairment of Ca²⁺ signaling in MCs is a chronic process in a range from 2 days to 7 days. In our case, a significant increase in SOCE and protein expression levels of STIM1/Orai1 occurred 7 days after HG treatment. The prolonged response indicates multiple intracellular processes involved. Apparently, further exploration of the intermediators linking HG with SOCE would be important for delineating the molecular mechanisms for HG-promoted SOCE. Interestingly, our study suggests that the mechanism for HG-induced STIM1 response is different from the mechanism mediating Orai1 response. STIM1 response was apparently attributed to elevated transcriptional activity, as indicated by a significant increase in mRNA expression level by HG treatment. Although the present study did not determine how HG activated STIM1 gene transcription, multiple transcription factors, such as NF- κ B and activated protein 1 (AP-1) which have been known to play a critical role in the development of DN (6; 28; 30; 36; 56; 82), are speculated to be downstream molecules of the HG signaling pathway. Particularly, NF- κ B has been reported to promote *stim1* transcription by binding to its promoter region (17). Different from STIM1, Orai1 response to HG may be through a post-transcription mechanism because HG treatment did not change the steady state level of Orai1 mRNA. Although the exact underlying mechanism is unknown from the present study, a ubiquitination and lysosomal degradation of Orai1 has been reported recently (41).

The pathological relevance of HG-regulated STIM1/Orai1 protein expressions was indicated by an increase in abundance of the two proteins in the renal glomeruli or cortex of both type I and II diabetic rats. While the pathogenesis of diabetes is different in type I and type II

diabetes, the natural history of DN is similar. Thus, it is not surprising that the STIM1/Orai1 proteins had a consistent change in both type I and II diabetic rats. MCs play a critical role in the development of DN in both early and late stages of diabetes (37; 38; 40; 88). A question raised from the *ex vivo* study is whether the increases in STIM1/Orai1 proteins were derived from MC response. Although contributions from other cell types, such as podocytes, endothelial cells, and tubular epithelial cells (in renal cortex), can't be ruled out, MCs constitute one third of the glomerular cell population (54) and thereby, the changes in STIM1/Orai1 protein expression in MCs are expected to be detectable at the tissue levels. Another question from the animal experiments is whether the increased STIM1/Orai1 proteins in diabetic kidneys were due to hyperglycemia. Indeed, hyperglycemia is the main determinant of initiation and progression of diabetic microvascular complications including nephropathy (29; 76). *In vitro* and *in vivo* studies have demonstrated that HG or hyperglycemia directly stimulates MCs, which subsequently results in mesangial dysfunction or malfunction (40; 51; 52; 58; 84). Combined with the data from cultured MCs and the fact that all diabetic rats used in the present study were hyperglycemic, we reason that the elevated cellular glucose level contributed, at least partially if not fully, to the STIM1/Orai1 response.

In addition to kidney, a recent study reported that STIM1/Orai1 protein expression levels were also upregulated in platelets isolated from patients with type II diabetes mellitus (86), suggesting that diabetes may have a general effect on SOCE.

What is the physiological and pathological relevance of the enhancement of SOCE in diabetic MCs? Ca^{2+} signaling in MCs involves multiple Ca^{2+} channels, each of which may have a specified downstream pathway and thus, have distinct functional consequences (47). For instance, our previous study demonstrated that among 4 subtypes of TRPC channels

endogenously expressed in mesangial cells, HG/diabetes either did not alter (TRPC1, 3, and 4) or decreased (TRPC6) the abundance of TRPC proteins (26). The downregulation of TRPC6 impairs contractile function of MCs by attenuating agonist-stimulated Ca^{2+} response, which may contribute to hyperfiltration at the early stage of diabetes (26). Different from TRPC channels (likely function as ROC)-mediated Ca^{2+} entry, SOCE is more related to sustained and chronic changes in cell function, such as gene transcription, cell proliferation, and apoptosis (59). Recently, SOCE was found to contribute to cardiac hypertrophy (35; 79) and STIM1-regulated Ca^{2+} homeostasis is crucial for smooth muscle cell proliferation, development, and growth response to injury (50). In contrast, SOCE constraints tuberous sclerosis complex-related tumor development in mice (60). Thus, the effect of SOCE on cell growth and protein synthesis may depend on cell types and downstream signaling pathways. Although the importance of SOCE in renal function and renal disease development has not been examined in the present study, it is certainly noteworthy to address this issue in near future.

In summary, our findings from the present study imply that HG/diabetes enhanced SOCE in MCs by increasing STIM1/Orai1 protein expressions. HG upregulates STIM1 by promoting its transcription, but increases Orai1 protein through a post-transcriptional mechanism.

Acknowledgements

We thank GlaxoSmithKline (GSK, Stevenage, UK) for providing GSK-7975A compound.

Grants

The work was supported by National Institutes of Health (NIH/NIDDK) Grant RO1 (5RO1DK079968-01, to R. Ma) and by Grant-in-Aid (11GRNT7560013) from American Heart Association Southwestern Affiliate (to R. Ma).

Table 1. Primers used for real-time PCR

Gene Name	Primer (5'-3')	GeneBank Accession Number
STIM1	F: ACAGGGACTGTGCTGAAGATGACA R: ACCAGCATGAAGTCCTTGAGGTGA	NM_003156.2
STIM2	F: CAACACACACCACACTCCTT R: GCCTCTTCCTCCTTCATTTTC	NM_001169117.1
Orai1	F: CAGAGCATGGAGGGAAGAGGATTT R: ACCTGGAGCTGGAAGAACAGGAAA	NM_032790.2

F: forward primer; R: reverse primer

Table 2. Diabetic parameters in LFD and HFD rats

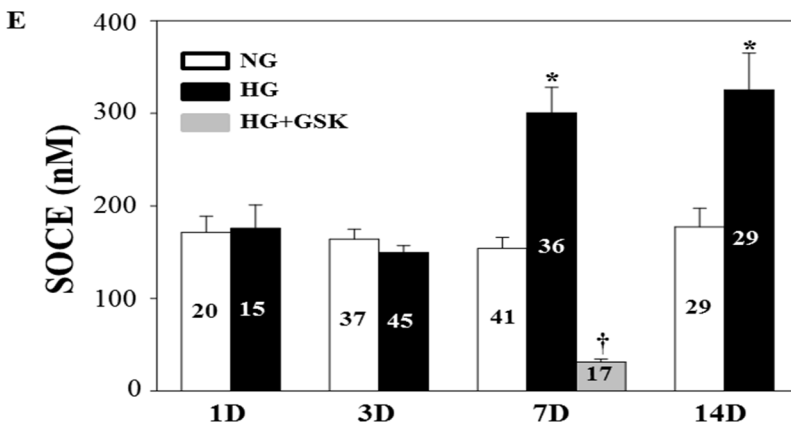
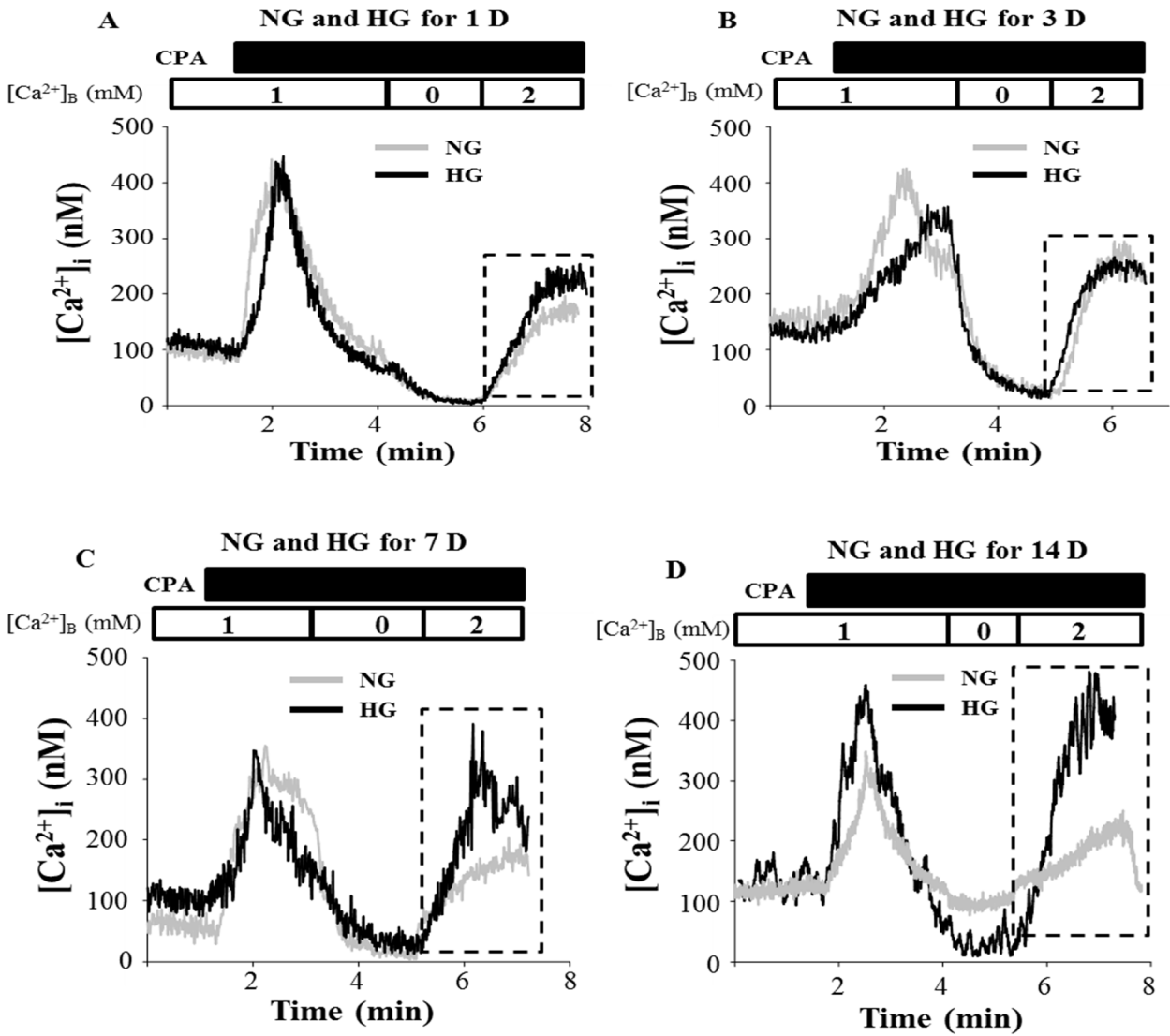
Index	LFD	HFD
Albumin/creatinine ratio ($\mu\text{g}:\text{mg}$)	508 \pm 137	4522 \pm 697**
Blood glucose (mg/dl)	85 \pm 2	350 \pm 15**
Body weight (g)	484 \pm 14	440 \pm 13
Urine output (ml/100 g BW/24 h)	1.4 \pm 0.1	36.9 \pm 2.7**
Serum insulin (ng/ml)	0.04 \pm 0.01	0.84 \pm 0.01**
Triglyceride (mg/dl)	61 \pm 7	333 \pm 31**
Cholesterol (mg/dl)	105 \pm 4	289 \pm 64**

N= 5 for each group. ** denotes $P < 0.01$, HFD vs. LFD (student t-test).

Figure 1. HG effect on SOCE in HMCs.

Fura-2 fluorescence ratiometry was used to assess the intracellular Ca^{2+} concentration ($[\text{Ca}^{2+}]_i$). HMCs were initially bathed in physiological saline solution (containing 1 mM Ca^{2+}). After $[\text{Ca}^{2+}]_i$ was stable (~2 min), 25 μM CPA was applied to the bath to deplete the internal Ca^{2+} stores, indicated by the first transient. When the CPA-induced initial Ca^{2+} spike declined steadily, the bathing solution was replaced with a Ca^{2+} free solution in the presence of CPA, which was followed by readdition of 2 mM Ca^{2+} solution containing CPA. SOCE was estimated by the increase in $[\text{Ca}^{2+}]_i$ upon switching the bathing solution from Ca^{2+} free to 2 mM Ca^{2+} solution, indicated by a dashed rectangle. **A-D:** Representative traces, showing CPA (25 μM)-evoked Ca^{2+} response in HMCs with NG and HG treatment for 1, 3, 7, and 14 days. $[\text{Ca}^{2+}]_B$ represents the Ca^{2+} concentration in the bathing solution. **E:** Summary data, showing time course effect of HG on SOCE in HMCs. * denotes $P < 0.05$, compared to NG at the same time period; † denotes $P < 0.05$, compared to HG for 7 days. The numbers inside bars indicate the number of cells analyzed in each group. GSK: GSK-A7975. **F:** Representative traces, showing Ca^{2+} response to readdition of Ca^{2+} , in the absence of CPA, in HMCs with NG and HG treatment for 7 days. **G:** Summary data from the experiments shown in Figure 1F. “n” indicates the number of cells analyzed in each group.

Figure 1



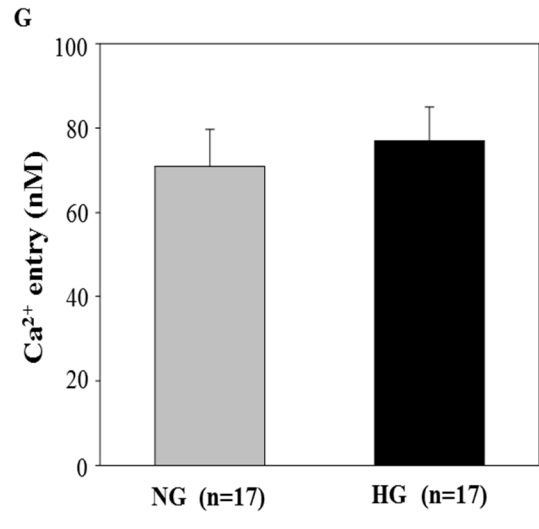
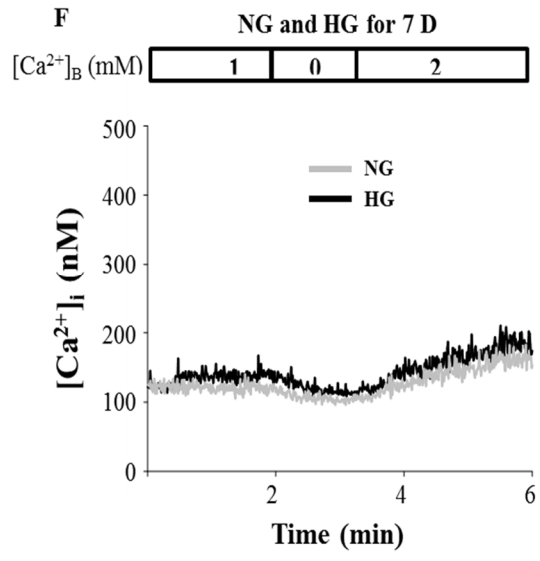


Figure 2. HG effect on SOC currents in HMCs

Whole cell currents in response to depletion of intracellular Ca^{2+} stores in HMCs with NG and HG treatment for 1 day and 7 days. The whole-cell current was recorded at a holding potential of -80mV . **A-D**: representative traces. Arrows indicate the membrane breaking-in. The horizontal bars indicate the type of the bathing solutions (Ca^{2+} or DVF solution) and the time of application of La^{3+} . **E-G**: Store depletion-induced membrane currents in Ca^{2+} solution (E) and DVF solution (F), and blockade of the currents by GSK-7975A ($10\ \mu\text{M}$) in HMCs with 7 day HG treatment (G). The response was calculated by the difference between the basal membrane current (before breaking-in) and the peak current after breaking-in. **H** shows the membrane currents reduced by $2\ \mu\text{M}\ \text{La}^{3+}$ in DVF solution. * indicates $P < 0.05$. The numbers under each bar represent the number of cells analyzed in each group.

Figure 2.

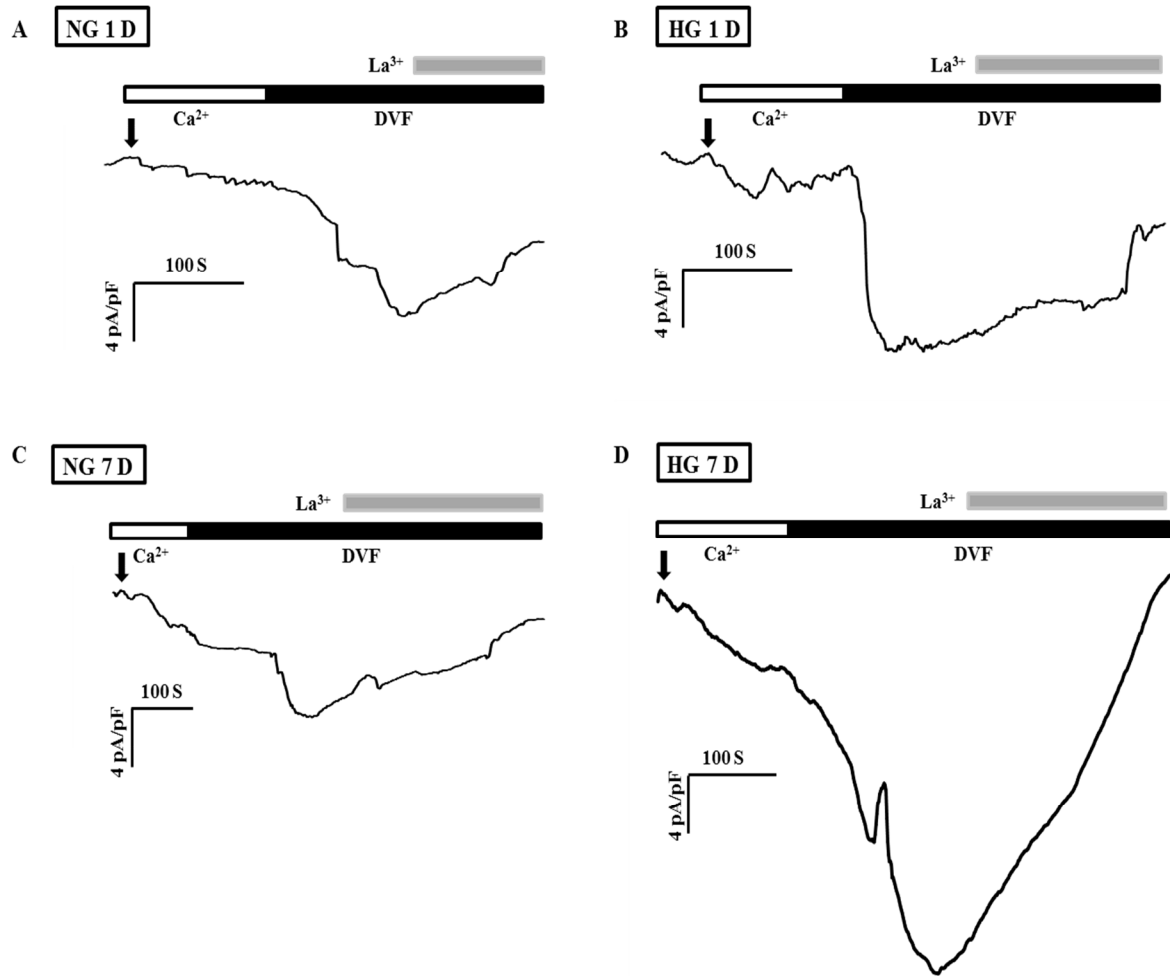


Figure 2.

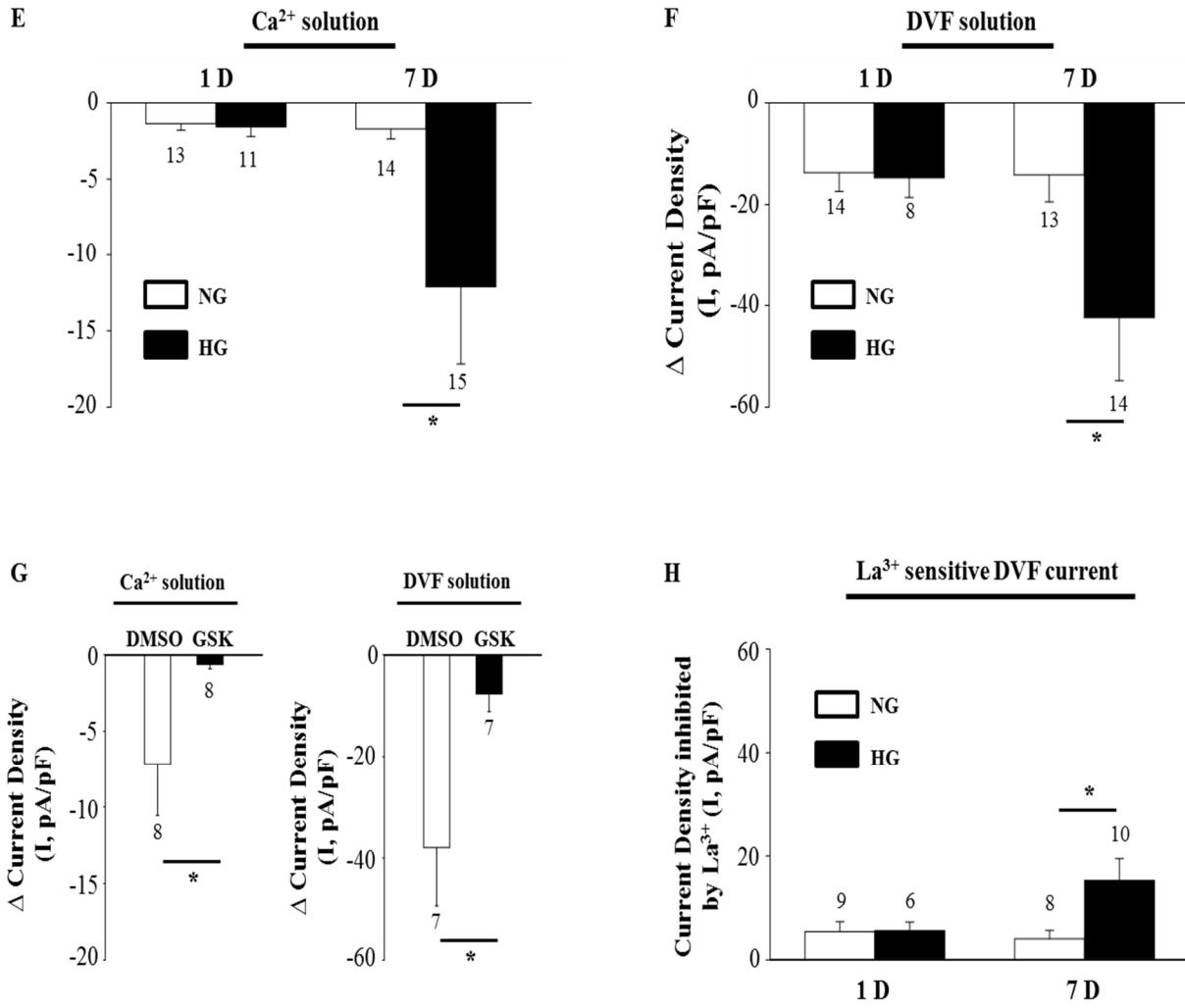


Figure 3. HG effect on ROCE in HMCs.

Fura-2 fluorescence ratiometry, showing SOCE and ROCE in HMCs with NG or HG treatment for 7 days. MCs were treated with 25 μM CPA for ~ 7 min to deplete the internal Ca^{2+} stores. SOCE was estimated by the elevation of $[\text{Ca}^{2+}]_i$ upon switching the bathing solution from Ca^{2+} free to 2 mM Ca^{2+} solution in the presence of CPA. ROCE was defined as the additional increase in $[\text{Ca}^{2+}]_i$ by adding Ang II (1 μM) in the presence of CPA. **A-C:** Representative traces, recorded ~ 4 min after CPA application. $[\text{Ca}^{2+}]_B$ represents the Ca^{2+} concentration in the bathing solution. Application of Ang II with and without diltiazem (Dil) or SKF96365 (SKF) is indicated by an arrow in graph. Traces were smoothed using the Sigmaplot software (version 11.0). **D:** Summary data averaged from groups of NG with Ang II treatment (n=29), HG with Ang II treatment (n=18), NG with Ang II+Dil treatment (n=16), and NG with Ang+SKF treatment (n=15). * denotes $P < 0.05$, compared to SOCE in NG group; † denotes $P < 0.01$, compared to ROCE in NG group.

Figure 3.

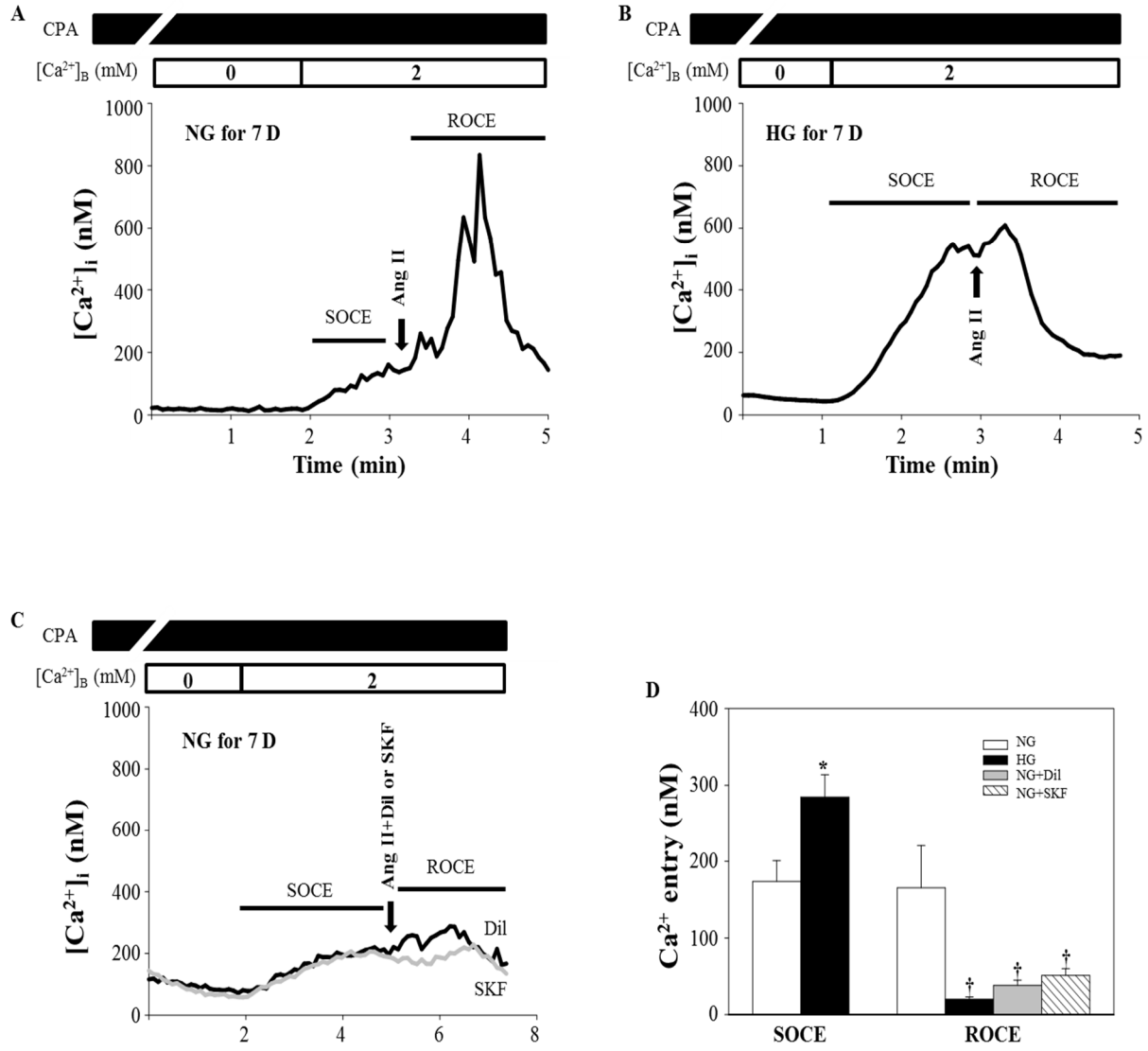


Figure 4. HG effect on STIM1 protein expression in HMCs.

A: HMCs were cultured in 0.5% FBS NG media for 3 days or in 0.5% FBS HG media for different time periods. **B:** HMCs were cultured in 0.5% FBS media with different concentration of D-glucose for 7 days. Appropriate concentrations of α -Mannitol were used as the osmotic control. **C and D:** Summary data showing the time course and dose dependent of HG effect on STIM1 protein expression. In C, ** indicates $P < 0.01$ and * indicates $P < 0.05$, NG vs. HG for the same time period. “n” indicates the number of independent western blot. In D, * indicates $P \leq 0.05$, vs. 5.6 mM glucose.

Figure 4.

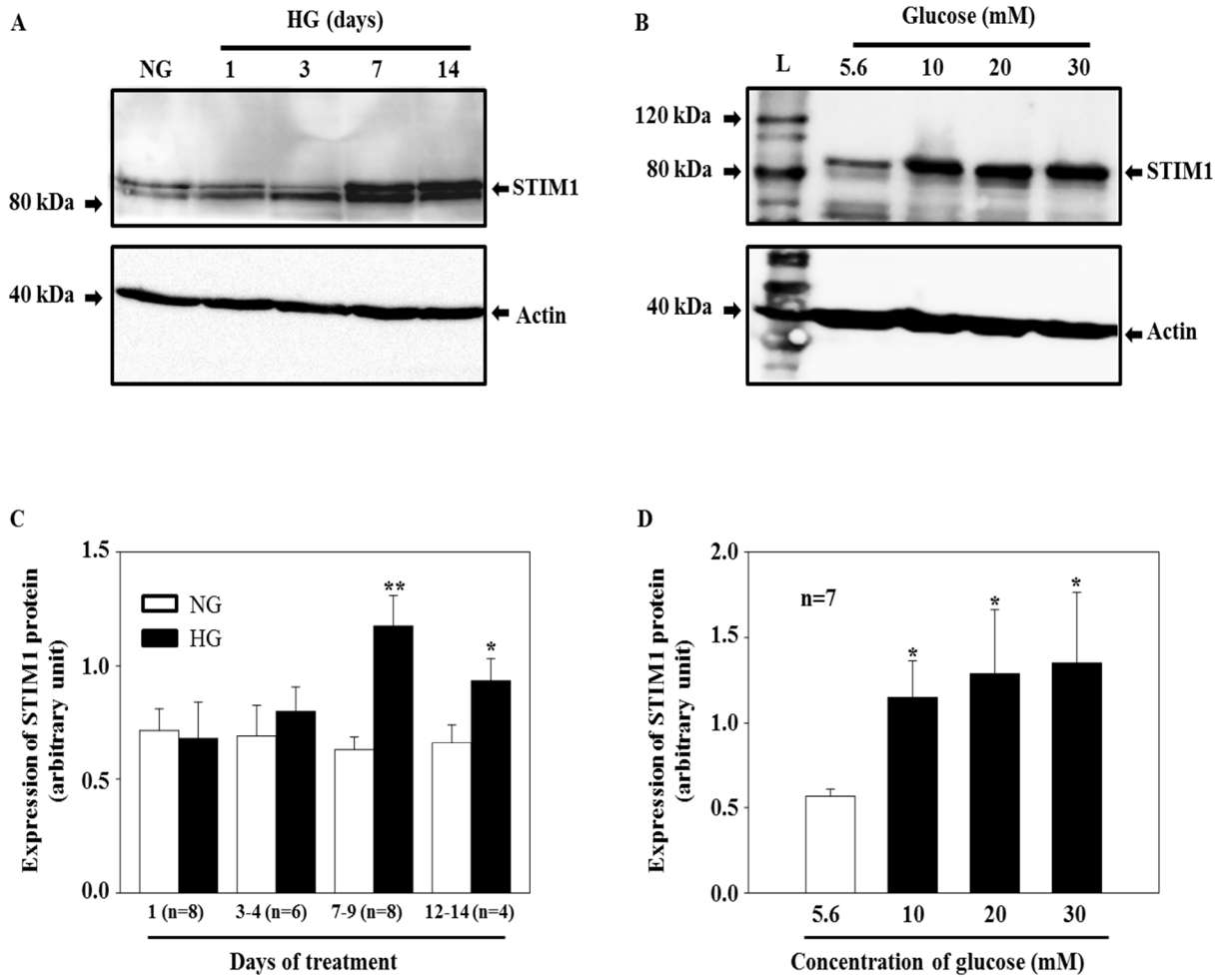


Figure 5. HG effect on Orai1 protein expression in HMCs.

A: HMCs were cultured in 0.5% FBS NG or HG media for different time periods. **B:** HMCs were cultured in 0.5% FBS media with different concentrations of D-glucose for 7 days. Appropriate concentrations of α -Mannitol were used as the osmotic control. In both A and B, orai1 is shown as two bands, a lower band at ~35 kDa and a upper band at ~42 kDa. Actin was used as a loading control. **C and D:** Summary data from experiments presented in A and B, respectively. In C, * indicates $P < 0.05$, NG vs. HG for the same time period. “n” indicates the number of independent western blot. In D, * indicates $P \leq 0.05$, vs. 5.6 mM glucose. **E:** Orai1 protein expression in HMCs with and without transfection of siRNA against human Orai1 (Orai1-siRNA) or scramble siRNA (Scramble). UT: untransfected MCs; L: a protein ladder. Actin was used as a loading control. **F:** Summary data from experiments presented in E. “n” indicates the number of independent experiments. † denotes $P < 0.05$, compared to both groups of Scramble and Orai1-siRNA. **G:** Fura-2 fluorescence ratiometry, showing SOCE in HMCs with NG or HG treatment for 7 days with transfection of scramble siRNA or Orai1-siRNA. Transfections were conducted on day 4 of HG treatment and the Ca^{2+} imaging experiments were performed 3 days of continuous HG treatment after transfection. * denotes $P < 0.05$, compared to NG, and † denotes $P < 0.05$, compared to both groups of HG and HG + Scramble. n indicates the number of cells analyzed in each group.

Figure 5.

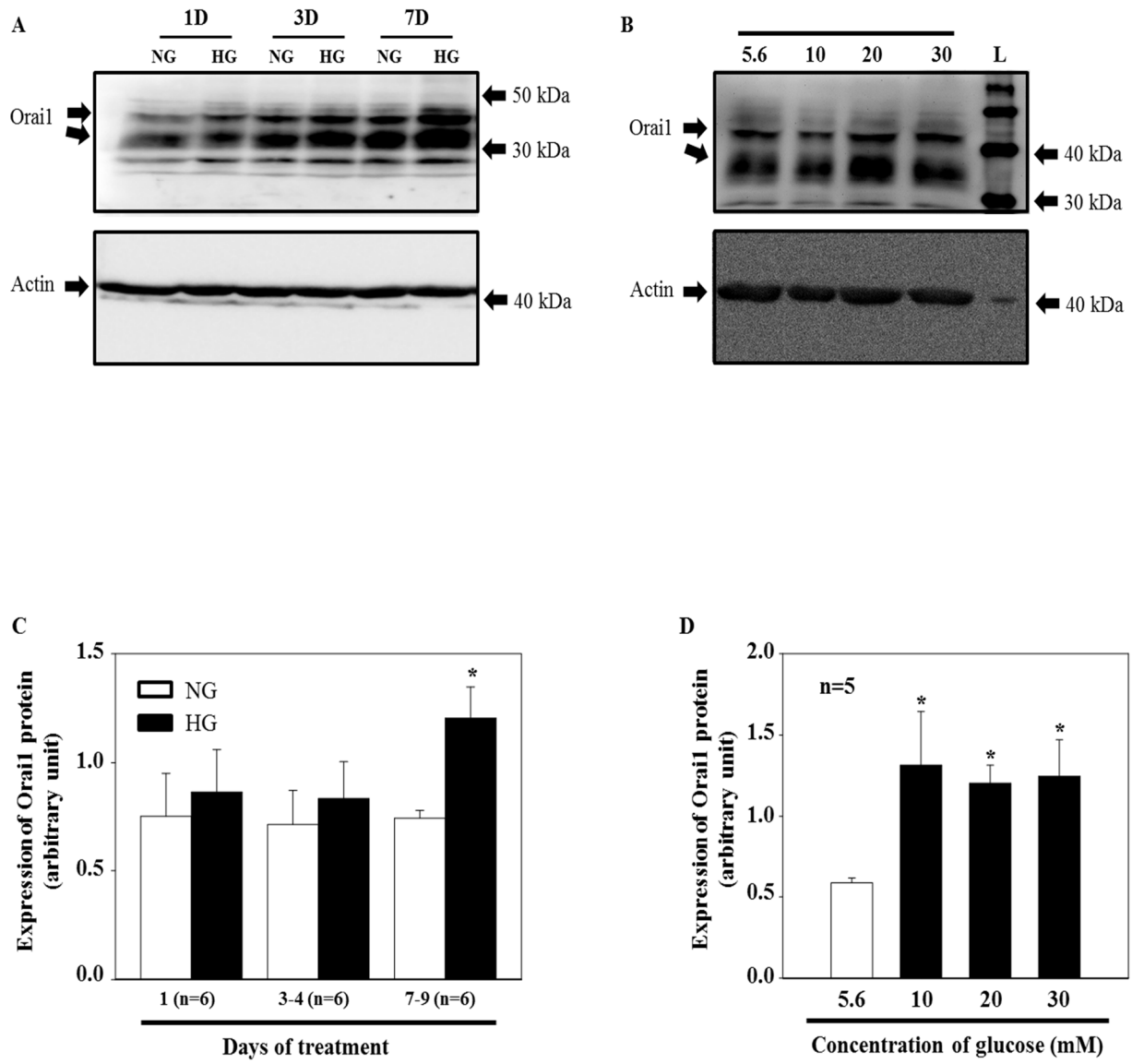


Figure 5.

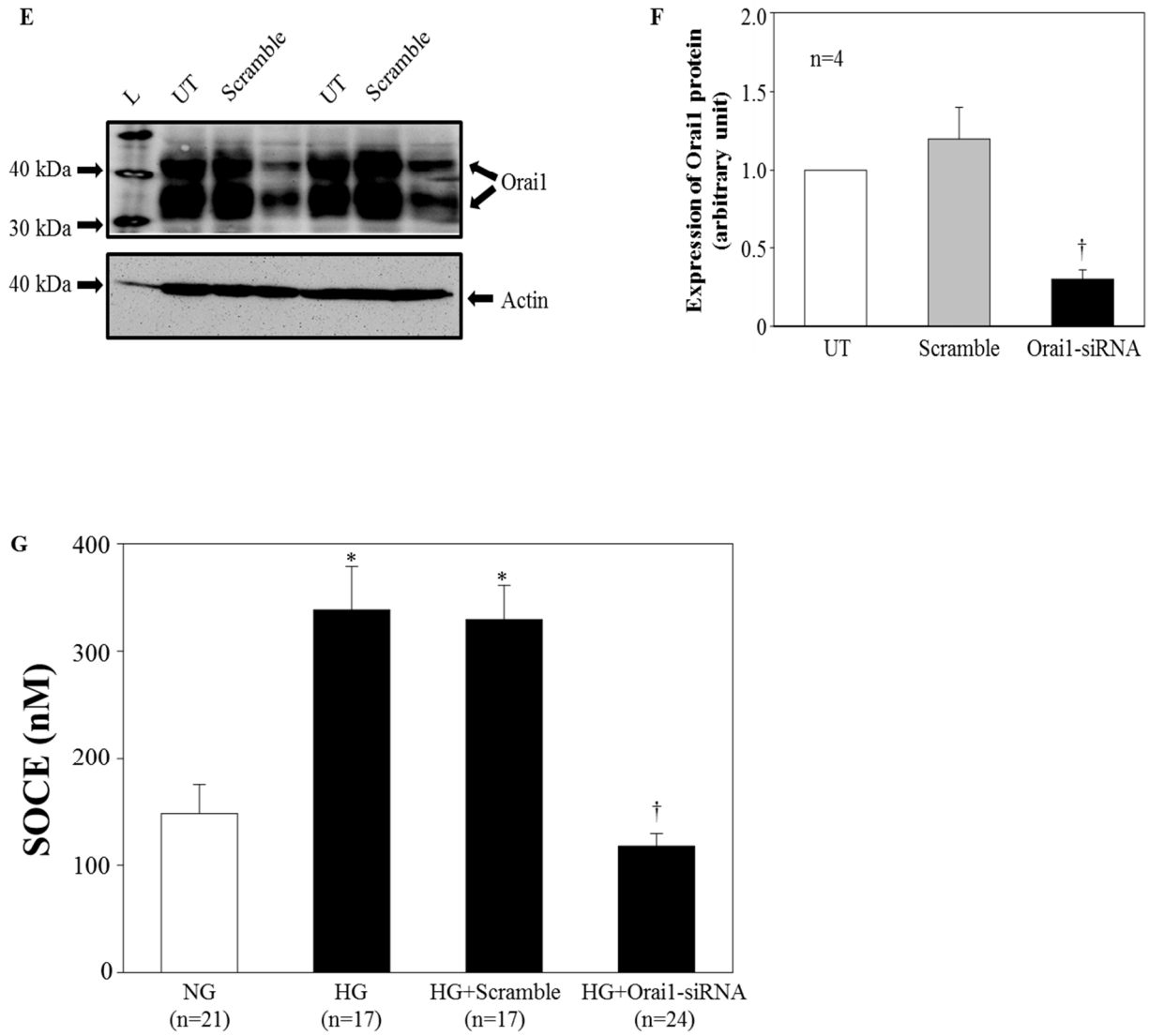


Figure 6. Effect of diabetes on STIM1 protein expression in rat kidney.

Western blot, showing STIM1 protein expression in extracts of glomeruli freshly isolated from rats with 2 weeks and 4 weeks after STZ injection (STZ-2W and STZ-4W, respectively) and with 4 weeks after vehicle injection (control) (A & B), and of renal cortex of LFD and HFD rats (C & D). In A and C, actin was used as a loading control. B and D are summary data from the experiments presented in A and C, respectively. * indicates $P < 0.05$, compared to control in B and LFD in D.

Figure 6.

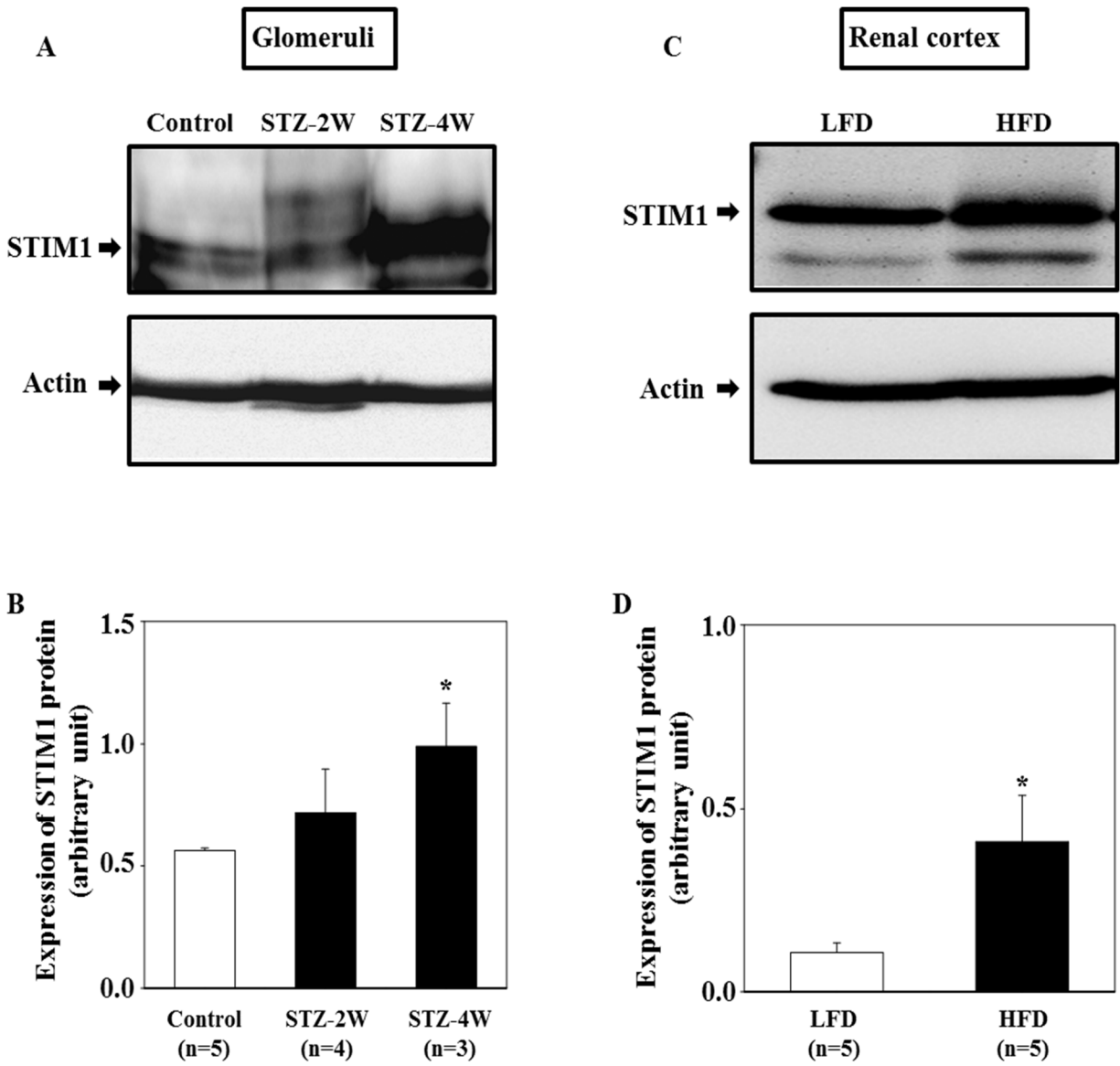


Figure 7. Effect of diabetes on Orai1 protein expression in rat kidney.

Western blot, showing Orai1 protein expression in extracts of glomeruli freshly isolated from rats with 4 weeks after STZ injection (STZ-4W) and with 4 weeks after vehicle injection (control) (A & B) and of renal cortex of LFD and HFD rats (C & D). In A and C, β -integrin and Tubulin were used as loading controls, respectively. B and D are summary data from the experiments presented in A and C, respectively. ** indicates $P < 0.01$, compared to control in B and LFD in D.

Figure 7.

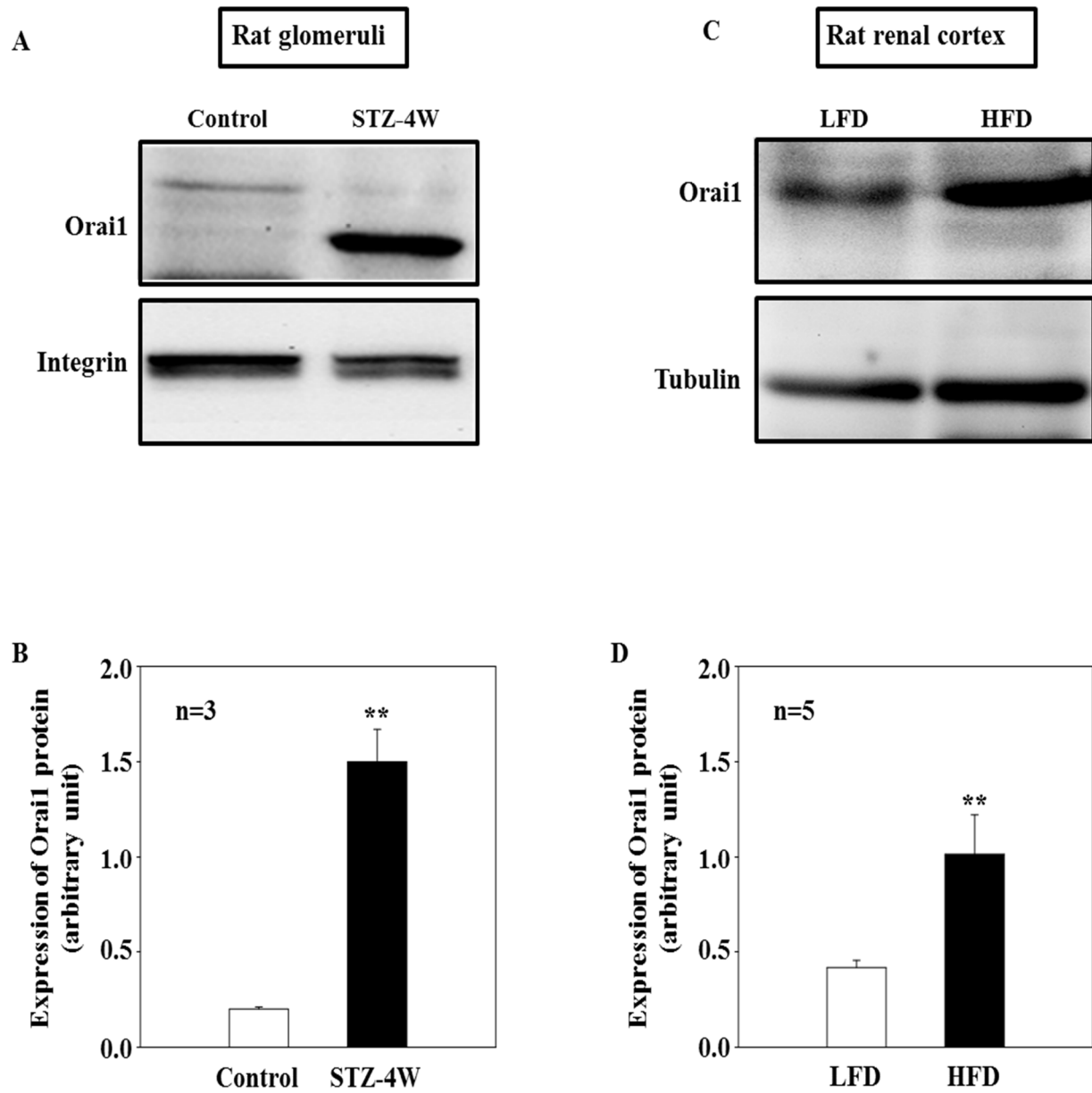
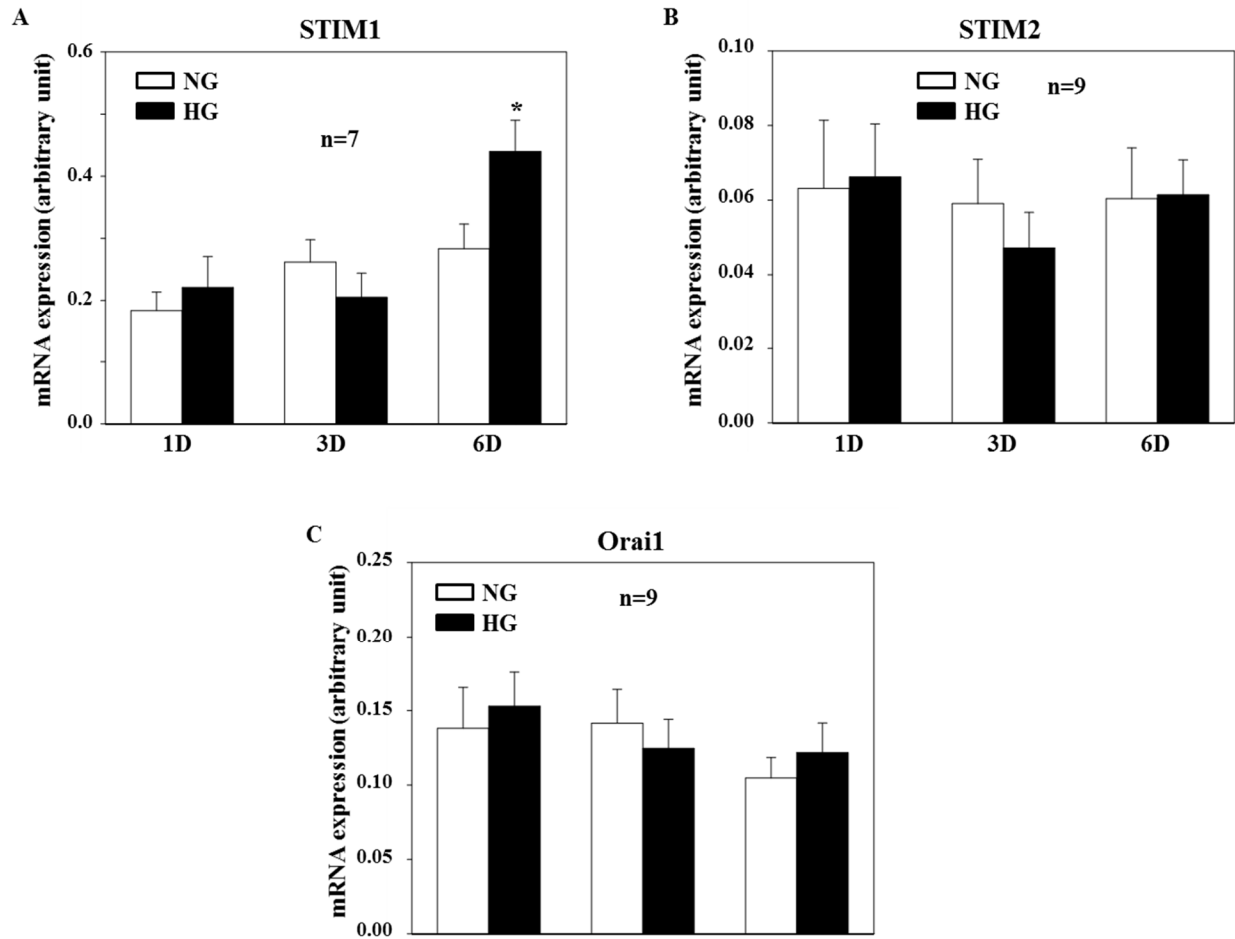


Figure 8. Quantitative real time RT-PCR, showing HG effect on STIM1, STIM2, and Orai1 mRNA expressions in HMCs.

HMCs were cultured in 0.5% FBS NG or HG media for different days. “D” indicates days of treatment. “*” in A denotes $P < 0.05$, HG vs. NG for 6 D treatment.

Figure 8.



Abbreviations

Ang II: angiotensin II

CPA: cyclopiazonic acid

ER: endoplasmic reticulum

HFD: high fat diet

HG: high glucose

HMCs: human mesangial cells

LFD: low fat diet

MCs: mesangial cells

NF- κ B: nuclear factor- κ B

ROC: receptor operated channels

ROCE: receptor operated Ca^{2+} entry

SOC: store-operated channels

SOCE: store operated calcium entry

STZ: streptozotocin

TRPC: canonical transient receptor potential channels

References

1. Abboud HE. Mesangial cell biology. *Exp Cell Res* 318: 979-985, 2012.
2. Ashmole I, Duffy SM, Leyland ML, Morrison VS, Begg M and Bradding P. CRACM/Orai ion channel expression and function in human lung mast cells. *J Allergy Clin Immunol* 129: 1628-1635, 2012.
3. Baba Y, Hayashi K, Fujii Y, Mizushima A, Watarai H, Wakamori M, Numaga T, Mori Y, Lino M, Hikida M and Kurosaki T. Coupling of STIM1 to store-operated Ca^{2+} entry through its constitutive and inducible movement in the endoplasmic reticulum. *PNAS* 103: 16704-16709, 2006.
4. Bakowski D and Parekh AB. Monovalent cation permeability and Ca^{2+} block of the store-operated calcium current I_{CRAC} in rat basophilic leukaemia cells. *Pflügers Arch* 443: 892-902, 2002.
5. Bakowski D and Parekh AB. Permeation through store-operated CRAC channels in divalent-free solution: potential problems and implications for putative CRAC channel genes. *Cell Calcium* 32: 379-391, 2002.
6. Banday AA, Fazili FR and Lokhandwala MF. Oxidative stress causes renal dopamine D1 receptor dysfunction and hypertension via mechanisms that involve nuclear factor- κB and protein kinase C. *J Am Soc Nephrol* 18: 1446-1457, 2007.
7. Bird GS, Dehaven WI, Smyth JT and Putney Jr JW. Methods for studying store-operated calcium entry. *Methods* 46: 204-212, 2008.
8. Broad LM, Cannon TR and Taylor CW. A non-capacitive pathway activated by arachidonic acid is the major Ca^{2+} entry mechanism in rat A7r5 smooth muscle cells stimulated with low concentrations of vasopressin. *J Physiol (Lond)* 517: 121-134, 1999.

9. Campos AH, Calixto JB and Schor N. Bradykinin induces a calcium-store-dependent calcium influx in mouse mesangial cells. *Nephron* 91: 308-315, 2002.
10. Che Q and Carmines PK. Src family kinase involvement in rat preglomerular microvascular contractile and $[Ca^{2+}]_i$ responses to Ang II. *Am J Physiol Renal Physiol* 288: F658-F664, 2005.
11. Danda RS, Habiba NM, Rincon-Choles H, Bhandari BK, Barnes JL, Abboud HE and Pergola PE. Kidney involvement in a nongenetic rat model of type 2 diabetes. *Kidney Int* 68: 2562-2571, 2005.
12. Deng X, Wang Y, Zhou Y, Soboloff J and Gill DL. STIM and Orai-dynamic intermembrane coupling to control cellular calcium signals. *J Biol Chem* 284: 22501-22505, 2009.
13. Derler I, Schindl R, Fritsch R, Heftberger P, Riedl MC, Begg M, House D and Romanin C. The action of selective CRAC channel blockers is affected by the Orai pore geometry. *Cell Calcium* 53: 139-151, 2013.
14. Dietrich A and Gudermann T. TRPC6. *Handb Exp Pharmacol* 179: 125-141, 2007.
15. Du J, Ding M, Sours-Brothers S, Graham S and Ma R. Mediation of angiotensin II-induced Ca^{2+} signaling by polycystin 2 in glomerular mesangial cells. *Am J Physiol* 294: F909-F918, 2008.
16. Du J, Sours-Brothers S, Coleman R, Ding M, Graham S, Kong D and Ma R. Canonical transient receptor potential 1 channel is involved in contractile function of glomerular mesangial cells. *J Am Soc Nephrol* 18: 1437-1445, 2007.
17. Eylenstein A, Schmidt S, Gu S, Yang W, Schmid E, Schmidt EM, Alesutan I, Szteyn K, Regel I, Shumilina E and Lang F. Transcription factor NF- κ B regulates the expressions of a

pore-forming unit, Orai1, and its activator, STIM1, to control Ca^{2+} entry and affect cellular functions. *J Biol Chem* 287: 2719-2730, 2012.

18. Fallet RW, Ikenaga H, Bast JP and Carmines PK. Relative contributions of Ca^{2+} mobilization and influx in renal arteriolar contractile responses to arginine vasopressin. *Am J Physiol Renal Physiol* 288: F545-F551, 2005.

19. Fellner S and Arendshorst WJ. Angiotensin II-stimulated calcium entry mechanism in afferent arterioles: role of transient receptor potential canonical channels and reverse $\text{Na}^+/\text{Ca}^{2+}$ exchange. *Am J Physiol Renal Physiol* 294: F212-F219, 2008.

20. Fellner SK and Arendshorst WJ. Angiotensin II Ca^{2+} signaling in rat afferent arteriols: stimulation of cyclic ADP ribose and IP3 pathways. *Am J Physiol Renal Physiol* 288: F785-F791, 2005.

21. Fellner SK and Arendshort WJ. Store-operated Ca^{2+} entry is exaggerated in fresh preglomerular vascular smooth muscle cells of SHR. *Kidney Int* 61: 2132-2141, 2002.

22. Feske S, Gwack Y, Prakriya M, Srikanth S, Puppel SH, Tanasa B, Hogan PG, Lewis RS, Daly M and Rao A. A mutation in Orai1 causes immune deficiency by abrogating CRAC channel function. *Nature* 441: 179-185, 2006.

23. Frecker H, Munk S, Wang H and Whiteside C. Mesangial cell reduced Ca^{2+} signaling in high glucose is due to inactivation of phospholipase C- β_3 by protein kinase C. *Am J Physiol Renal Physiol* 289: F1078-F1087, 2005.

24. Gaikwad AB, Gupta J and Tikoo K. Epigenetic changes and alteration of *Fbn1* and *Col3A1* gene expression under hyperglycaemic and hyperinsulinaemic conditions. *Biochem J* 432: 333-341, 2010.

25. Gerasimenko JV, Gryshchenko O, Ferdek PE, Stapleton E, Hebert TO, Bychkova S, Peng S, Begg M, Gerasimenko OV and Petersen OH. Ca^{2+} release-activated Ca^{2+} channel blockade as a potential tool in antipancreatitis therapy. *PNAS* 110: 13186-13191, 2013.
26. Graham S, Ding M, Sours-Brothers S, Yorio T, Ma JX and Ma R. Downregulation of TRPC6 protein expression by high glucose, a possible mechanism for the impaired Ca^{2+} signaling in glomerular mesangial cells. *Am J Physiol Renal Physiol* 293: F1381-F1390, 2007.
27. Graham S, Gorin Y, Abboud HE, Ding M, Lee DY, Shi H, Ding Y and Ma R. Abundance of TRPC6 protein in glomerular mesangial cells is decreased by ROS and PKC in diabetes. *Am J Physiol Cell Physiol* 301: C304-C315, 2011.
28. Gruden G, Setti G, Hayward A, Sugden D, Duggan S, Burt D, Buckingham RE, Gnudi L and Viberti G. Mechanical stretch induces monocyte chemoattractant activity via an NF-kappaB-dependent monocyte chemoattractant protein-1-mediated pathway in human mesangial cells: inhibition by rosiglitazone. *J Am Soc Nephrol* 16: 688-696, 2005.
29. Ha H, Yu M and Kim KH. Melatonin and taurine reduce early glomerulopathy in diabetic rats. *Free Radical Biol Med* 26: 944-950, 1999.
30. Ha H, Yu MR, Choi YJ, Kitamura M and Lee HB. Role of high glucose-induced nuclear factor- κ B activation in monocyte chemoattractant protein-1 expression by mesangial cells. *J Am Soc Nephrol* 13: 894-902, 2002.
31. Hall D, Carmines PK and Sansom SC. Dihydropyridine-sensitive Ca^{2+} channels in human glomerular mesangial cells. *Am J Physiol (Renal Physiol)* 278: F97-F103, 2000.
32. Hewavitharana T, Deng X, Soboloff J and Gill DL. Role of STIM and Orai proteins in the store-operated calcium signaling pathway. *Cell Calcium* 42: 173-182, 2007.

33. Hoth M and Penner R. Depletion of intracellular calcium stores activates a calcium current in mast cells. *Nature* 355: 353-356, 1992.
34. Hoth M and Penner R. Calcium release-activated calcium current in rat mast cells. *J Physiol (Lond)* 465: 359-386, 1993.
35. Hulot JS, Fauconnier J, Ramanujam D, Chaanine A, Aubart F, Sassi Y, Merkle S, Cazorla O, Ouillé A, Dupuis M, Hadri L, Jeong D, Mühlstedt S, Schmitt J, Braun A, Bénard L, Saliba Y, Laggerbauer B, Nieswandt B, Lacampagne A, Hajjar RJ, Lompré AM and Engelhardt S. Critical role for stromal interactionmolecule 1 in cardiac hypertrophy. *Circulation* 124: 796-805, 2011.
36. Iwamoto M, Mizuiri S, Arita M and Hemmi H. Nuclear factor- κ B activation in diabetic rat kidney: evidence for involvement of P-selectin in diabetic nephropathy. *Tohoku J Exp Med* 206: 163-171, 2005.
37. Kanwar YS, Akagi S, Sun L, Nayak B, Xie P, Wada J, Chugh SS and Danesh FR. Cell biology of diabetic kidney disease. *Nephron Exp Nephrol* 101: e100-e110, 2005.
38. Kanwar YS, Wada J, Sun L, Xie P, Wallner EI, Chen S, Chugh S and Danesh FR. Diabetic nephropathy: mechanisms of renal disease progression. *Exp Biol Med* 233: 4-11, 2008.
39. Kashgarian M and Sterzel RB. The pathobiology of the mesangium. *Kidney Int* 41: 524-529, 1992.
40. Kikkawa R, Kitamura E, Fujiwara Y, Arimura T, Haneda M and Shigeta Y. Impaired contractile responsiveness of diabetic glomeruli to angiotensin II: a possible indication of mesangial dysfunction in diabetes mellitus. *Biochem Biophys Res Commun* 136: 1185-1190, 1986.

41. Lee JE, Jeon IS, Han NE, Song HJ, Kim EG, Choi JW, Song KD, Lee HK and Choi JK. Ubiquilin 1 interacts with Orai1 to regulate calcium mobilization. *Mol Cells* 35: 41-46, 2013.
42. Lewis RS. The molecular choreography of a store-operated calcium channel. *Nature* 446: 284-287, 2007.
43. Li WP, Tsiokas L, Sansom SC and Ma R. Epidermal growth factor activates store-operated Ca^{2+} channels through an IP_3 independent pathway in human glomerular mesangial cells. *J Biol Chem* 279: 4570-4577, 2004.
44. Liao Y, Erxleben C, Abramowitz J, Flockerzi V, Zhu MX, Armstrong DL and Birnbaumer L. Functional interactions among orai1, TRPCs, and STIM1 suggest a STIM-regulated heteromeric Orai/TRPC model for SOCE/Icrac channels. *PNAS* 105: 2895-2900, 2008.
45. Liou J, Kim ML, Heo WD, Jones JT, Myers JW, Ferrell JE and Meyer T. STIM is a Ca^{2+} store sensor essential for Ca^{2+} -store-depletion-triggered Ca^{2+} influx. *Current Biol* 15: 1235-1241, 2005.
46. Luan JJ, Li W, Han J, Zhang W, Gong W and Ma R. Renal protection of in vivo administration of tempol in streptozotocin-induced diabetic rats. *J Pharmacol Scien* 119: 167-176, 2012.
47. Ma R, Pluznick JL and Sansom SC. Ion channels in mesangial cells: function, malfunction, or fiction. *Physiology* 20: 102-111, 2005.
48. Ma R and Sansom SC. Epidermal growth factor activates store-operated calcium channels in human glomerular mesangial cells. *J Am Soc Nephrol* 12: 47-53, 2001.
49. Ma R, Smith S, Child A, Carmines PK and Sansom SC. Store-operated Ca^{2+} channels in human glomerular mesangial cells. *Am J Physiol* 278: F954-F961, 2000.

50. Mancarella S, Potireddy S, Wang Y, Gao H, Gandhirajan RK, Autieri M, Scalia R, Cheng Z, Wang H, madesh M, Houser SR and Gill DL. Targeted STIM deletion impairs calcium homeostasis, NFAT activation, and growth of smooth muscle. *FASEB J* 27: 893-906, 2013.
51. Menè P, Pascale C, Teti A, Bernardini SV, Cinotti GA and Pugliese F. Effects of advanced glycation end products on cytosolic Ca²⁺ signaling of cultured human mesangial cells. *J Am Soc Nephrol* 10: 1478-1486, 1999.
52. Mené P, Pugliese G, Pricci F, DiMario U, Cinotti GA and Pugliese F. High glucose level inhibits capacitative Ca²⁺ influx in cultured rat mesangial cells by a protein kinase C-dependent mechanism. *Diabetologia* 40: 521-527, 1997.
53. Mené P, Pugliese G, Pricci F, Dimaro V, Cinotti GA and Pugliese F. High glucose inhibits cytosolic calcium signaling in cultured rat mesangial cells. *Kidney Int* 43: 585-591, 1993.
54. Menè P, Simonson MS and Dunn MJ. Physiology of mesangial cell. *Physiol Rev* 69: 1347-1424, 1989.
55. Menè P, Teti A, Pugliese F and Cinotti GA. Calcium release-activated calcium influx in cultured human mesangial cells. *Kidney Int* 46: 122-128, 1994.
56. Mezzano S, Aros C, Droguett A, Burgos ME, Ardiles L, Flores C, Schneider H, Ruiz-Ortega M and Egidio J. NF-κB activation and overexpression of regulated gene in human diabetic nephropathy. *Nephrol Dial Transplant* 19: 2505-2512, 2004.
57. Misra RP. Isolation of glomeruli from mammalian kidneys by graded sieving. *Am J Clin Pathol* 58: 135-139, 1972.
58. Nutt LK and O'Neil RG. Effect of elevated glucose on endothelin-induced store-operated and non-store-operated calcium influx in renal mesangial cells. *J Am Soc Nephrol* 11: 1225-1235, 2000.

59. Parekh AB and Putney Jr. JW. Store-operated calcium channels. *Physiol Rev* 85: 757-810, 2005.
60. Peng H, Liu J, Chen R, Wang Y, Duan J, Li C, Li B, Jing Y, Chen X, Mao Q, Xu KF, Walker CL, Li J, Wang J and Zhang H. mTORC1 enhancement of STIM1-mediated store-operated Ca^{2+} entry constrains tuberous sclerosis complex-related tumor development. *Oncogene* 32: 4702-4711, 2013.
61. Prakriya M, Feske S, Gwack Y, Srikanth S, Rao A and Hogan PG. Orail1 is an essential pore subunit of the CRAC channel. *Nature* 443: 230-233, 2006.
62. Prakriya M and Lewis RS. Separation and characterization of currents through store-operated CRAC channels and Mg^{2+} -inhibited cation (MIC) channels. *J Gen Physiol* 119: 487-508, 2002.
63. Putney Jr JW. Recent breakthroughs in the molecular mechanism of capacitative calcium entry (with thoughts on how we got here). *Cell Calcium* 42: 103-110, 2007.
64. Putney Jr JW. A model for receptor-regulated calcium entry. *Cell Calcium* 7: 1-12, 1986.
65. Reed MJ, Meszaros K, Entes LJ, Claypool MD, Pinkett JG and Reaven GM. A new rat model of type 2 diabetes: the fat-fed, streptozotocin-treated rat. *Metabolism* 49: 1390-1394, 2000.
66. Rice LV, Bax HJ, Russell LJ, Barrett VJ, Walton SE, Deakin AM, Thomson SA, Lucas F, Solari R, Hous D and Begg M. Characterization of selective calcium-release activated calcium channel blockers in mast cells and T-cells from human, rat, mouse and guinea-pig preparations. *Eur J Pharmacol* 704: 49-57, 2013.

67. Roos J, DiGregorio PJ, Yeromin AV, Ohlsen K, Lioudyno M, Zhang S, Safrina O, Kozak JA, Wagner SL, Cahalan MD, Velicelebi G and Stauderman KA. STIM1, an essential and conserved component of store-operated Ca^{2+} channel function. *J Cell Biol* 169: 435-445, 2005.
68. Schlöndorff D and Bana B. The mesangial cell revisited: no cell is an island. *J Am Soc Nephrol* 20: 1179-1187, 2009.
69. Scindia YM, Deshmukh US and Bagavant H. Mesangial pathology in glomerular disease: targets for therapeutic intervention. *Adv Drug Deliv Rev* 62: 1337-1343, 2010.
70. Soboloff J, Spassova M, Xu W, He LP, Cuesta N and Gill DL. Role of endogenous TRPC6 channels in Ca^{2+} signal generation in A7r5 smooth muscle cells. *J Biol Chem* 280: 39786-39794, 2005.
71. Song JH, Jung SY, Hong SB, Kim MJ and Suh CK. Effects of high glucose on basal intracellular calcium regulation in rat mesangial cell. *Am J Nephrol* 23: 343-352, 2003.
72. Sours S, Du J, Chu S, Zhou JX, Ding M and Ma R. Expression of canonical transient receptor potential (TRPC) proteins in human glomerular mesangial cells. *Am J Physiol Renal Physiol* 290: F1507-F1515, 2006.
73. Sours-brothers S, Ding M, Graham S and Ma R. Interaction between TRPC1/TRPC4 assembly and STIM1 contributes to store-operated Ca^{2+} entry in mesangial cells. *Exp Biol Med* 234: 673-682, 2009.
74. Stockand JD and Sansom SC. Glomerular mesangial cells: electrophysiology and regulation of contraction. *Physiol Rev* 78: 723-744, 1998.
75. Sugano M, Yamato H, Hayashi T, Ochiai H, Kakuchi J, Goto S, Nishijima F, Lino N, Kazama JJ, Takeuchi T, Mokuda O, Ishikawa T and Okazaki R. High-fat diet in low-dose-streptozotocin-treated heminephrectomized rats induces all features of human type 2 diabetic

nephropathy: a new rat model of diabetic nephropathy. *Nutrition Met Cardiovas Dis* 16: 477-484, 2006.

76. The Diabetes Control and Complications Trial Research Group. The effect of intensive treatment of diabetes on the development and progression of long-term complications in insulin-dependent diabetes mellitus. *N Engl J Med* 329: 977-986, 1993.

77. Trebak M, Bird GSJ, McKay RR and Putney Jr JW. Comparison of human TRPC3 channels in receptor-activated and store-operated modes. Differential sensitivity to channel blockers suggests fundamental differences in channel composition. *J Biol Chem* 277: 21617-21623, 2002.

78. Vig M, Peinelt C, Beck A, Koomoa DL, Rabah D, Koblan-Huberson M, Kraft S, Turner H, Fleig A, Penner R and Kinoshita JP. CRACM1 is a plasma membrane protein essential for store-operated Ca^{2+} entry. *Science* 312: 1220-1223, 2006.

79. Voelkers M, Salz M, Herzog N, Frank D, Dolatabadi N, Frey N, Gude N, Friedrich O, Koch WJ, Katus HA, Sussman MA and Most P. Orai1 and Stim1 regulate normal and hypertrophic growth in cardiomyocytes. *J Mol Cell Cardiol* 48: 1329-1334, 2010.

80. Wang Y, Deng X and Gill DL. Calcium signaling by STIM and Orai: intimate coupling details revealed. *Sci Signal* 3: pe42-1-pe42-4, 2010.

81. Wang Y, Ding M, Chaudhari S, Ding Y, Yuan J, Stankowska D, He S, Krishnamoorthy R, Cunningham JT and Ma R. Nuclear factor κ B mediates suppression of canonical transient receptor potential 6 expression by reactive oxygen species and protein kinase C in kidney cells. *J Biol Chem* 288: 12852-12865, 2013.

82. Weigert C, Sauer U, Brodbeck K, Pfeiffer A, Häring HU and Schleicher ED. AP-1 proteins mediate hyperglycemia-induced activation of the human TGF- β 1 promoter in mesangial cells. *J Am Soc Nephrol* 11: 2007-2016, 2000.
83. Welsh DG, Morielli AD, Nelson MT and Brayden JE. Transient receptor potential channels regulate myogenic tone of resistance arteries. *Cir Res* 90: 248-250, 2002.
84. Whiteside CI, Hurst RD and Stevanovic ZS. Calcium signaling and contractile response of diabetic glomerular mesangial cells. *Kidney Int* 48: S28-S33, 1995.
85. Williams RT, Manji SSM, Parker NJ, Hancock MS, van Stekelenburg L, Eid JP, Senior PV, Kazenwadel J, Shandala T, Saint R and Smith PJ. Identification and characterization of the STIM (stromal interaction molecule) gene family: coding for a novel class of transmembrane proteins. *Biochem J* 357: 673-685, 2001.
86. Zbidi H, Lopez JJ, Amor NB, Bartegi A, Salido GM and Rosado JA. Enhanced expression of STIM1/Orai1 and TRPC3 in platelets from patients with type 2 diabetes mellitus. *Blood Cells Mol Dis* 43: 211-213, 2009.
87. Zhang SL, Yeromin AV, Zhang XHF, Yu Y, Safrina O, Penna A, Roos J, Stauderman KA and Cahalan MD. Genome-wide RNAi screen of Ca²⁺ influx identifies genes that regulate Ca²⁺ release-activated Ca²⁺ channel activity. *PNAS* 103: 9357-9362, 2006.
88. Ziyadeh FN and Sharma K. Role of transforming growth factor- β in diabetic glomerulosclerosis and renal hypertrophy. *Kidney Int* 48: S34-S36, 1995.

CHAPTER III

STORE-OPERATED CA^{2+} CHANNELS IN MESANGIAL CELLS INHIBIT MATRIX PROTEIN EXPRESSION

Peiwen Wu, Yanxia Wang, Mark E. Davis, Jonathan E. Zuckerman, Sarika Chaudhari,
Malcolm Begg and Rong Ma

Journal of The American Society of Nephrology,26:2691–2702,2015.

doi: 10.1681/ASN.2014090853

Excerpts for this Chapter are taken from the published manuscript as in Appendix.

Abstract

Accumulation of extracellular matrix derived from glomerular mesangial cells (MCs) is an early feature of diabetic nephropathy. Ca^{2+} signals mediated by store-operated Ca^{2+} channel (SOC) can regulate protein production in a variety of cell types. The aim of the present study is to determine the effect of SOC in MCs on extracellular matrix protein expression using both *in vitro* and *in vivo* settings. In cultured human MCs (HMCs), activation of SOC by thapsigargin significantly decreased fibronectin protein expression, but inhibition of SOC by 2-APB significantly increased both fibronectin and collagen IV expressions. Knockdown of calcium release-activated calcium channel protein 1 (Orai1) increased fibronectin protein expression. Moreover, thapsigargin abrogated high glucose-induced fibronectin and collagen IV expressions. Consistent with the *in vitro* findings, *in vivo* knockdown of Orai1, the pore-forming unit of SOC, specifically in MCs of mice using a targeted nanoparticle siRNA delivery system resulted in an increase in glomerular fibronectin and collagen IV expressions. Consistently, the mice treated with nanoparticles carrying siRNA against Orai1 showed significant mesangial expansion. These results suggest that SOC in MCs negatively regulates extracellular matrix protein expression in kidney, which may serve as an endogenous renoprotective mechanism in diabetes.

Keywords: extracellular matrix, mesangial cells, SOC, Orai1

Introduction

Diabetic nephropathy (DN) is the most common cause of the end stage renal disease (1,2). One of early features of DN includes accumulation of extracellular matrix (ECM) proteins in glomerular mesangium (3,4). This pathological change in glomerulus may, with time, progress to glomerulosclerosis and ultimately to irreversible end stage renal disease (5,6). Over production of ECM, including fibronectin and collagen IV (Col IV) by glomerular mesangial cells (MCs) and deposition of these proteins to mesangium is an important contributor to mesangial expansion in the early stage of DN (7-9). Therefore, suppression of ECM production in MCs may be a therapeutic option to protect kidney from diabetic damages.

Mesangial cells sit between glomerular capillary loops and maintain the structural architecture of the capillary networks. These cells play important roles in mesangial matrix homeostasis, regulation of glomerular filtration rate and phagocytosis of apoptotic cells in the glomerulus (7,10,11). MC dysfunction is closely associated with several kidney diseases, including DN (12,13). Like many other cell types, MC function is controlled by intracellular Ca^{2+} signals (11,14). In this regard, store-operated Ca^{2+} channel (SOC) plays a pivotal role in many physiological processes in MCs (14). SOC is activated upon depletion of the endoplasmic reticulum (ER) in response to activation of G protein coupled receptors (15). Two proteins, STIM1 (16,17) and Orai1 (18-20), have been identified as required components of the SOC pathway. STIM1 is located in the ER membrane and functions as an ER Ca^{2+} sensor, while Orai1 is located in the plasma membrane and functions as a Ca^{2+} channel (21,22). Over past decades, we and others have demonstrated that SOC mediates MC Ca^{2+} responses to a variety of circulating and locally produced hormones, such as angiotensin II (Ang II) (23-27). We have also demonstrated that STIM1 was required for activation of SOC in MCs (28). Recently, we found

that store operated calcium entry (SOCE) was enhanced in human MCs (HMCs) with prolonged high glucose treatment (29). Consistently, abundance of both STIM1 and Orai1 proteins was significantly increased in MCs with chronic high glucose treatment, and in the glomerulus/renal cortex of rats with diabetes (29). However, the role of SOC in MCs in the development of DN is completely unknown. In the present study, we used both *in vitro* and *in vivo* systems and tested a hypothesis that SOC in MCs regulated ECM protein expression.

Materials and Methods

Animals. All procedures were approved by University of North Texas Health Science Center (UNTHSC) Institutional Animal Care and Use Committee. A total of 10 male C57BL/6 mice were used in this study. All mice were between 2 and 4 months of age. Mice were purchased from Charles River (Wilmington, MA). All animals were maintained at the animal facility of UNTHSC under local and National Institutes of Health guidelines.

In vivo delivery of nanoparticles into the kidney of mice. The targeted NP-delivery system was used to deliver siRNA against Orai1 to the kidney of mice. Mice were randomly divided into control and Orai1-knocked down groups (3 mice each group). The mice in Orai1-knocked down group were given NPs containing Cy3-tagged siRNA against mouse Orai1 (NP-Cy3-siOrai1) via tail vein injection at a dose of 10mg/kg siRNA in ~100 μ l injection volume. The mice in control group were only given NPs (NP-Con) through the same route in the same injection volume. Mice on both groups received the iv injection on day 1 and 3 of experiment, and were euthanized on day 5 for kidney harvesting.

siRNA-CDP-NP formulation. siRNA NPs were formed by using cyclodextrin-containing polycations (CDP) and adamantine-polyethylene glycol (AD-PEG) as previously described (pre-

complexation) (80). NPs were formed in 5 % glucose in deionized water (D5W) at a charge ratio of 3 +/- and a siRNA concentration of 2 mg/ml. The Cy3 labeled siRNA oligos targeting mouse *Orai1* were purchased from Integrated DNA Technologies, Inc. (Chicago, IL). The sense strand sequence is 5'-/5Cy3/GGGUUGCUCUCAUCGUCUUUAGUGC-3'.

Immunohistochemistry. Mice were euthanized by intraperitoneal injection of pentobarbital (100 mg/kg body weight) at indicated time points. After washing out blood with phosphate buffer saline (PBS), the left kidneys were removed and fixed in 4 % paraformaldehyde in PBS overnight. Formalin-fixed organs were dehydrated and embedded in molten paraffin to generate sections of 4- μ m in thickness (Cryostat 2800 Frigocut-E, Leica Instruments). Anti-OX 7 mouse monoclonal antibody at 1:100 and Alexa Fluor 488 (for mice) or 568 (for rats) goat anti-mouse IgG (Invitrogen, Grand Island, NY) at 1:200 were used to label glomerular MCs. Sections were examined using an Olympus microscope (BX41) equipped for epifluorescence and an Olympus DP70 digital camera with DP manager software (version 2.2.1). Images were converted to 16-bit format and uniformly adjusted for brightness and contrast using Image J (version 1.47, NIH). Semi-quantification of colocalizations of NP-Cy3-si*Orai1* with MC marker or podocyte marker (Figure 5D) was examined using BioimageXD software.

Assessment of mesangial area. Four- μ m paraffin-embedded kidney sections were stained with Periodic Acid-Schiff (PAS) (Sigma-Aldrich, St. Louis, MO). Images were captured using an Olympus DP70 digital camera with DP manager software (version 2.2.1) and traced using Image J software (v. 1.47, NIH). Mesangial area was defined as PAS-positive and nuclei-free area in the mesangium, and expressed as a ratio to a total glomerular area.

Extraction of renal cortical proteins. Right kidneys were removed from mice immediately after euthanization. Renal cortex was separated from the other region of kidney using a sharp

blade and the cortical tissue was minced using two sharp blades. The cortical tissues were sonicated in a lysis buffer followed by centrifugation at 20817 g for 15 min at 4°C. The supernatants were collected for immunoblots.

Cell culture and transfection. HMCs were purchased from Lonza (Walkersville, MD). Cells were cultured in DMEM medium (Gibco, Carlsbad, CA) supplemented with 25 mM HEPES, 4 mM glutamine, 1.0 mM sodium pyruvate, 0.1 mM nonessential amino acids, 100 U/ml penicillin, 100 µg/ml streptomycin and 20% FBS. Cells less than 10 generations were used in the present study.

All transfections in the present study were transient transfection using LipofectAmine and Plus reagent (Invitrogen-BRL, Carlsbad, CA) following the protocols provided by the manufacturer. Experiments were conducted ~48 hours after transfection.

Immunoblots. Whole cell lysates or renal cortical extracts were fractionated by 10% SDS-PAGE, transferred to PVDF membranes, and probed with primary fibronectin, Col IV, β -actin, α -tubulin, STIM1, and Orail antibodies. Bound antibodies were visualized with Super Signal West Pico or Femto Luminol/Enhancer Solution (Thermo Scientific, Rockford, IL). The specific protein bands were visualized and captured using an AlphaEase FC Imaging System (Alpha Innotech, San Leandro, CA). The Integrated Density Value (IDV) of each band was measured by drawing a rectangle outlining the band using AlphaEase FC software with auto background subtraction. The expression levels of targeted proteins were quantified by normalization of the IDVs of those protein bands to that of actin or tubulin band on the same blot.

Materials. Thapsigargin (TG), 2-aminoethyl diphenylborinate (2-APB), rabbit polyclonal anti-fibronectin and α -tubulin antibodies, methanol, and DMSO were purchased from Sigma-Aldrich (Sigma, ST. Louis, MO). GSK-7975A was kindly donated by GlaxoSmithKline (Brentford, UK).

Anti-Orai1 and anti-CD90/Thy1 (MRC OX-7) antibodies were purchased from Abcam (Cambridge, MA). Mouse monoclonal anti-Col IV antibody was purchased from Meridian Life Science, Inc. (Memphis, TN).

Statistical Analysis Data were reported as means \pm SE. The one-way ANOVA plus Student-Newman-Keuls post-hoc analysis and Student unpaired t-test were used to analyze the differences among multiple groups and between two groups, respectively, unless indicated in individual figure legends. $P < 0.05$ was considered statistically significant. Statistical analysis was performed using SigmaStat (Jandel Scientific, San Rafael, CA).

Results

SOC suppressed ECM protein expression in HMCs.

Treatment of cultured HMCs with 1 μ M TG, a classical and widely used activator of SOC (15), for 2 days significantly reduced fibronectin protein content (Figure 1 A&D). This inhibitory effect was abolished by GSK-7975A, a selective SOC inhibitor (30-33). Consistently, inhibition of SOC with 50 μ M 2-APB, but not its vehicle control (methanol) significantly increased fibronectin protein expression (Figure 1 B&E). The 2-APB response was also observed for Col IV, another matrix protein (Figure 1 C&F). These data suggest that SOC negatively regulates ECM protein expression in HMCs.

Knockdown of Orai1 increased fibronectin expression in HMCs.

Knocking down of orai1 the pore forming unit of SOC, using previously characterized synthetic siRNA (29) significantly increased fibronectin content (Figure 2, A and B) This data further support an inhibitory effect of SOC on ECM protein expression.

Activation of SOC inhibited high glucose-induced ECM protein content in MCs.

High glucose is a pathogenic stimulator for ECM expression during the progress of DN (5,9,30-33). We examined if activation of SOC could inhibit high glucose-induced fibrotic response. As shown in Figure 3, high glucose significantly increased content of both fibronectin and Col IV proteins. The high glucose responses were significantly abolished by TG, but not by its vehicle. Furthermore, TG treatment reduced fibronectin and Col IV contents to a level lower than that in untreated-MCs (NG in Figure 3) even though it did not attain statistical significance. These data suggest a beneficial role of SOC in diabetic kidney.

***In vivo* knock down of Orai1 in MCs increased ECM protein expression in renal cortex and glomerulus, and induced mesangial expansion in mice.**

Orai1 is the pore-forming unit of SOC (21,22). Our recent study demonstrated that knocking down Orai1 using siRNA nearly eliminated SOC-mediated Ca^{2+} influx in cultured MCs (29). We speculated that we could inhibit SOC function in MCs *in vivo* by delivery of siRNAs against Orai1 to intact animals. We have previously shown specific delivery of ~75 nm PEGylated gold nanoparticles (NP) into MCs in mouse kidney (34). We have also previously demonstrated that ~75 nm cyclodextrin-containing NP carrying siRNA (siRNA-CDP-NPs) accumulate in the glomerulus (35) and that these siRNA-CDP-NPs can be used for the selective delivery of functional siRNA to mouse MC *in vivo* (36). In the present study, we formulated the siRNA-CDP-NPs with Cy3-tagged siRNA against mouse Orai1 (NP-Cy3-siOrai1) and injected these siRNA-CDP-NPs into mice via the tail vein. Consistent with our previous reports (34), the siRNA-CDP-NP complexes were accumulated in glomeruli with scarce distribution in other

regions (Figure 4A). Immunoblot of renal cortex extracts verified the efficiency of knocking down *Orai1* (Figure 4B). To confirm delivery of siRNA-CDP-NPs to the MCs, we counterstained kidney sections from mice that received Cy3-siRNA containing NP with the MC marker thymic antigen 1 (*Thy1*) using the OX-7 antibody and with podocyte marker synaptopodin protein using anti-synaptopodin antibody. We found persistent Cy3-siRNA fluorescent signal after administration of the siRNA-CDP-NPs that highly co-localized with the OX-7, but not with synaptopodin antibody staining (Figure 4C). Semi-quantitative co-localization analysis revealed 85% OX-7 staining co-localization with Cy3-fluorescence and 90% co-localization of Cy3-siRNA fluorescence with OX-7 staining (Figure 4D). However, both values of co-localization of Cy3-siRNA fluorescence with synaptopodin staining were minimal (Figure 4D). These data show that siRNA-CDP-NPs were predominantly deposited in glomerular MCs.

We conducted biochemical, immunohistochemical and histological examinations to assess the changes in glomerular ECM protein expression and mesangial expansion in the mice with and without knockdown of *Orai1*. As expected, abundance of fibronectin protein in renal cortex was significantly increased in the mice treated with siRNA-CDP-NPs carrying Cy3-si*Orai1* (Figure 5A&B). Consistently, further immunohistochemical examinations showed remarkable increases in both fibronectin and Col IV staining in the glomeruli of mice receiving siRNA-CDP-NPs (Figure 5 C&D). In agreement with those changes, the mice treated with siRNA-CDP-NPs carrying Cy3-si*Orai1* showed significant expansion of mesangium (Figure 5 E&F). In summary, the use of siRNA-CDP-NP delivery in mice provided *in vivo* evidence that inhibition of SOC in MCs increased glomerular ECM protein expression and induced mesangial expansion.

Discussion

Diabetes is the leading cause of end-stage renal disease (ESRD) world-wide. The early changes in the diabetic kidney include accumulation of ECM proteins in glomerulus, which ultimately progresses to glomerulosclerosis and irreversible ESRD. There is no curative therapy currently available for DN. Despite the increased use of antihypertensive medications and renin-angiotensin system (RAS) inhibitors in the patients with DN, the improvement of renal function is slight (37). Therefore, new therapeutic approaches are needed. The present study provides *in vitro* and *in vivo* evidence that SOC in MCs inhibits glomerular matrix protein expression. This inhibitory effect of SOC could play a role under resting state and stress because *in vivo* knock down of Orai1 in MCs in normal animals resulted in mesangial expansion (Figures 5 E&F), and activation of SOC prevented high glucose-induced ECM protein expression (Figure 3). Thus, SOC in MCs is a protective mechanism in diabetic kidneys. Theoretically, selective enhancement of the renoprotective SOC function, and any component in its signaling pathway, would be expected to ameliorate renal damage in diabetes and limit the development of DN.

Interestingly, our previous study demonstrated that the abundance of STIM1/Orai1 proteins (essential components of SOC pathway) was increased in glomerulus by diabetes and in MCs by high glucose (29). This paradoxical phenomenon suggests that in addition to well-known deleterious processes, diabetes simultaneously activates a beneficial SOC pathway in MCs as a compensatory mechanism to counteract detrimental pathways generated in diabetic kidneys.

Store operated channel function is distinct in different tissues and cell types (15,38). In general, the SOC-associated signaling pathway promotes protein synthesis and cell growth (15), for instance, contributing to cardiac hypertrophy (39,40). However, a recent study revealed that the SOC-mediated Ca^{2+} influx suppressed cell growth in mouse embryonic fibroblasts and rat uterine

leiomyoma cells through inhibition of AKT1 (41). Thus, the effect of SOC on protein production might be cell type specific and/or cell context dependent. Our data suggest that SOC-mediated Ca^{2+} signaling in glomerular MCs negatively regulates ECM protein expression. A similar example is the regulation of protein secretion by Ca^{2+} in juxtaglomerular (JG) cells. Like MCs, JG cells are modified smooth muscle cells that synthesize, store, and release renin into the blood stream for initiating the RAS system. Usually, Ca^{2+} signal through SOC stimulates protein secretion in granular cells (15). In contrast, activation of SOC in JG cells inhibits renin secretion (42). It is possible that in MCs, the intermediators that regulate ECM protein expression may be functionally linked or be physically adjacent to SOC. Thus, the local Ca^{2+} signals delimited to the SOC-associated Ca^{2+} microdomains can be sensed by these molecules and subsequently inhibit ECM protein expression.

The mechanism for SOC inhibiting ECM protein expression in MCs is not elucidated in the present study. Accumulation of ECM in DN involves many molecules and multiple pathways, such as Ang II (43-45) reactive oxygen species (3,9,46), the mitogen-activated protein kinase (3,33,47), protein kinase C (3,33,48), and the TGF- β /Smad pathway (3,4,33,49-52). It is possible that the SOC-mediated Ca^{2+} signals modulate one or more of those pathways leading to suppression of ECM expression.

Here, we used the siRNA-CDP-NP delivery system to introduce RNAi sequences into MCs in mice. This approach is built on the anatomical properties of glomerular capillary. The glomerular capillary walls have 70-100 nm diameter endothelial fenestrations. The surrounding glomerular basement membrane generates a size-selective barrier with a pore size of 4 nm. MCs directly adjoin the endothelium without intervening the basement membrane (7,53). Thus, particles in a size of 4-100 nm can permeate through the fenestrated glomerular capillary wall and yet be

restricted in passing through the glomerular basement membrane, and therefore come into the mesangial region under a high transmural pressure gradient. Shimizu, et al. (53) have successfully delivered nanocarriers containing siRNA in the 10-20 nm-size range to MCs in animals. We employed similar approach using ~75 nm siRNA-CDP-NPs that have been demonstrated to accumulate within the glomeruli of mice (35). In agreement with those studies, the siRNA-CDP-NPs in the present study were predominantly localized in MCs with very limited distribution in extraglomerular region and glomerular podocytes (Figure 5 A&C). Both mouse and HMCs could rapidly internalize the siRNA-NPs *in vitro* (data not shown). Therefore, the decrease in Orai1 protein expression in renal cortex (Figure 5B) was most likely due to knockdown of Orai1 in MCs. We further reason that the increases in fibronectin and Col IV expression in renal cortex and glomerulus, and glomerular mesangial expansion (Figure 5 E and F) were attributed to reduced Orai1 protein (i.e. inhibition of SOC) in MCs.

In summary, the present study strongly suggests a beneficial effect of SOC in MCs by inhibiting ECM protein expression, which may protect kidney from diabetic injury at early stage of DN. Thus, SOC could be a promising therapeutic option to limit progress of DN. Furthermore, MCs do not have a cell type specific promoter, and thereby it is impossible to genetically manipulate a MC-specific gene expression. We have shown in this study that the nanocarriers of a particular size can be used as MC-specific siRNA delivery systems by systemic injection. Since the siRNA-CDP-NPs system has been used as a research tool as well as a human therapeutic (34, 53-55) and MC injury is associated with many renal diseases (7,10), systemic administration of a MC-selective siRNA-CDP-NPs targeting a particular protein may have a potential for the treatment of renal diseases.

Acknowledgements and Grants

The work was supported by National Institutes of Health (NIH) Grant RO1 (5RO1DK079968-01) from NIDDK (to R. Ma) and National Natural Science Foundation of China (81400805, to P. Wu). We thank GlaxoSmithKline (GSK, Stevenage, UK) for providing GSK-7975A compound.

Figure 1. Effect of SOC on ECM protein expression in cultured HMCs.

A-C: Representative immunoblots, showing activation of SOC on fibronectin (FN) (A), inhibition of SOC on FN (B), and inhibition of SOC on Collagen IV (Col IV) (C) expressions. UT: untreated cells; TG: thapsigargin (1 μ M); GSK: GSK-7975A (10 μ M); Meth: methanol, vehicle control for 2-APB (50 μ M); TB: tubulin. Both actin and Tubulin (TB) were used as a loading control. Serum starved cells (in 0.5% FBS) were with or without treatments for 2 days before harvested. **D, E, and F:** Summary data, corresponding to experiments presented in A, B, and C. * denotes $P < 0.05$, compared to other two groups. “n” indicates the number of independent experiments.

Figure 1.

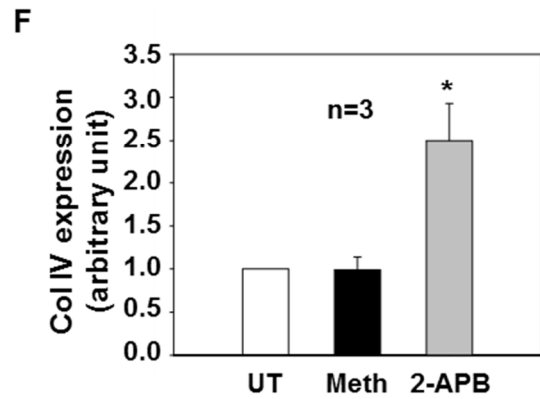
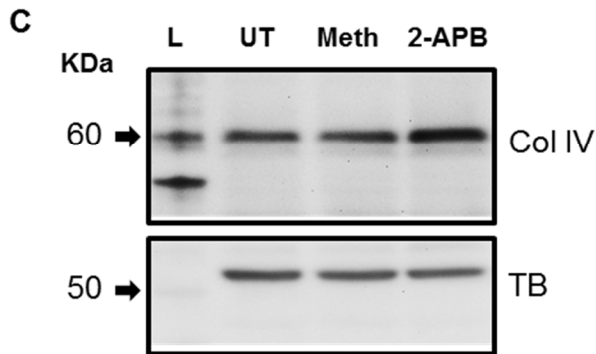
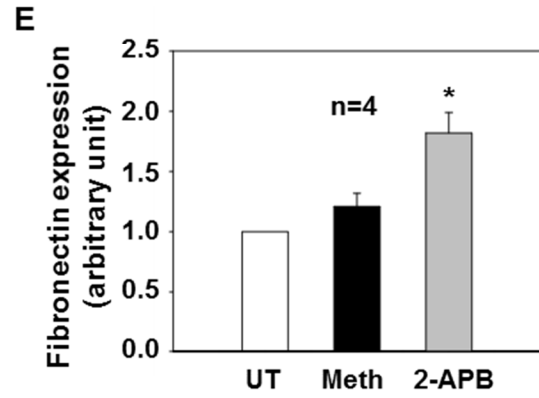
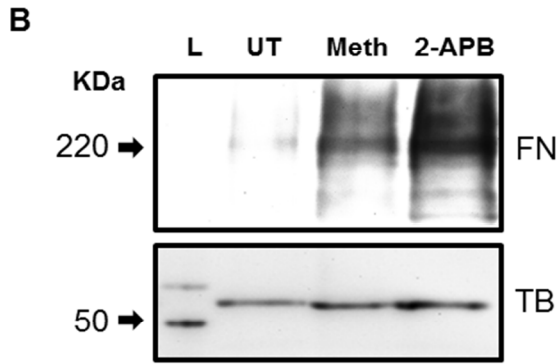
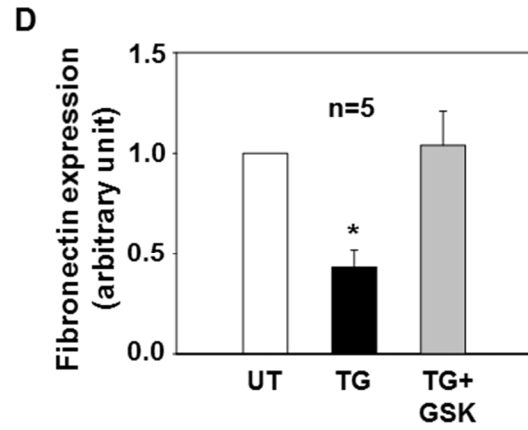
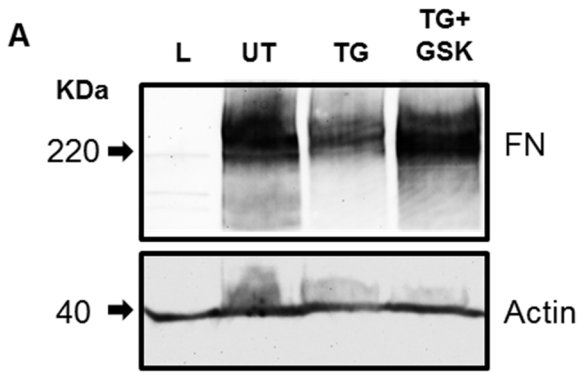


Figure 2. Effect of knockdown of Orai1 on fibronectin (FN) expression in HMCs.

A: Representative immunoblot, showing FN expression in HMCs without transfection (UTran) and the cells transfected with Scramble and Orai1 siRNA (50 nM). Tubulin was used as a loading control. **B:** Summary data from the experiments presented in A, showing FN (B) expression levels in HMCs with different treatments by normalized to tubulin. * denotes $P < 0.05$, compared to all other groups. “n” indicates the number of independent experiments.

Figure 2.

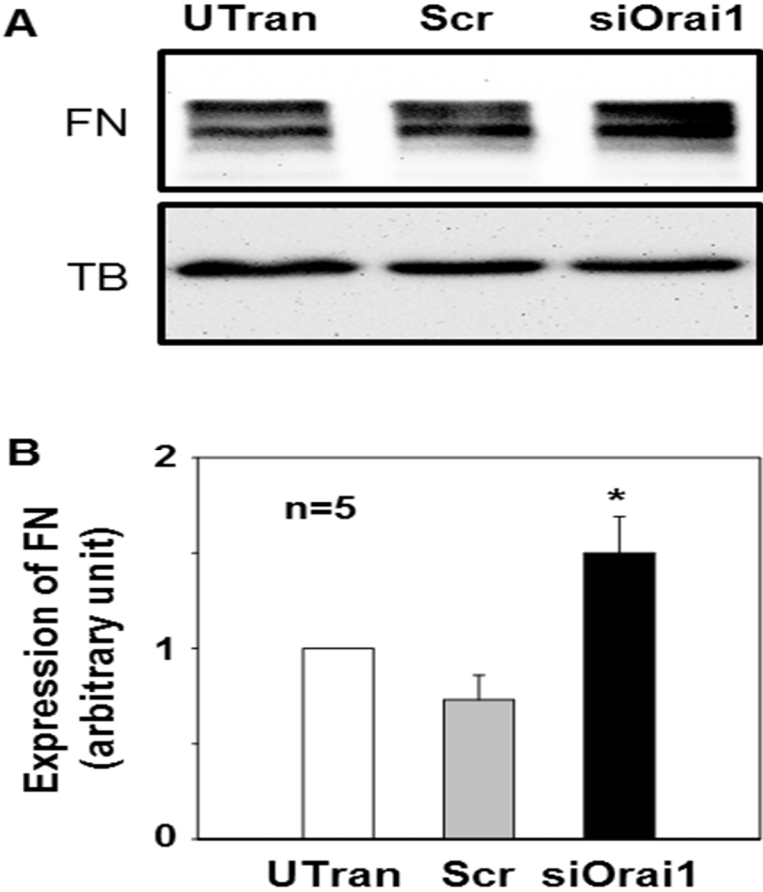


Figure 3. Effect of SOC on HG-stimulated ECM protein content in HMCs.

A and B: Representative immunoblots, showing FN (A) and Col IV (B) expression in MCs cultured in NG (5.6 mM glucose + 20 mM mannitol) or in HG (25 mM glucose) in the absence or presence of DMSO (1:1000, vehicle control) and TG (1 μ M). Tubulin (TB) was used as a loading control. MCs were with and without various treatments for 2 (A) or 3 (B) days in 0.5% FBS medium. **C and D:** Summary data from the experiments presented in A and B, respectively. FN and Col IV expression levels were normalized to tubulin. * denotes $P < 0.05$, compared to NG group and † denotes $P < 0.05$, compared to both HG and HG+DMSO groups. “n” indicates the number of independent experiments.

Figure 3.

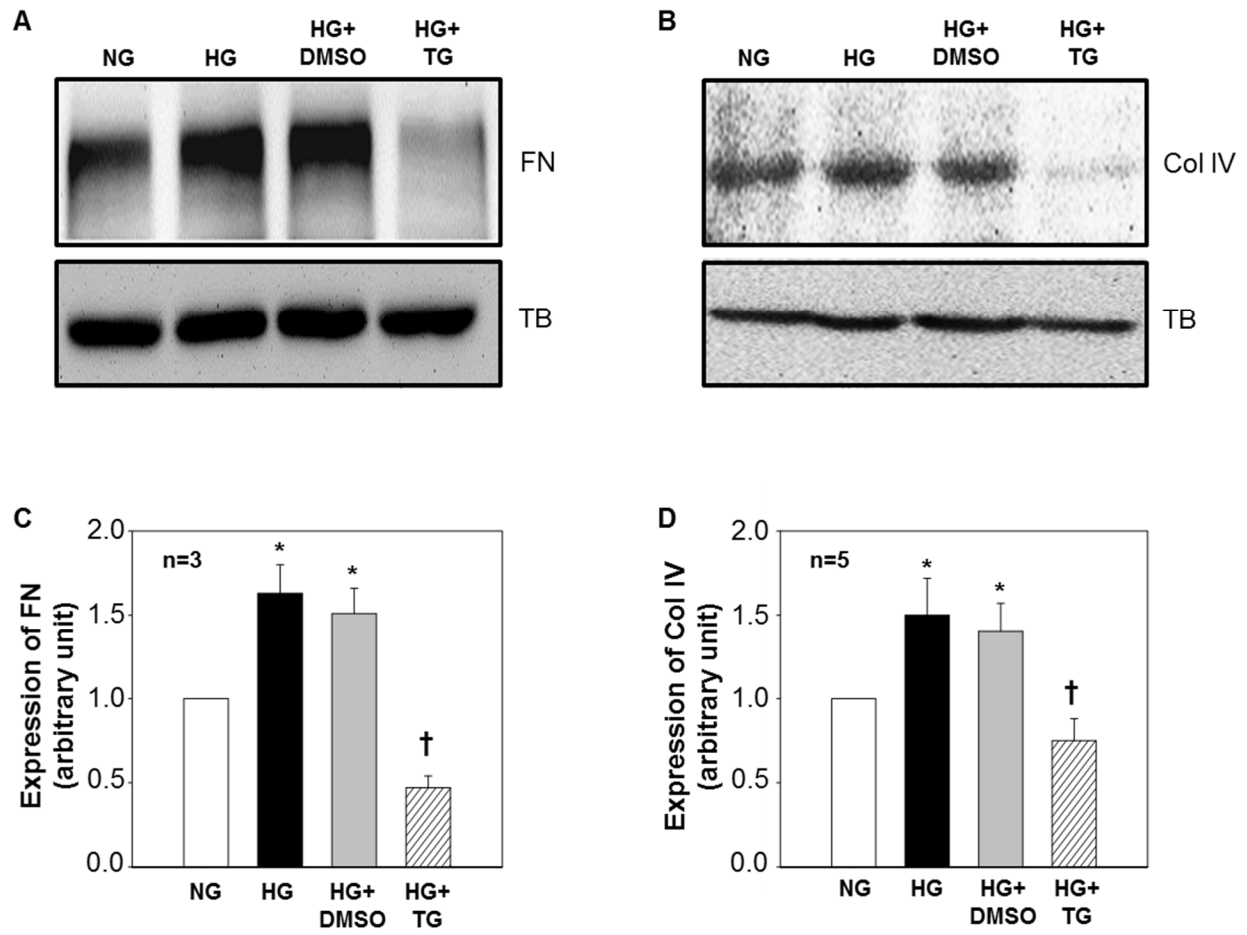


Figure 4. Distribution of NP-Cy3-siOrai1 in mouse kidney.

A: Representative images from 3 mice, showing localization of NP-Cy3-siOrai1 (red) in glomeruli (indicated by arrows), but not in tubules. Original magnification: 200X. **B:** Representative immunoblot of renal cortex extracts from 3 independent experiments, showing Orai1 expression in the mouse with injection of NP control (NP-Con) and NP-Cy3-siOrai1. Although the predicted size of Orai1 is ~33 kDa, the antibody actually detects a band at ~50 kDa. Tubulin: loading control. L: protein ladder. **C:** Localization of NP-Cy3-siOrai1 in MCs (upper panels) and podocytes (POD) (bottom panels), representative from 3 mice. MCs were stained with OX-7 (green) and podocytes were stained with synaptopodin (green). NP-Cy3-siOrai1 was shown as red signals. Original magnification: 200X. **D:** Semiquantification of the co-localizations of MC and podocyte markers with NP-Cy3-siOrai1 shown in “C” using BioimageXD software.

Figure 4.

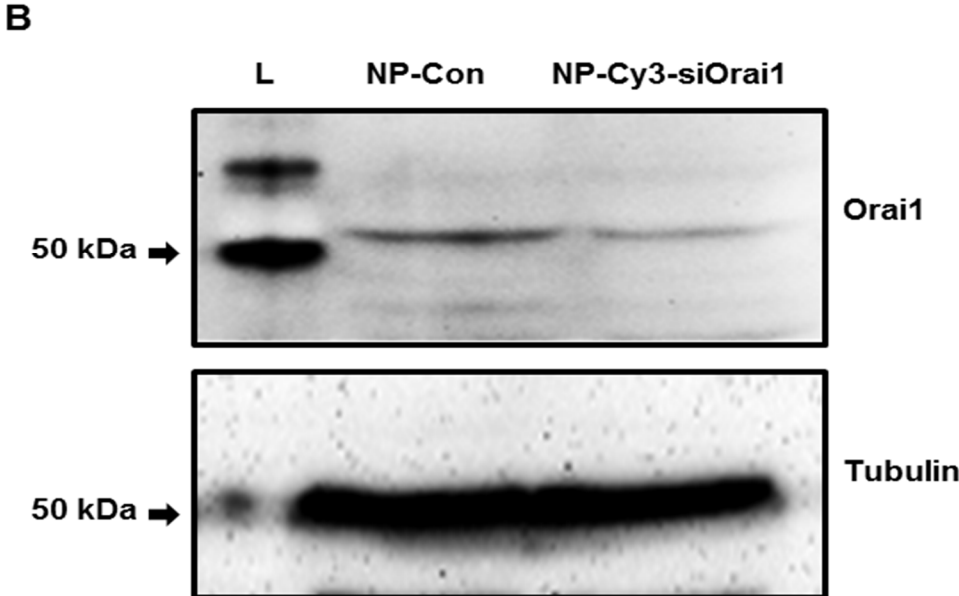
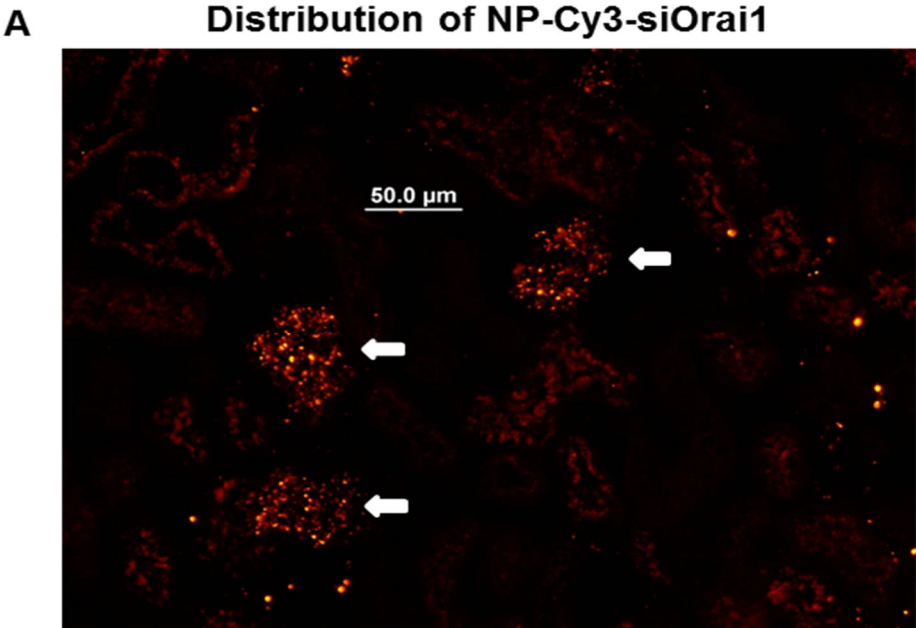


Figure 4.

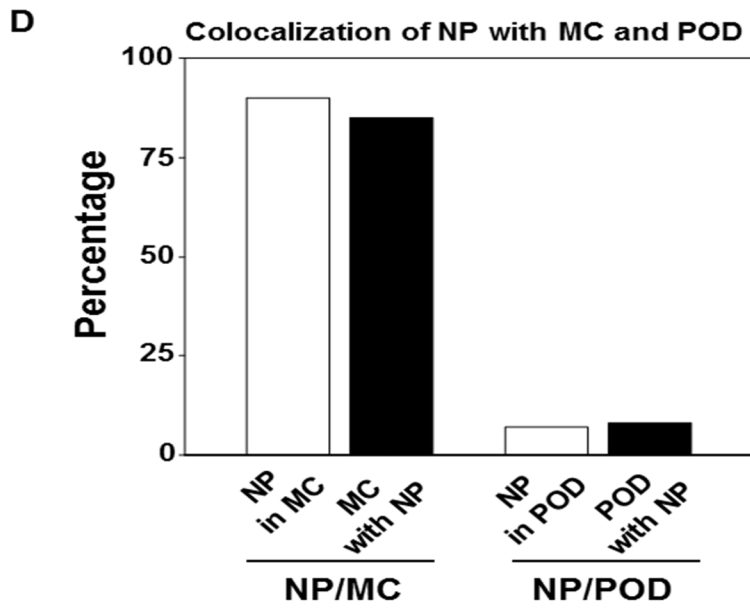
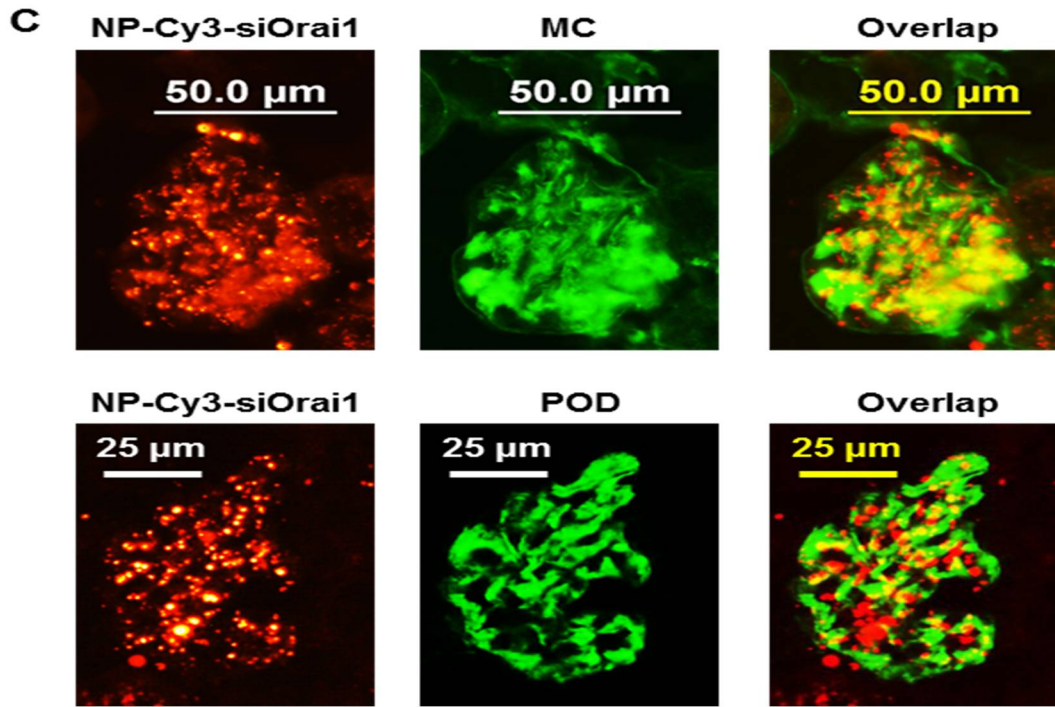


Figure 5. Effect of *in vivo* knockdown of Orai1 in MCs on ECM protein expression in mice.

A and B: Immunoblot of renal cortex extracts, showing expressions of FN protein in the cortex of kidney from the mouse treated with control NP (NP-Con) and NP-Cy3-siOrai1 (knockdown of Orai1). TB: α -tubulin, a loading control. **A:** Representative blot. **B:** summary data. * denotes $P < 0.05$, compared to NP-Con. “n” indicates the number of independent experiments. **C and D:** Immunohistochemistry, showing expressions of FN (C) and Col IV (D) in the glomeruli of the mouse treated with control NP (NP-Con) and NP-Cys-siOrai1 (knockdown of Orai1). Both FN and Col IV are shown as green staining. In NP-Con, a bright field image was captured to show the glomerulus. In NP-Cy3-siOrai1, the distribution of NP-Cy3-siOrai1 is indicated by Cy3 signals (red). Arrows indicate glomerulus. Original magnification: 200X. **E:** Representative PAS staining, showing mesangial matrix expansion in the glomerulus from the mouse treated with NP-siRNA-Orai1. Original magnification: 200X. **F:** Summary data from 50 glomeruli (n=50) from 5-7 sections/kidney/mouse of 3 mice. * denotes $P < 0.05$.

Figure 5.

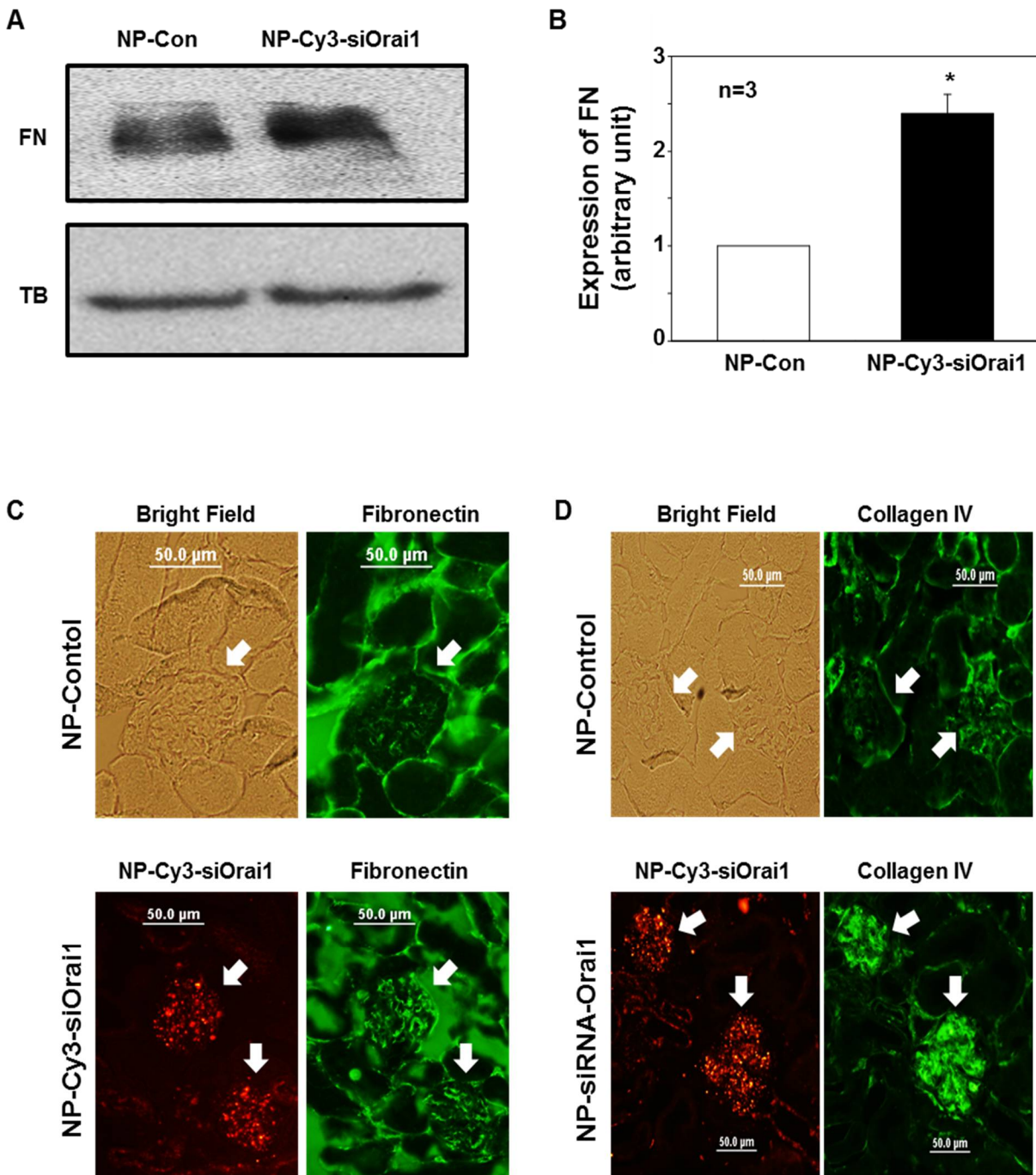
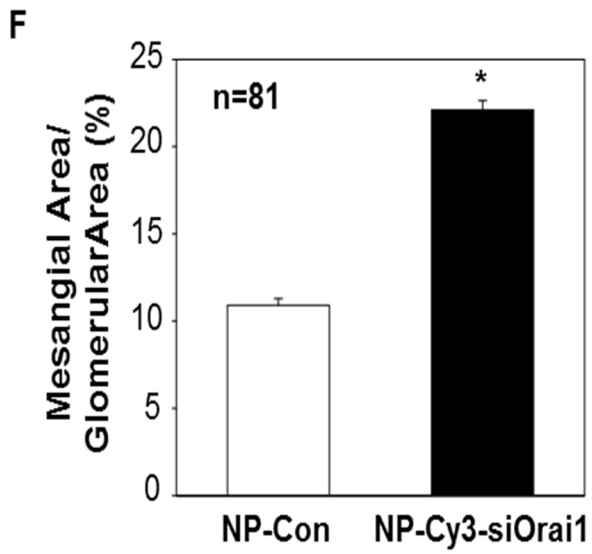
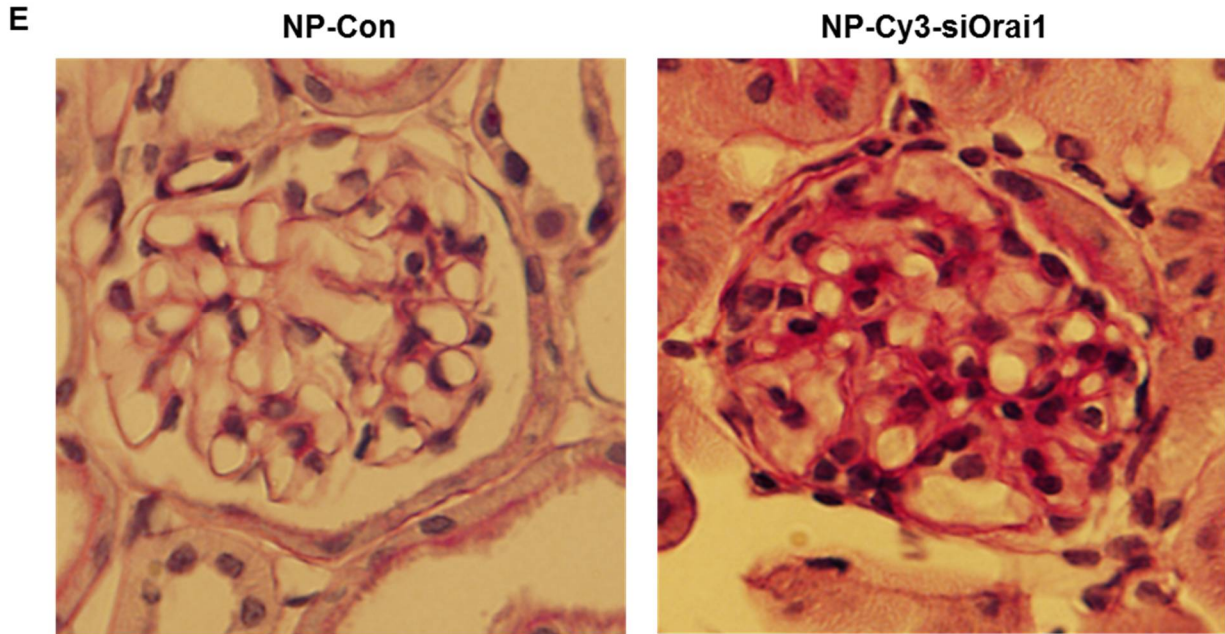


Figure 5.



Abbreviations

Ang II: angiotensin II

DN: Diabetic nephropathy

ECM: extracellular matrix

ER: endoplasmic reticulum

ESRD: end stage renal disease

HMCs: human mesangial cells

MCs: mesangial cells

SOC: store-operated channels

SOCE: store-operated Ca²⁺ entry

Col IV: collagen IV

NP-Cy3-siOrai1: nanoparticles containing Cy3-tagged siRNA against mouse Orai1

CDP: cyclodextrin-containing polycations

AD-PEG: adamantine-polyethylene glycol

PAS: Periodic Acid-Schiff

TG: Thapsigargin

2-APB: 2-aminoethyl diphenylborinate

NP: nanoparticles

siRNA-CDP-NPs: cyclodextrin-containing nanoparticle carrying siRNA

Thy1: thymic antigen 1

RAS: rennin-angiotensin system

JG: juxtaglomerular

References

1. Townsend RR, Feldman HI: Chronic kidney disease progression. *NephSAP* 8:271-288, 2009
2. Townsend RR, Feldman HI: Chronic kidney disease: past problems, current challenges, and future facets. *NephSAP* 8:239-243, 2009
3. Kanwar YS, Akagi S, Sun L, Nayak B, Xie P, Wada J, Chugh SS, Danesh FR: Cell biology of diabetic kidney disease. *Nephron Exp Nephrol* 101:e100-e110, 2005
4. Ziyadeh FN, Sharma K: Role of transforming growth factor- β in diabetic glomerulosclerosis and renal hypertrophy. *Kidney Int* 48:S34-S36, 1995
5. Kanwar YS, Wada J, Sun L, Xie P, Wallner EI, Chen S, Chugh S, Danesh FR: Diabetic nephropathy: mechanisms of renal disease progression. *Exp Biol Med* 233:4-11, 2008
6. Simonson MS: Phenotypic transitions and fibrosis in diabetic nephropathy. *Kidney Int* 71:846-854, 2007
7. Schlöndorff D, Bana B: The mesangial cell revisited: no cell is an island. *J Am Soc Nephrol* 20:1179-1187, 2009
8. Gooch JL, Barnes JL, Garcia S, Abboud HE: Calcineurin is activated in diabetes and is required for glomerular hypertrophy and ECM accumulation. *Am J Physiol Renal Physiol* 284:F144-F154, 2003
9. Gorin Y, Block K, Hernandez J, Bhandari B, Wagner B, Barnes JL, Abboud HE: Nox4 NAD(P)H oxidase mediates hypertrophy and fibronectin expression in the diabetic kidney. *J Biol Chem* 280:39616-39626, 2005
10. Abboud HE: Mesangial cell biology. *Exp Cell Res* 318:979-985, 2012

11. Stockand JD, Sansom SC: Glomerular mesangial cells: electrophysiology and regulation of contraction. *Physiol Rev* 78:723-744, 1998
12. Kashgarian M, Sterzel RB: The pathobiology of the mesangium. *Kidney Int* 41:524-529, 1992
13. Scindia YM, Deshmukh US, Bagavant H: Mesangial pathology in glomerular disease: targets for therapeutic intervention. *Adv Drug Deliv Rev* 62:1337-1343, 2010
14. Ma R, Pluznick JL, Sansom SC: Ion channels in mesangial cells: function, malfunction, or fiction. *Physiology* 20:102-111, 2005
15. Parekh AB, Putney Jr. JW: Store-operated calcium channels. *Physiol Rev* 85:757-810, 2005
16. Roos J, DiGregorio PJ, Yeromin AV, Ohlsen K, Lioudyno M, Zhang S, Safrina O, Kozak JA, Wagner SL, Cahalan MD, Velicelebi G, Stauderman KA: STIM1, an essential and conserved component of store-operated Ca^{2+} channel function. *J Cell Biol* 169:435-445, 2005
17. Liou J, Kim ML, Heo WD, Jones JT, Myers JW, Ferrell JE, Meyer T: STIM is a Ca^{2+} store sensor essential for Ca^{2+} -store-depletion-triggered Ca^{2+} influx. *Current Biol* 15:1235-1241, 2005
18. Feske S, Gwack Y, Prakriya M, Srikanth S, Puppel SH, Tanasa B, Hogan PG, Lewis RS, Daly M, Rao A: A mutation in *Orai1* causes immune deficiency by abrogating CRAC channel function. *Nature* 441:179-185, 2006
19. Vig M, Peinelt C, Beck A, Koomoa DL, Rabah D, Koblan-Huberson M, Kraft S, Turner H, Fleig A, Penner R, Kinet JP: CRACM1 is a plasma membrane protein essential for store-operated Ca^{2+} entry. *Science* 312:1220-1223, 2006

20. Zhang SL, Yeromin AV, Zhang XHF, Yu Y, Safrina O, Penna A, Roos J, Stauderman KA, Cahalan MD: Genome-wide RNAi screen of Ca²⁺ influx identifies genes that regulate Ca²⁺ release-activated Ca²⁺ channel activity. *PNAS* 103:9357-9362, 2006
21. Deng X, Wang Y, Zhou Y, Soboloff J, Gill DL: STIM and Orai-dynamic intermembrane coupling to control cellular calcium signals. *J Biol Chem* 284:22501-22505, 2009
22. Wang Y, Deng X, Gill DL: Calcium signaling by STIM and Orai: intimate coupling details revealed. *Sci Signal* 3:pe42-1-pe42-4, 2010
23. Campos AH, Calixto JB, Schor N: Bradykinin induces a calcium-store-dependent calcium influx in mouse mesangial cells. *Nephron* 91:308-315, 2002
24. Menè P, Teti A, Pugliese F, Cinotti GA: Calcium release-activated calcium influx in cultured human mesangial cells. *Kidney Int* 46:122-128, 1994
25. Nutt LK, O'Neil RG: Effect of elevated glucose on endothelin-induced store-operated and non-store-operated calcium influx in renal mesangial cells. *J Am Soc Nephrol* 11:1225-1235, 2000
26. Ma R, Sansom SC: Epidermal growth factor activates store-operated calcium channels in human glomerular mesangial cells. *J Am Soc Nephrol* 12:47-53, 2001
27. Li WP, Tsiokas L, Sansom SC, Ma R: Epidermal growth factor activates store-operated Ca²⁺ channels through an IP₃ independent pathway in human glomerular mesangial cells. *J Biol Chem* 279:4570-4577, 2004
28. Sours-brothers S, Ding M, Graham S, Ma R: Interaction between TRPC1/TRPC4 assembly and STIM1 contributes to store-operated Ca²⁺ entry in mesangial cells. *Exp Biol Med* 234:673-682, 2009

29. Chaudhari S, Wu P, Wang Y, Ding Y, Yuan J, Begg M, Ma R: High glucose and diabetes enhanced store-operated Ca^{2+} entry and increased expression of its signaling proteins in mesangial cells. *Am J Physiol Renal Physiol* 306:F1069-F1080, 2014
30. Blaes N, Pecher C, Mehrenberger M, Cellier E, Praddaude F, Chevalier J, Tack I, Couture R, Girolami JP: Bradykinin inhibits high glucose- and growth factor-induced collagen synthesis in mesangial cells through the B2-kinin receptor. *Am J Physiol Renal Physiol* 303:F293-F303, 2012
31. Tahara A, Tsukada J, Tomura Y, Yatsu T, Shibasaki M: Effects of high glucose on AVP-induced hyperplasia, hypertrophy, and type IV collagen synthesis in cultured rat mesangial cells. *Endocr Res* 37:216-227, 2012
32. Jung DS, Li JJ, Kwak SJ, Lee SH, Park J, Song YS, Yoo TH, Han SH, Lee JE, Kim DK, Moon SJ, Kim YS, Han DS, Kang SW: FR167653 inhibits fibronectin expression and apoptosis in diabetic glomeruli and in high glucose-stimulated mesangial cells. *Am J Physiol Renal Physiol* 295: F595-F604, 2008
33. Wolf G, Ziyadeh FN: Molecular mechanisms of diabetic renal hypertrophy. *Kidney Int* 56:393-405, 1999
34. Choi CHJ, Zuckerman JE, Webster P, Davis ME: Targeting kidney mesangium by nanoparticles of defined size. *PNAS* 108:6656-6661, 2011
35. Zuckerman JE, Choi CHJ, Han H, Davis ME: Polycation-siRNA nanoparticles can disassemble at the kidney glomerular basement membrane. *PNAS* 109:3137-3142, 2012
36. Zuckerman JE, Gale A, Wu P, Ma R, Davis ME: siRNA delivery to the glomerular mesangium using polycationic cyclodextrin nanoparticles containing siRNA. *Submitted* 2014

37. Pavkov ME, Mason CC, Bennett PH, Curtis JM, Knowler WC: Change in the distribution of albuminuria according to estimated glomerular filtration rate in Pima Indians with type 2 diabetes. *Diabetes Care* 32:1845-1850, 2009
38. Nesin V, Wiley G, Kousi M, Ong EC, Lehmann T, Nicholl DJ, Suri M, Shahrizaila N, Katsanis N, Gaffney Pm, Wierenga KJ, Tsiokas L: Activating mutations in *STIM1* and *ORAI1* cause overlapping syndromes of tubular myopathy and congenital miosis. *PNAS* 111:4197-4202, 2014
39. Hulot JS, Fauconnier J, Ramanujam D, Chaanine A, Aubart F, Sassi Y, Merkle S, Cazorla O, Ouillé A, Dupuis M, Hadri L, Jeong D, Mühlstedt S, Schmitt J, Braun A, Bénard L, Saliba Y, Laggerbauer B, Nieswandt B, Lacampagne A, Hajjar RJ, Lompré AM, Engelhardt S: Critical role for stromal interaction molecule 1 in cardiac hypertrophy. *Circulation* 124:796-805, 2011
40. Voelkers M, Salz M, Herzog N, Frank D, Dolatabadi N, Frey N, Gude N, Friedrich O, Koch WJ, Katus HA, Sussman MA, Most P: *Orai1* and *Stim1* regulate normal and hypertrophic growth in cardiomyocytes. *J Mol Cell Cardiol* 48:1329-1334, 2010
41. Peng H, Liu J, Chen R, Wang Y, Duan J, Li C, Li B, Jing Y, Chen X, Mao Q, Xu KF, Walker CL, Li J, Wang J, Zhang H: mTORC1 enhancement of STIM1-mediated store-operated Ca^{2+} entry constrains tuberous sclerosis complex-related tumor development. *Oncogene* 32:4702-4711, 2013
42. Schweda F, Riegger GAJ, Kurtz A, Kramer BK: Store-operated calcium influx inhibits renin secretion. *Am J Physiol Renal Physiol* 279:F170-F176, 2000
43. Wolf G, Ziyadeh FN: The role of angiotensin II in diabetic nephropathy: emphasis on nonhemodynamic mechanisms. *Am J Kid Dis* 29:153-163, 1997

44. kenefick TM, Anderson S: Role of angiotensin II in diabetic nephropathy. *Semin Nephrol* 17:441-447, 1997
45. Mima A, Matsubara T, Arai H, Abe H, Nagai K, Kanamori H, Sumi E, Takahashi T, Iehara N, Fukatsu A, Kita T, Doi T: Angiotensin II-dependent Src and Smad1 signaling pathway is crucial for the development of diabetic nephropathy. *Lab Invest* 86:927-939, 2006
46. Gorin Y: Nox4 as a potential therapeutic target for treatment of uremic toxicity associated to chronic kidney disease. *Kidney Int* 83:541-543, 2013
47. Gorin Y, Ricono JM, Wagner B, Kim NH, Bhandari B, Choudhury GG: Angiotensin II-induced ERK1/ERK2 activation and protein synthesis are redox-dependent in glomerular mesangial cells. *Biochem J* 381:231-239, 2004
48. Kanzaki M, Zhang YQ, mashima H, Li L, Shibata H, Kojima I: Translocation of a calcium-permeable cation channel induced by insulin-like growth factor-1. *Nat Cell Biol* 1:165-170, 1999
49. Li J, Qu X, Yao J, Caruana G, Ricardo SD, Yamamoto Y, Yamamoto H, Bertram JF: Blockade of endothelial-mesenchymal transition by a Smad3 inhibitor delays the early development of streptozotocin-induced diabetic nephropathy. *Diabetes* 59:2612-2624, 2010
50. Tu Y, Wu T, Dai A, Pham Y, Chew P, de Haan JB, Wang Y, Toh BH, Zhu H, Cao Z, Cooper ME, Chai Z: Cell division autoantigen 1 enhances signaling and the profibrotic effects of transforming growth factor-b in diabetic nephropathy. *Kidney Int* 79:199-209, 2011
51. Wei X, Xia Y, Li F, Tang Y, Nie J, Liu Y, Zhou Z, Zhang H, Hou FF: Kindlin-2 mediates activation of TGF-b/Smad signaling and renal fibrosis. *J Am Soc Nephrol* 24:1387-1398, 2013

52. Kretzschmar M, Liu F, Hata A, Doody J, Massagué J: The TGF-beta family mediator Smad1 is phosphorylated directly and activated functionally by the BMP receptor kinase. *Genes Dev* 11:984-995, 1997
53. Shimizu H, Hori Y, Kaname S, Yamada K, Nishiyama N, Matsumoto S, Miyata K, Oba M, Yamada A, Kataoka K, Fujita T: siRNA-Based therapy ameliorates glomerulonephritis. *J Am Soc Nephrol* 21:622-633, 2010
54. Davis ME, Zuckerman JE, Choi CHJ, Seligson D, Tolcher A, Alabi CA, Yen Y, Heidel JD, Ribas A: Evidence of RNAi in humans from systemically administered siRNA via targeted nanoparticles. *Nature* 464:1067-1071, 2010
55. Chaudhary K, Moore H, Tandon A, Gupta S, Khanna R, Mohan RR: Nanotechnology and adeno-associated virus based decorin gene therapy ameliorates peritoneal fibrosis. *Am J Physiol Renal Physiol* in press: 2014

CHAPTER IV

STORE OPERATED CALCIUM ENTRY SUPPRESSED TGF β 1-SMAD3 SIGNALING PATHWAY IN GLOMERULAR MESANGIAL CELLS

Sarika Chaudhari, Weizu Li, Yanxia Wang, Hui Jiang, and Rong Ma

Manuscript to be submitted

Abstract

Our previous study demonstrated that the abundance of extracellular matrix (ECM) proteins was suppressed by store-operated calcium entry (SOCE) in mesangial cells (MCs). The present study was conducted to investigate the underlying mechanism focused on the transforming growth factor beta 1 (TGF β 1) - Smad3 pathway, a critical pathway for ECM expansion in diabetic kidneys. We hypothesized that SOCE suppressed ECM protein expression by inhibiting this pathway in MCs. In cultured human MCs (HMCs), we observed that TGF β 1 (5 ng/ml for 15 hours) significantly increased Smad3 phosphorylation (p-Smad3) as evaluated by immunoblot. However, this response was markedly inhibited by thapsigargin (TG) (1 μ M), a classical activator of store-operated Ca²⁺ channel (SOC). Consistently, immunocytochemistry and immunoblot showed that TGF β 1 significantly increased nuclear translocation of Smad3 in a manner prevented by pre-treatment with TG. Importantly, the TG effect was reversed by Lanthanum (La³⁺) (5 μ M) and GSK-7975A (10 μ M), both of which are selective blockers of SOC. Furthermore, knockdown of Orai1, a SOC channel protein, significantly augmented TGF β 1-induced Smad3 phosphorylation. Overexpression of Orai1 augmented the inhibitory effect of TG on TGF β 1-induced phosphorylation of Smad3. *In vivo* knockdown of Orai1 specific to MCs in mice using a targeted nanoparticle siRNA delivery system resulted in an increase in glomerular Smad3 phosphorylation and nuclear translocation in mice. Taken together, our results indicate that SOCE in MCs negatively regulates the TGF β 1-Smad3 signaling pathway. Because the TGF β 1-Smad3 pathway is a critical pro-fibrotic pathway, enhancing SOCE specifically in MCs, may be a therapeutic option for patients with glomerular fibrosis.

Keywords: mesangial cells, ECM, SOCE, Orai1, TGF β 1, Smad3

Introduction

Progressive accumulation of extracellular matrix (ECM) proteins in the glomerulus is one of the consistent pathological changes initiated at an early stage in kidney diseases such as diabetic nephropathy (DN) (1,2). The magnitude of matrix accumulation in both the glomeruli and the interstitium is intensely and independently associated with the degree of renal insufficiency and proteinuria in these patients (3,4). Over extended period of time, this ECM accumulation and its dysregulated remodeling contributes to irreversible fibrotic changes that lead to chronic kidney disease and ultimately kidney failure in the form of end stage renal disease (5-8). Glomerular mesangial cells (MCs) which are a major source of ECM proteins are also an important target of metabolic abnormalities in diabetic environment (9,10). Since ECM expansion in the mesangium is one early feature of DN (1,11), it is justifiable to study the mechanisms that alter ECM dynamics in MCs.

Store operated Ca^{2+} entry (SOCE), which regulates many physiological and pathological functions in variety of cells, is an important Ca^{2+} signaling pathway in MCs (12-14). In our previous study, we demonstrated a negative effect of SOCE on the content of ECM proteins like fibronectin and collagen-IV in MCs (15), suggesting an anti-fibrotic effect of SOCE in MCs. However, the mechanism underlying the inhibitory effect of SOCE on ECM protein expression is not known. Transforming growth factor beta1 ($\text{TGF}\beta$ 1), a multifunctional cytokine, plays a critical role in ECM protein dynamics (16-19). It exerts its potent fibrotic effect intracellularly via receptor operated Smad (R-Smad) proteins particularly Smad3 (20-25). Activation of Smad3 by $\text{TGF}\beta$ 1 through phosphorylation and subsequent translocation into the nucleus, regulates the transcription of target genes including those of ECM proteins (22,26-28). In this study, we

investigated if the ability of SOCE to suppress both fibronectin and collagen-IV is mediated by the inhibition of the TGF β 1-Smad3 pathway.

Material and Methods

Mesangial Cell culture. Human MCs (HMCs) belong to the Clonetics renal MC system and were purchased from Lonza (Catalogue no:CC2559, Walkersville, MD). HMCs in a 75-cm² flask were cultured in normal glucose (5.6 mM; NG) DMEM (GIBCO, Carlsbad, CA) supplemented with 25 mM HEPES, 4 mM glutamine, 1.0 mM sodium pyruvate, 0.1 mM nonessential aminoacids, 100 U/ml penicillin, 100 μ g/ml streptomycin, and 20% fetal bovine serum (FBS). When HMCs reached 90% confluence, the cells were split into 60 mm or 35 mm culture plates for various treatments as specified in figure legends. The cell growth was arrested with 0.5% FBS medium during treatments. Every alternate day the culture media was replaced with fresh media. Activators or inhibitors of SOCE were added 20 min before the TGF β 1 treatment. Cells used were with sub-passages not more than nine generations.

Transient transfection of HMCs. Small interfering (si) RNA against human Orai1 or scrambled control siRNA (both 50 nM) were transfected into HMCs using Dharmafect 2 transfection reagent (Thermo Scientific, Rockford, IL) in serum free DMEM media following the protocol provided by the manufacturer. Media was changed to 20% FBS DMEM media after 6 h. Cells were harvested for Western blot 72 h after transfection. Expression plasmid of Orai1, mCherry Flag-red Orai1 plasmid (0.5 μ g/ml) and empty vector yellow fluorescent protein, YFP (0.5 μ g/ml) were transfected into the HMCs using Lipofectamine and Plus reagent (Invitrogen-BRL, Carlsbad, CA) following the protocols provided by the manufacturer. Cells were collected 48 h after transfection for Western blot analysis.

Preparation of nuclear extracts. Preparation of nuclear extracts from HMCs was performed using NE-PER Nuclear and Cytoplasmic Extraction Reagents (Catalogue No: 78833, Thermo Scientific, Rockford, IL) following the manufacturer's protocol. The extracts were stored at -80°C until use.

Immunoblot Analysis. Immunoblot Analysis was performed as described in our previous publications(29). Briefly, the whole-cell lysates were fractionated by 10% SDS-PAGE (except for TGF β 1 protein which was fractionated by 15% SDS-PAGE), transferred to PVDF membranes, and probed with primary antibodies to Smad3, phospho-Smad3 (p-Smad3), Orail, TGF β 1, Flag, TATA binding protein (TBP) and tubulin. Bound antibodies were visualized with Super Signal West Femto or Pico Luminol/ Enhancer Solution (Catalogue No: 34095 and 34087, Thermo Scientific, Rockford, IL). The specific protein bands were visualized and captured using the AlphaEase FC Imaging System (Alpha Innotech, San Leandro, CA). The integrated density value (IDV) of each band was measured by drawing a rectangle outlining the band using AlphaEase FC software with autobackground subtraction. If a protein had double bands, a total IDV by summation of each band IDV was used. The expression of Smad3, p-Smad3, Orail, TGF β 1, Flag proteins were quantified by normalization of the IDVs of those protein bands to that of tubulin bands on the same blot. In Figure 6, the expression of nuclear p-Smad3 proteins were normalized to TBP.

ELISA. Abundance of TGF β 1 in supernatant media was determined by a solid-phase sandwich enzyme-linked immunosorbent assay (ELISA) using a DuoSet ELISA Development kit for TGF β 1 (Catalogue No: DY240-05, R&D System, Minneapolis, MN, USA). Briefly, HMCs were plated in 24 well plates as 1.8×10^4 cells per well and after confluency were serum deprived till the end of experiment. SOCE was activated by treating these cells with $1\mu\text{M}$ thapsigargin (TG)

for 8 h before sample collection. Supernatant media was collected, centrifuged at 1500 rpm for 10 min at 4°C and stored at -80°C until use. Latent TGFβ1 in the cell supernatants was activated with acidification of samples by 1.0 N HCl and subsequent neutralization with 1.2 N NaOH/0.5 M HEPES and assayed immediately using the protocol provided by the manufacturer. The optical density was determined using the microplate reader set to 450 nm. TGFβ1 concentration in the media was determined from the standard curve obtained using the Sigma plot software version 11.

Immunofluorescence Cytochemistry. HMCs were plated on 22 X 22, 1 mm glass coverslips in 35 mm culture dishes. Cells were treated with TGFβ1 (5 ng/ml) for 15 h, with or without (TG 1μM) and GSK-7975A (10 μM). GSK was added 20 min before TG which was added 20 min prior to TGFβ1 treatment. After 15 h, cells were washed with PBS and fixed with 4% paraformaldehyde for 15 min at room temperature. After another wash with PBS, the cells were then incubated with ice-cold acetone at -20°C for 10 min. After 30 min of incubation with blocking buffer, the cells were incubated with mouse anti-Smad3 primary antibody at 1:100 in PBS plus 10% donkey serum and 0.2% Triton X-100 at 4 °C overnight. After three washes with PBS, the cells were then incubated with donkey anti-mouse secondary antibody conjugated with Alexa Fluor 568 (Catalogue No: A10037, Invitrogen) at a concentration of 1:500 for 1 h at 4°C in dark. DAPI (Catalogue No: H-1200, Invitrogen) was used for staining nuclei. Fluorescent staining was examined using an Olympus microscope (BX41) equipped for epifluorescence and an Olympus DP70 digital camera with DP manager software (version 2.2.1). Images were converted to 16-bit format and uniformly adjusted for brightness and contrast using ImageJ (version 1.47; NIH).

Animals. All procedures were approved by the University of North Texas Health Science Center (UNTHSC) Institutional Animal Care and Use Committee. 10 male C57BL/6 mice were purchased from Charles River Laboratories (Wilmington, MA). All mice used in this study were between 2 and 4 months of age. The animals were maintained at the animal facility of UNTHSC under local and National Institutes of Health guidelines.

In Vivo Delivery of nanoparticles (NP) into the Kidney of Mice. NPs having an Orail siRNA concentration of 2 mg/ml and size of about 70 nm were obtained using the protocol as previously described (30). These siRNAs against Orail were delivered to the kidneys of mice using the targeted NP delivery system as described previously (15). Mice were randomly divided into control and Orail-knocked down groups (five mice in each group). Tail vein injection of NPs containing Cy3- tagged siRNA against mouse Orail (NP-Cy3- siOrail) were given at a dose of 10 mg/kg siRNA in a volume of 100 μ l to the mice in the Orail-knocked down group. The mice in the control group were only given unconjugated NPs through the same route in the same injection volume. These intravenous injections were given on day 1 and 3 of the experiment and the mice were euthanized on day 5. Mice were euthanized via intraperitoneal injection of pentobarbital (100 mg/kg body weight). Kidneys were perfused with PBS to wash out the blood and after removal the left kidneys were fixed in 4% paraformaldehyde in PBS overnight. Paraformaldehyde fixed organs were dehydrated and embedded in molten paraffin to generate sections of 4 μ m in thickness (Cryostat 2800 Frigocut-E; Leica Instruments).

Immunofluorescence histochemistry. Anti α 8 integrin rabbit polyclonal antibody at 1:50 and Alexa Fluor 488 Donkey anti-rabbit IgG (Catalogue no: A21206, Invitrogen, Eugene, OR) at 1:200 were used to label mouse glomerular MCs. Anti synaptopodin goat polyclonal antibody at 1:50 and Alexa Fluor 488 donkey anti goat IgG (Catalogue no: A11055, Life Technologies,

Eugene, OR) at 1:200 was used to label the podocytes. Sections were examined using an Olympus microscope (BX41) equipped for epifluorescence and an Olympus DP70 digital camera with DP manager software (version 2.2.1). Images were converted to 16-bit format and uniformly adjusted for brightness and contrast using Image J (version 1.47, NIH).

Immunohistochemistry with DAB staining. After rehydration, antigen retrieval was achieved by heating the sections in 10 mM citrate buffer in a microwave for 10 min. The sections were blocked by 5% goat serum for 30min at room temperature and then were incubated with anti p-Smad3 rabbit antibody at 1:100 overnight at 4⁰C. The sections were incubated with anti-rabbit poly HRP IHC reagent (Catalogue no: IHC-2291, General Bioscience Corporation) at room temperature for 1 h, followed by incubation with Peroxidase substrate solution for about 2-3min, dipping the slides in hematoxylin solution for 90 seconds, dehydration in incubator at 60⁰C for 30 min and cover slipped with mounting media. Sections were examined using an Olympus microscope (BX41) and an Olympus DP70 digital camera with DPmanager software (version 2.2.1). Images were converted to 16-bit format and uniformly adjusted for brightness and contrast using ImageJ (version 1.47; NIH).

Materials

Primary antibodies against p-Smad3 (ab51451) and TBP (ab818) were purchased from Abcam (Cambridge, MA), Smad3 (sc101154), integrin α 8:H-180 (sc-25713), synaptopodin (P-19) (sc-21537) and α -tubulin(sc-5286) from Santa Cruz biotechnologies, Orai1(O8264) from Sigma-Aldrich,(Israel). Secondary antibodies for western blot, goat anti mouse Ig HRP (sc2005) and goat anti rabbit Ig HRP (sc2003) were purchased from Santa Cruz biotechnologies. Small interfering (si) RNA against human Orai1, Cy3-labeled siRNA against mouse Orai1 were

purchased from Integrated DNA Technologies, Inc. (Chicago, IL). (Table 1) Scramble control siRNA (ON-TARGETplus Non-targeting control siRNA#1) (D-001810-01-20) was purchased from Dharmacon, GE. mCherry Flag red Orail plasmid and the mouse Flag antibody were obtained from Dr Yuan at UNTHSC.

TG(T9033), BSA (A7030), Hematoxylin (GHS3) were purchased from Sigma-Aldrich. HCl (BDH3419-1), NaOH (VW3247-1) were from VWR, (West Chester, PA), DMSO (4-X) was purchased from ATCC, (Manassas, VA), Human recombinant TGF β 1 (240-B-002) was purchased from R&D systems. GSK-7975A was kindly donated by GlaxoSmithKline (Brentford, UK). Peroxidase substrate solution (DAB Peroxidase substrate kit SK-4100) was purchased from Vector Laboratories (Burlingame, CA).

Statistical Analyses. Data were reported as mean \pm SEM. The one-way ANOVA plus Newman-Keuls post hoc analysis and unpaired t-test were used to analyze the differences among multiple groups and between two groups, respectively, unless indicated in individual figures. $P < 0.05$ was considered statistically significant. Statistical analysis was performed using SigmaStat (Jandel Scientific, San Rafael, CA).

Results

SOCE activation did not affect abundance and secretion of TGF β 1 in cultured HMCs. MCs are known to synthesize and secrete TGF β 1 (31-33). To study if Ca^{2+} entry via SOC suppresses ECM proteins by inhibiting production and/or secretion of TGF β 1 by HMCs, we activated SOC by treating the cells with 1 μ M TG for 8 h. ELISA assay showed SOC activation did not significantly change the concentration of TGF β 1 in the culture media (Figure 1 A). Consistently immunoblot analysis showed that there was no significant difference in abundance of TGF β 1

protein in HMCs with and without TG treatment (Figure 1B and 1C). These results indicate that activation of SOC did not affect the secretion and amount of TGF β 1 protein.

SOCE inhibited TGF β 1 induced phosphorylation of Smad3

A variety of stimuli such as Angiotensin II, high glucose, advanced glycosylation end products, and reactive oxygen species activate TGF β 1 to regulate expression of matrix proteins by MCs (34-36). One of the major intracellular downstream pathways mediating this effect has been demonstrated to be via the activation of Smad proteins, particularly Smad3 (28,37-41). We indeed found that administration of TGF β 1 (5 ng/ml) but not its vehicle control (HCl) for 15 h induced a robust increase in the content of phospho-Smad3, the active form of Smad3, in HMCs (Figure 2A and 2B). Activation of SOC in these cells by TG significantly attenuated TGF β 1 response. However, the content of total Smad3 did not have significant difference among these groups. These results indicate that SOCE inhibits activation of the Smad3 pathway by TGF β 1 in HMCs.

Knockdown of Orai1 increased while overexpression of Orai1 decreased the TGF β 1 induced phosphorylation of Smad3.

Further, we speculated that knocking down the pore forming unit of SOC may have opposite effect to that of activation of SOC. Indeed, TGF β 1 induced phosphorylation of Smad3 was further and significantly increased in HMCs transfected with Orai1 siRNA as compared to untransfected cells and scramble siRNA-transfected cells. (Figure 3A and 3B). Simultaneous activation of SOC using 1 μ M TG attenuated the enhanced response. The knockdown efficiency of Orai1 siRNA as demonstrated by Orai1 bands in Figure 3, showed 80% reduction of Orai1 protein abundance.

To support these findings, we next overexpressed Orai1 protein in HMCs with mCherry-Flag-red human Orai1 plasmid. The Flag-tagged exogenous Orai 1 band was detected at approximately 80 kDa (Figure 4C). As shown in Figure 4A and 4B, activation of SOCE by TG significantly decreased TGF β 1-induced phosphorylation of Smad3. This inhibition was further augmented with overexpressing Orai 1.

Activation of SOCE decreases TGF β 1 mediated translocation of Smad3 in the nucleus.

Activation of Smad3 by TGF β 1 involves its phosphorylation and subsequent translocation to the nucleus where it regulates the transcription of target genes. Translocation is the rate limiting step for TGF β 1 signaling. We studied the expression of TGF β 1-induced phosphorylated Smad3 in the nuclear extracts of HMCs with activation or inhibition of SOC respectively. As shown in Figure 5A and 5B, translocation of p-Smad3 to the nucleus was significantly increased by TGF β 1 treatment. TG significantly reduced this translocation while simultaneous treatment with La³⁺ (5 μ M) a SOC blocker reversed the TG effect. Consequently, immunocytological examination showed that Smad3 was localized in the cytosol in many HMCs without stimulation. However, in the cells treated with TGF β 1, Smad3 was localized in the nucleus (Figure 5C). Furthermore, TG inhibited this translocation indicated by presence of Smad3 in the cytosol. The inhibitory effect of TG was abolished when the cells were simultaneously treated with a selective SOC inhibitor, GSK-7975A (10 μ M).

***In Vivo* knockdown of Orai1 in MCs increased phosphorylation and nuclear translocation of Smad3 in mice.**

We next verified our in vitro findings in mice with knockdown of Orai1 in MCs using the established targeted NP-siRNA delivery system (42,43). The NP carriers containing Cy3-tagged siRNA against mouse Orai 1 (NP-Cy3-siOrai1) were injected into mice via the tail vein

(15,43,44). These NP-siRNA complexes were predominantly distributed in glomeruli with limited distribution in surrounding tubules (Figure 6A). Next, we counterstained kidney sections from mice that received NP-Cy3-siOrai1 (red signals) with the MC marker integrin $\alpha 8$ (green staining). As shown in Figure 6B, the NP-Cy3-siOrai 1 complexes highly co-localized with the integrin α -8, suggesting that the NP-siRNA complexes were specifically delivered into MCs.

We conducted immunohistological examination of the kidney sections from the mice with and without delivery of NP-Cy3-siOrai1. As shown in Figure 7, the abundance of p-Smad3 (indicated by the brown color) was markedly increased in the glomeruli of mice with Orail knockdown. Also, the NP-Cy3-siOrai1 treatment stimulated translocation of p-Smad3 to the nuclei, indicated by intense brown color.

Discussion

Store operated calcium entry is a ubiquitous intracellular Ca^{2+} signaling pathway, serving diverse functions in many non-excitabile and excitable cells (14,45-50). Apart from its physiological functions, this pathway is also involved in many pathological disorders. For instance, an altered SOCE is associated with many diabetic complications (51). We have previously demonstrated that SOCE in MCs suppressed ECM protein expression (15). It is known that multiple pathways regulate synthesis and degradation of ECM proteins and thus, affect expression level of ECM proteins (52,53). TGF β 1, a pleotropic cytokine and the most common and best characterized isoform of TGF β , is a known pro-fibrotic factor to stimulate production of ECM proteins in MCs (41). Also, TGF β 1 signaling pathway plays a critical role in mesangial expansion and renal fibrosis in diabetic kidney disease (16,17). Serum levels of TGF β 1 are positively correlated with the severity of diabetic nephropathy (DN), while in diabetic

patients without DN those are not significantly different as compared to nondiabetic subjects (18). Various studies have indicated the potent fibrotic effect of TGF β 1 to be mediated via the receptor operated intracellular Smad signaling, particularly through Smad3 (22,24,25,37,38). Our results from the present study suggest that TGF β 1/Smad3 pathway is a target of SOCE for inhibition of ECM protein expression.

SOCE could inhibit the TGF β 1-Smad3 signaling by acting on one or more sites of this pathway in MCs. First, it could inhibit the production or secretion of TGF β 1 by MCs. Second, SOCE could inhibit the activation of Smad3, i.e. its phosphorylation, and the third, SOCE could inhibit the nuclear translocation of Smad3. Our findings suggest that SOCE may not influence TGF β 1 production and secretion by MCs in presence of NG because activation of SOC did not change the abundance of TGF β 1 in MCs and in media culturing MCs (Figure 1).

Further our study suggests that activation (phosphorylation) and nuclear translocation of Smad3 are the regulatory sites for SOCE-induced inhibition of TGF β 1/Smad3 pathway. Receptor activation after TGF β 1 binding, leading to C-terminal phosphorylation of R-Smad is an important step which destabilizes Smad interaction with Smad anchor for receptor activation (SARA), allowing dissociation of Smad from the complex and the subsequent exposure of a nuclear import region on the Smad MH2 domain (54). In addition, R-Smad phosphorylation augments its affinity for Smad4 (55). The association of these two proteins translocates to the nucleus and interacts with transcriptional regulation complexes. In this study, activation of SOC significantly reduced the TGF β 1-induced phosphorylation of Smad3 in MCs (Figure 2). However, the abundance of total Smad3 remained unaffected. Since phosphorylated Smad3 is the active form of Smad3, a decrease in the ratio of p-Smad3 to total Smad3 indicates an inhibition of the Smad3 signaling pathway.

The inhibitory effect of SOCE on Smad3 activation (phosphorylation) was further supported by the data from experiments of manipulating Orai1 protein expression. Orai1 is the pore forming unit of SOC and therefore, knocking down this channel protein would be expected to reduce SOCE. Consistent with the findings described above, knocking down Orai1 significantly enhanced TGF β 1-induced phosphorylation of Smad3 in HMCs (Figure 3A and 3B). In agreement with the results, over expressing Orai1 significantly augmented the inhibitory effect of SOCE on TGF β 1-stimulated Smad3 phosphorylation (Figure 4). These findings are also in line with our previous reports that Orai1 knocked down increased ECM protein expression in MCs (15). Interestingly, one group recently reported that phosphorylation of Smad2/Smad3 was decreased by knocking down Orai1 in HK2 cells (56). However, if this decrease was specifically due to decrease in both Smad2 and Smad3 or only Smad2 or Smad3 was not clear. This is important because Smad2 and Smad3 may have totally opposite downstream effects, Smad3 being pro-fibrotic and Smad2 as anti-fibrotic, as demonstrated by many studies (57,58) . Another possibility is that the effect of SOCE is cell type or cell context specific. Also, some studies have reported decreased SOCE with overexpression of Orai1 which was not measured in this study. It might be possible that the abundance of STIM1 is more in MCs and hence overexpression of Orai1 may not change the stoichiometry to the extent to reduce the SOCE.

It is not known how SOCE inhibited phosphorylation of Smad3 by TGF β 1 from this study. Several possibilities exist. At the level of TGF β receptor, SOCE may inhibit the type II or type I receptor kinase which in turn, suppresses the subsequent phosphorylation of Smad3. Another mechanism could be that SOCE either activates a Ca²⁺ dependent phosphatase, such as calcineurin or a receptor specific phosphatase PP1c that dephosphorylate TGF β receptor I (59)

reducing the subsequent Smad3 phosphorylation and thus inhibiting its activation and translocation. Alternatively, SOCE could facilitate the interaction between inhibitory Smad7 and the TGF β receptors, resulting in suppression of downstream TGF β 1/R-Smad signaling, including phosphorylation of R-Smad.

Phosphorylation of Smad3 renders the receptor-operated Smad protein suitable for nuclear import, a critical step for its regulation of gene transcription. Because SOCE inhibited Smad3 phosphorylation, it is not surprising that the nuclear translocation of Smad3 was depressed by activation of SOC and was promoted by inhibition of SOC (Figure 5). However, the content of nuclear Smad3 is regulated by multiple mechanisms. The change in nuclear Smad3 in response to SOCE may not only be secondary to its inhibition on phosphorylation. Effect of SOCE on other pathways regulating nuclear localization of Smad3 can't be ruled out. For example, SOCE may also facilitate phosphorylation in the linker region by cyclin dependent kinases (CDKs) or mitogen associated protein kinases (MAPKs) rendering Smad3 unsuitable for nuclear transport or interacts with other kinases that can affect interaction of Smad3 with import machinery like nucleoporins, nuclear retention factors (60-62). Increased export of Smad3 out of the nucleus can also be a mechanism for suppressed nuclear content of p-Smad3 by SOCE. Nuclear localized protein phosphatase PP1MA/PP2C α , a Smad2/3 SXS-motif specific phosphatase, dephosphorylates Smad2/3 in the nuclei and also facilitates the interaction of dephosphorylated Smad2/3 with a nuclear export factor, RanBP3(Ran-binding protein 3). (63)

In summary, we defined a negative regulation of TGF β 1-Smad3 pathway by SOCE in MCs. This inhibition was through suppression of phosphorylation and nuclear translocation of Smad3, but not by decreasing abundance of TGF β 1 protein in MCs. A diagram presented in Figure 8 illustrates the possible mechanism for suppression of TGF β 1-Smad3 pathway by SOCE

in MCs. Because TGF β 1-Smad3 signaling pathway plays a critical role in renal fibrosis in many kidney diseases, our findings highlight that SOC may be considered as an alternative therapeutic option for treating patients with renal fibrosis.

Acknowledgments and Grants

We thank GlaxoSmithKline for providing GSK-7975A compound and Dr. Joseph Yuan at UNTHSC, for providing the mCherry Flag red human Orail plasmid and Flag antibody. The work was supported by RO1 grant from National Institutes of Health (Ma), Doctoral Student Bridge Grant from UNTHSC (Chaudhari) and Grant - in - Aid Research Grant for doctoral student from Sigma Xi (Chaudhari)

Table1. siRNAs used for transient transfection.

siRNA	Sequence	Gene Accession number/ catalog number
ON_TARGETplus Non-targeting control siRNA#1 Target sequence	UGGUUUACAUGUCGACUAA	D-001810-01-20
Human Orai1 siRNA (sense strand)	5'-UGGAACUGUCGGUCAGUCUUAUGGC-3'	NM_032790
Cy3 Mouse Orai1 siRNA (sense strand)	5'-/5Cy3/ GGGUUGCUCAUUCGUCUUUAGUGC-3'	NM_175423

Figure 1. Effect of SOCE on TGF β 1 secretion or production in cultured HMCs.

A: ELISA showing TGF β 1 concentration in culture media. HMCs were in serum free DMEM media for 72 h. One group was without any treatment and the other two groups were treated with DMSO (1:1000) or TG (1 μ M) for 8 h. prior to collection of media. 'n' indicates the number of independent experiments. **B:** Representative immunoblot showing the effect of SOCE on TGF β 1 protein content in cultured HMCs. HMCs were without treatment or treated with DMSO (1:1000) or TG (1 μ M) in presence of NG for 24 h. DMSO (1:1000) is the vehicle control for TG. α -tubulin was used as the loading control. **C:** Summary data from the experiment indicated in B. 'n' indicates the number of independent experiments.

Figure 1.

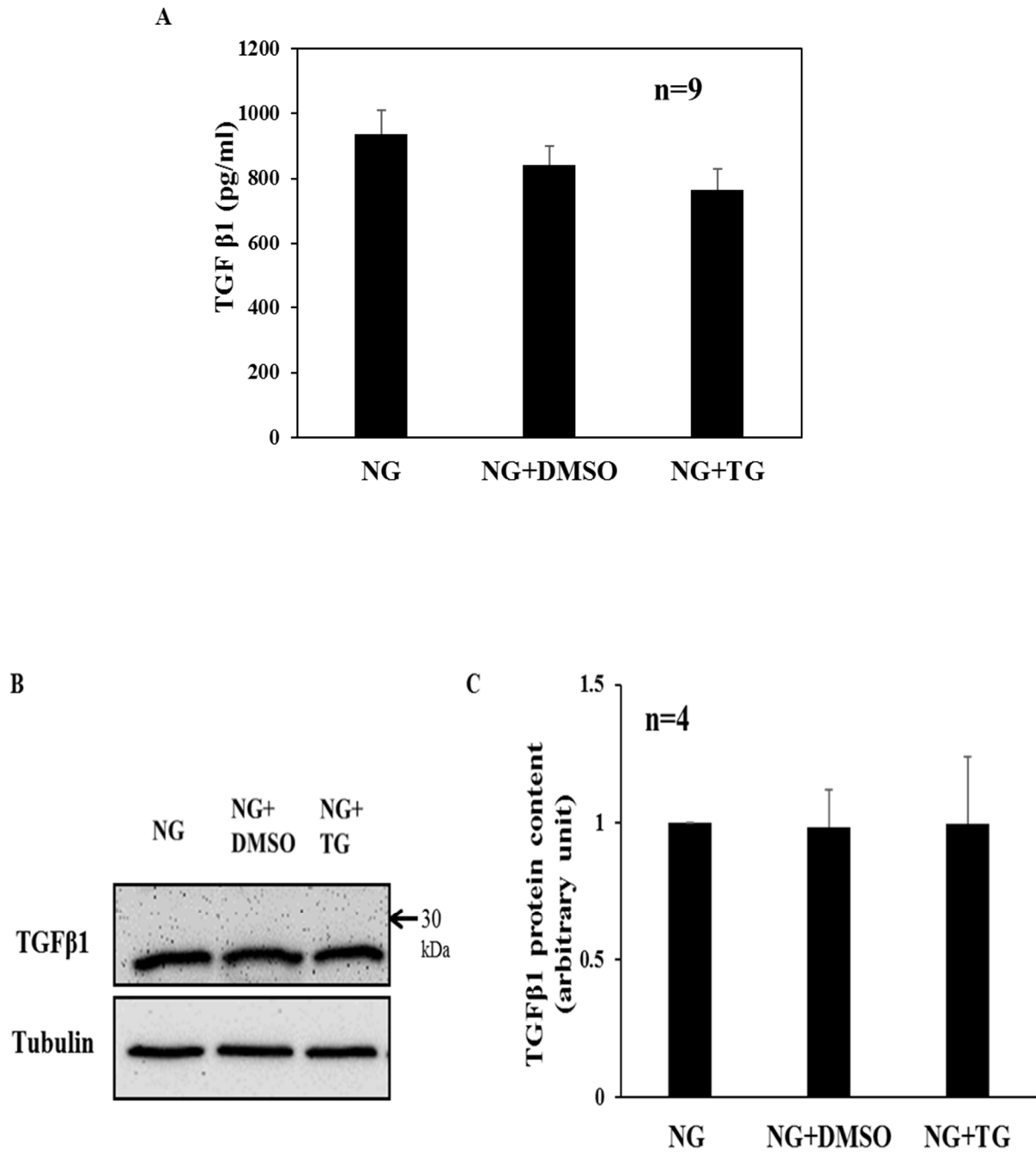


Figure 2. SOCE inhibited TGFβ1-induced phosphorylation of Smad3 in cultured HMCs.

A: Representative immunoblot showing changes in p-Smad3 and Smad3 proteins in different treatment groups. HMCs were treated with recombinant human TGFβ1 (5 ng/ml) in presence or absence of TG (1μM) for 15 h. UT: the cells without any treatment, HCl: 4 mM HCl with 0.1% BSA at 1:4000, the vehicle control for TGFβ1. DMSO (1:1000): the vehicle control for TG. α-tubulin was used as the loading control. **B:** summary data showing changes in the ratio of p-Smad3 to Smad3 in different treatment groups. ***p<0.001 vs UT and HCl; **p<0.01 vs TGFβ1 and TGFβ1 + DMSO. 'n' indicates the number of independent experiments.

Figure 2.

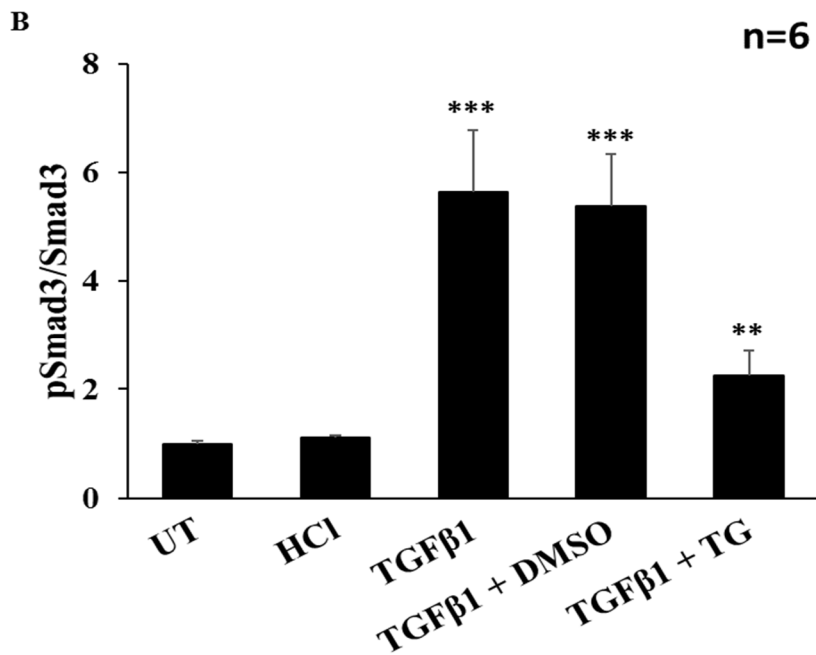
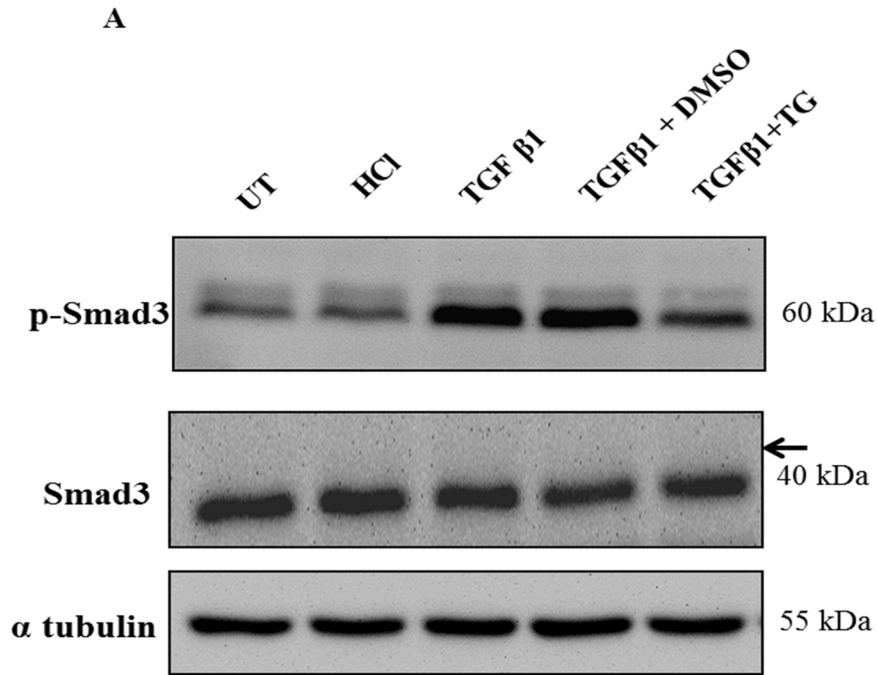


Figure 3. Knockdown of Orai1 increased the TGFβ1-induced phosphorylation of Smad3.

A: Representative immunoblot, showing effect of knockdown of Orai1 on p-Smad3 and Smad3 protein abundance in different groups. HMCs were transfected with scramble (scr) or Orai1 siRNA (siOrai1). On day 3 after transfection cells were treated with TGFβ1(5 ng/ml) in the presence or absence of TG (1 μM) for 15 h. UT: cells were without any treatment. α-tubulin was used as the loading control. L: ladder. **B:** Summary data from experiments presented in A. The abundance of p-Smad3 is expressed as the ratio of p-Smad3 to Smad3. **p<0.01 ***p<0.001 vs UT; *p<0.05 vs TGFβ1, TGFβ1+Scr and TGFβ1+siOrai1+TG; #p<0.05 vs TGFβ1+siOrai1+TG; ##p<0.01 vs TGFβ1+siOrai1. 'n' indicates the number of independent experiments.

Figure 3.

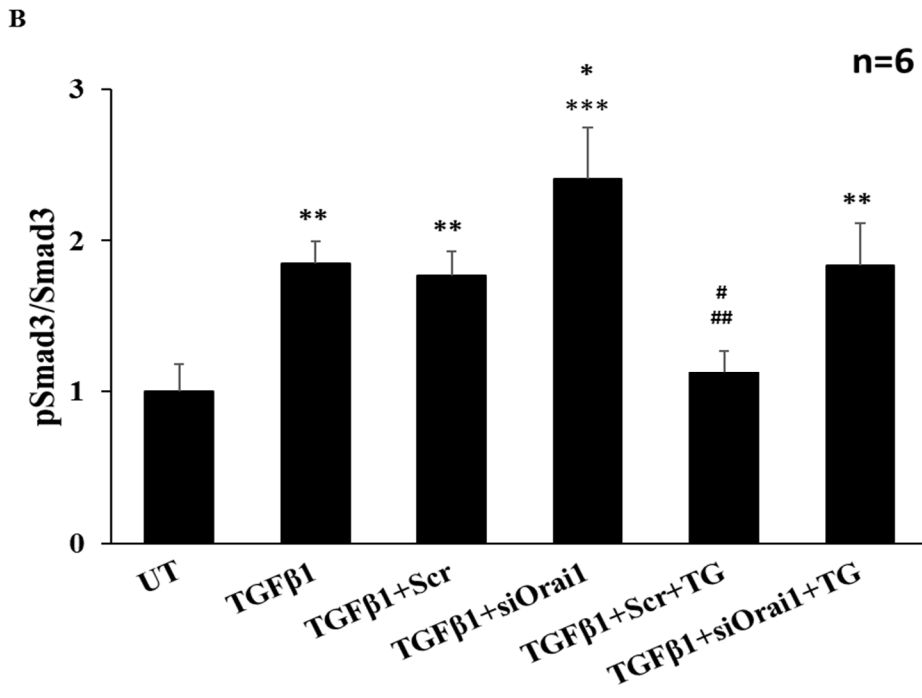
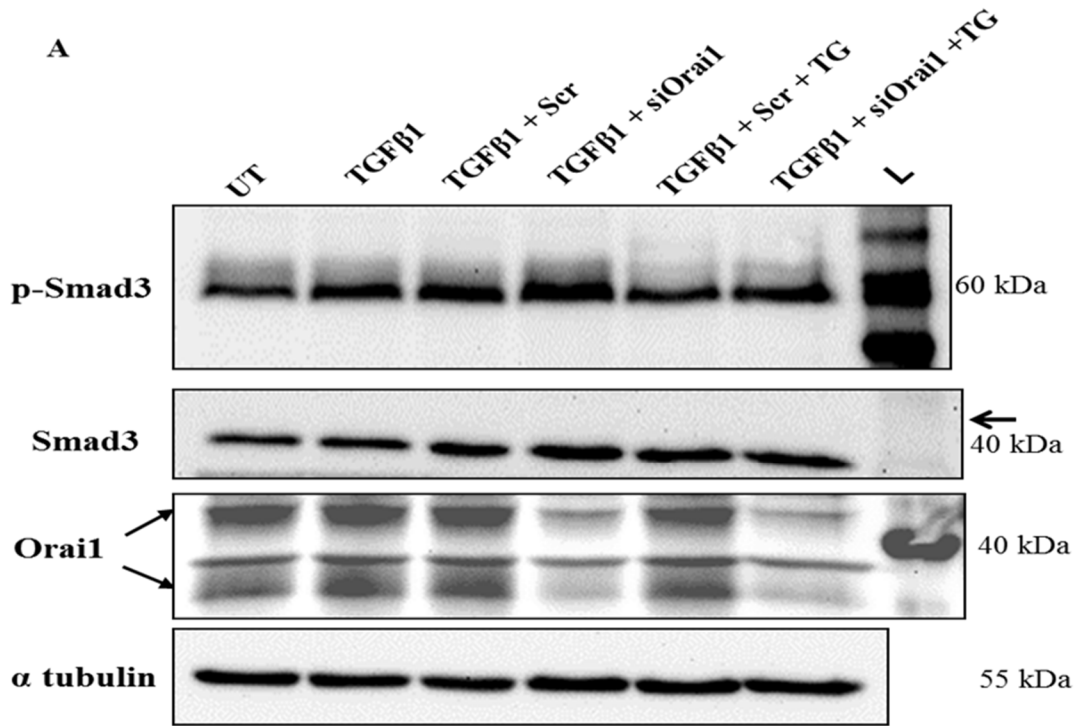


Figure 4. Overexpression of Orai1 decreased the TGFβ1-induced phosphorylation of Smad3.

A: Representative immunoblot, showing p-Smad3 and total Smad3 protein abundance in HMCs in different groups. HMCs were without transfection or were with YFP plasmid (YFP) or mCherry FLAG Red Orai1 plasmid (pOrai1). On day 2 after transfection, cells were treated with TGFβ1 (5ng/ml) in the presence or absence of TG (1μM) for 15 h. UT: cells without transfection and treatment, DMSO (1:1000): vehicle control for TG. α-tubulin was used as the loading control. **B:** Summary data showing changes in p-Smad3/ Smad3 ratio in different groups. ***p<0.01, vs UT; *p<0.05, vs TGFβ1, TGFβ1+DMSO, TGFβ1+ pOrai1+TG. 'n' indicates the number of independent experiments. **C:** Immunoblot, showing endogenous Orai1 and expressed Orai1 protein expression HMCs transfected with YFP and pOrai1.

Figure 4.

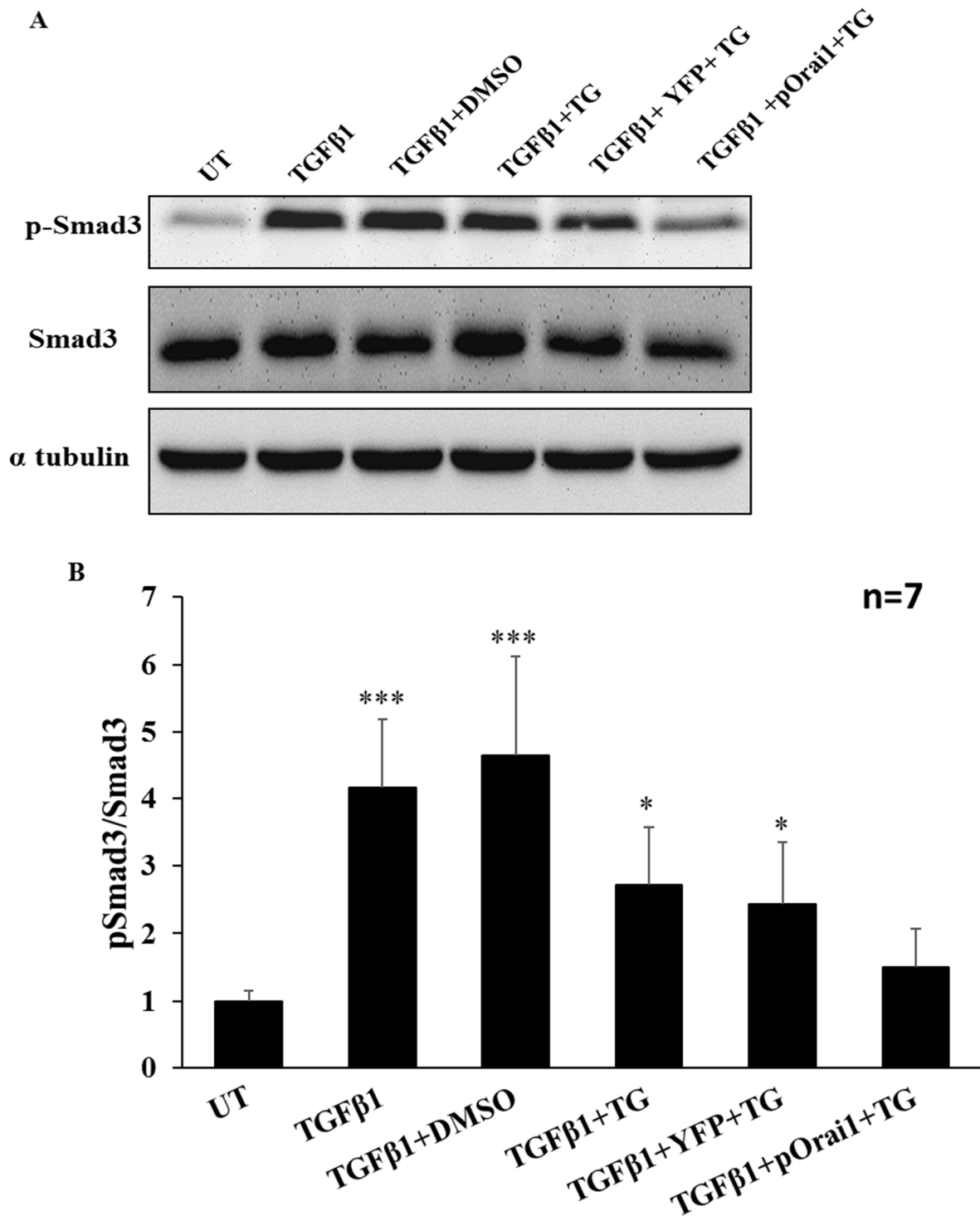


Figure 4.

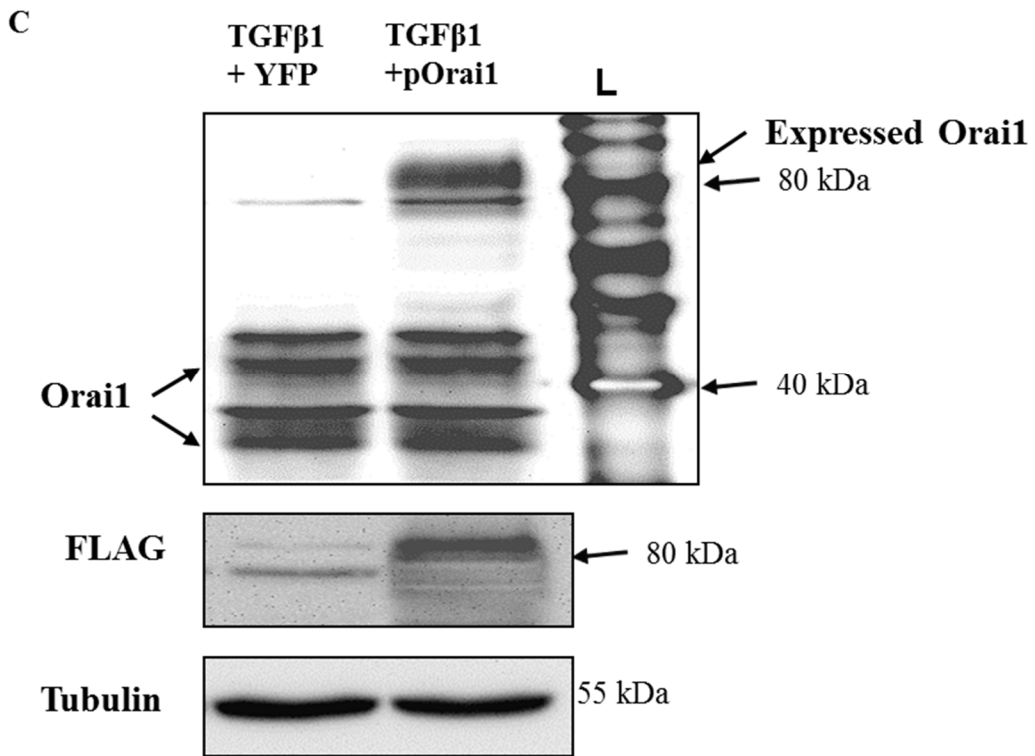
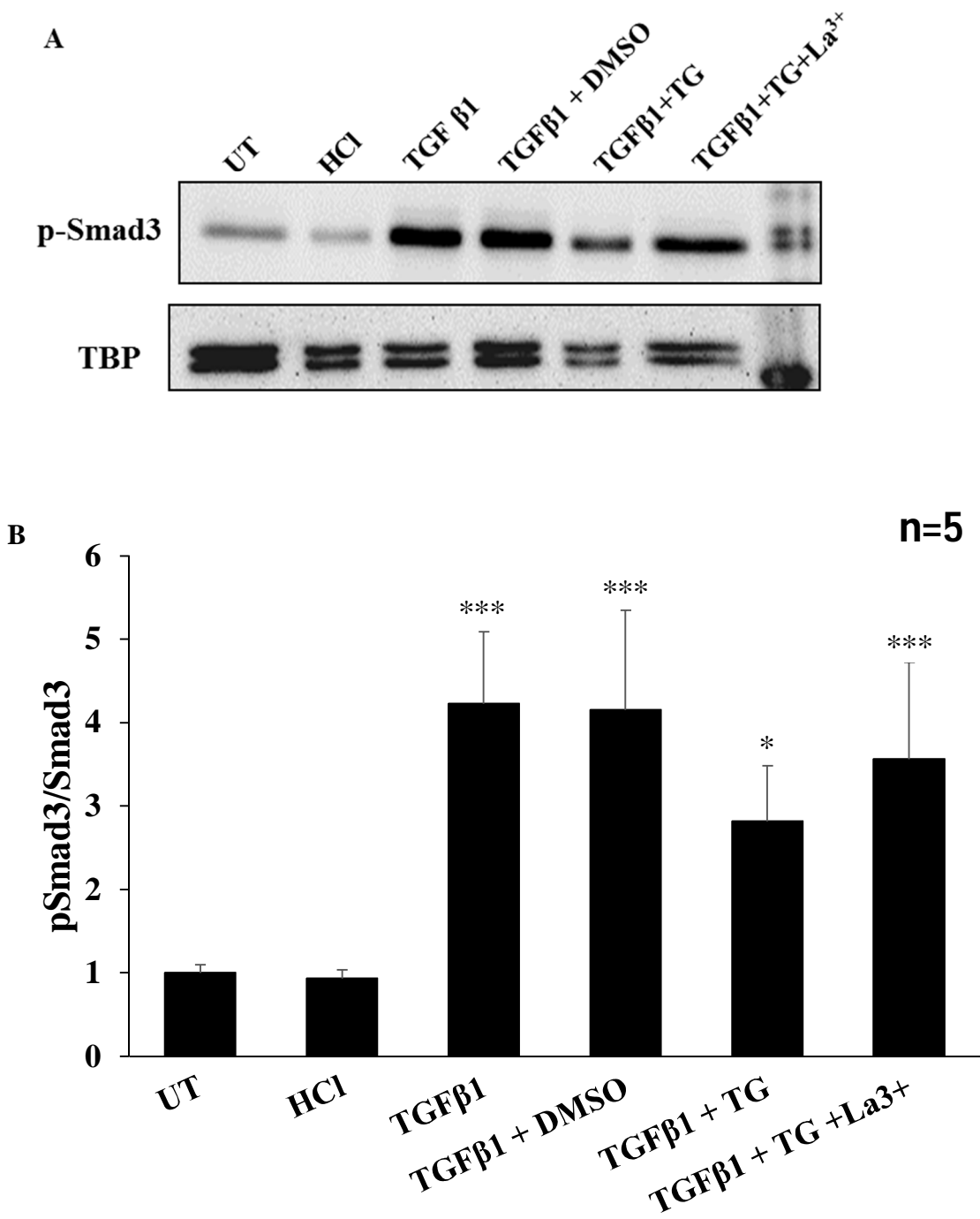


Figure 5. Activation of SOC decreased TGF β 1-stimulated translocation of Smad3 to the nucleus.

A: Representative immunoblot showing p-Smad3 protein abundance in nuclear extracts of HMCs. HMCs were either without treatment (UT) or treated with recombinant human TGF β 1 (5 ng/ml) in the presence or absence of TG (1 μ M) or a selective blocker of SOCE, La³⁺ (5 μ M) for 15 h. HCl: vehicle control for TG, DMSO: vehicle control for TG. TBP was used as the loading control for the nuclear proteins. **B:** Summary data from experiments in A. ***p<0.001, vs. UT and HCl; *p<0.05 vs. TGF β 1, TGF β 1+DMSO, TGF β 1+TG+La³⁺. 'n' indicates the number of independent experiments. **C.** Immunofluorescence staining showing Smad3 expression in HMCs treated with TGF β 1 (5 ng/ml) in the presence or absence of TG (1 μ M) or GSK-7975A (10 μ M) for 15 h. UT: cells without treatment, DMSO: vehicle control for TG. Smad3 is shown as red. Nuclei was stained with DAPI and shown as blue. Purple indicates co-localization of Smads with nuclei. Arrows indicate presence of Smad3 in the cytosol.

Figure 5.



C

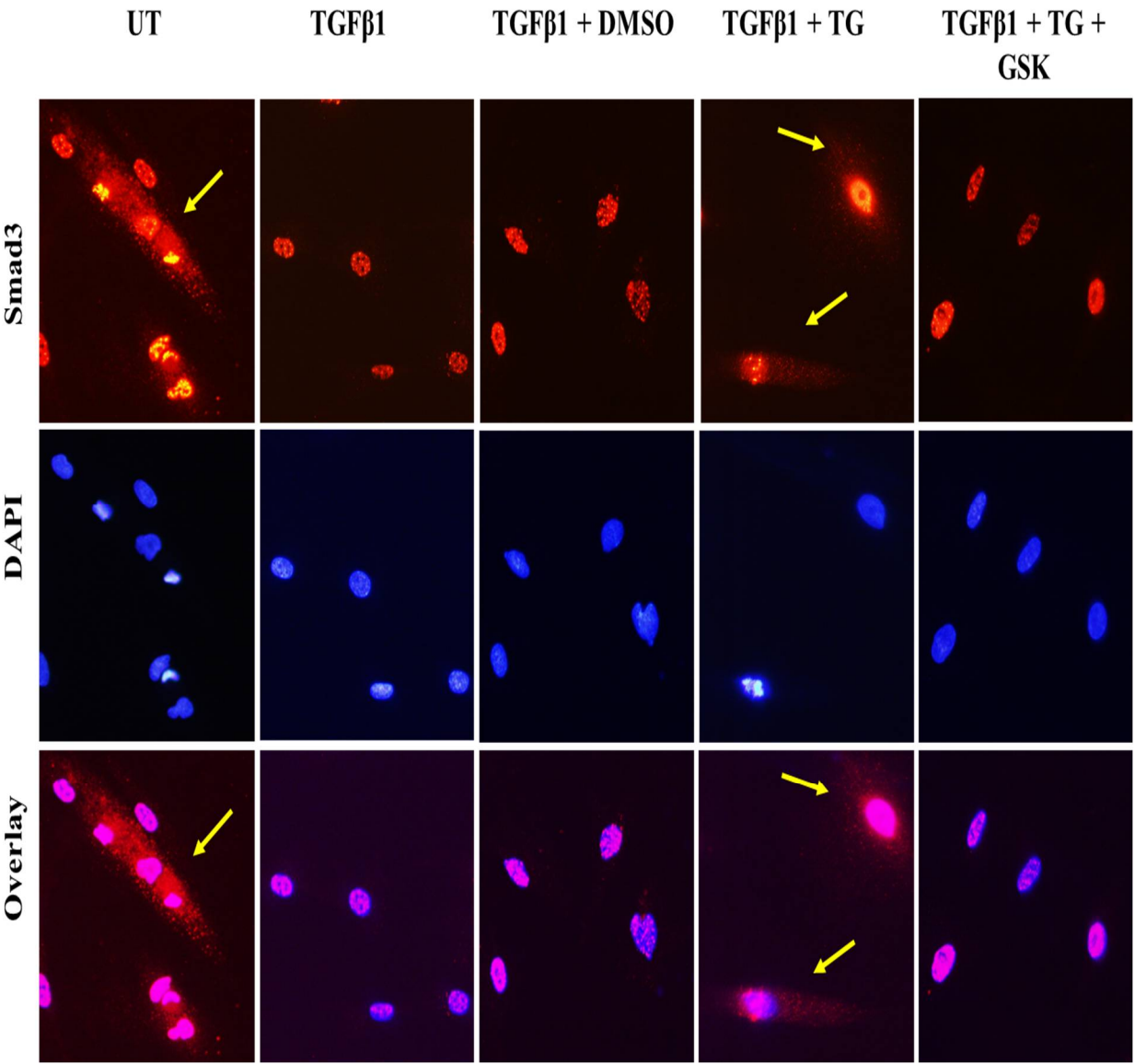


Figure 6. Distribution of NP-Cy3-siOrai1 predominantly in MCs in mouse kidney.

A: Representative images from 3 mice, showing localization of NP-Cy3-siOrai1 (red) in glomeruli (indicated by arrows), but not in tubules. Original magnification: 200X. **B:** Localization of NP-Cy3-siOrai1 in MCs (upper panel) and podocytes (lower panel) representative from 3 mice. MCs and podocytes were stained with Integrin- α 8 and synaptopodin (green) respectively in different sections. NP-Cy3-siOrai1 was shown as red signals. Original magnification: 200X.

Figure 6.

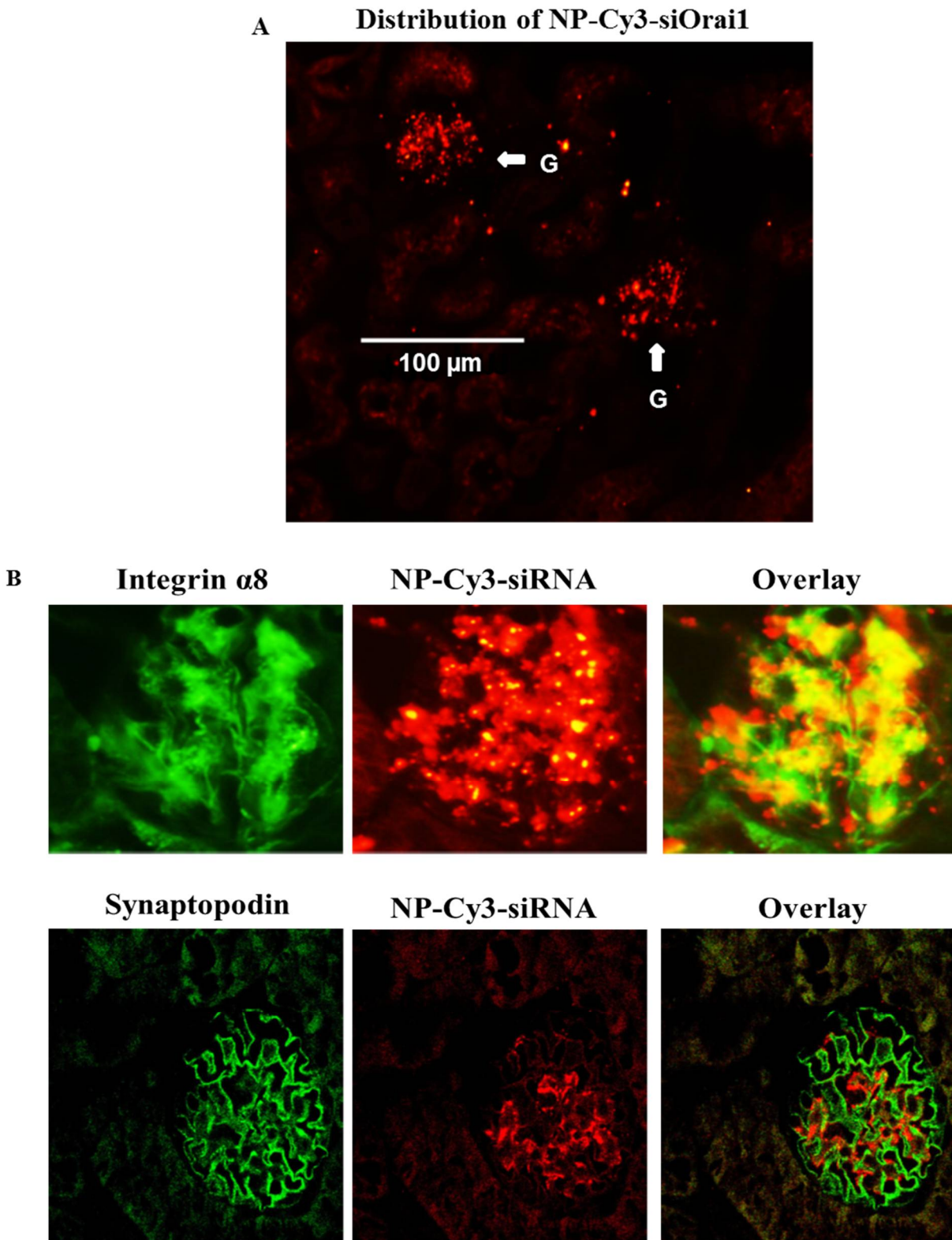


Figure 7. Knockdown of Orai1 in MCs increased phosphorylation and nuclear translocation of Smad3 in mice.

A: Representative images for immuno-histochemical staining of p-Smad3 on paraffin embedded kidney sections from NP-alone and NP-Cy3-siOrai1 injected mice. p-Smad3 staining is indicated by brown while nuclei are shown blue. Glomeruli are indicated by arrows. Original magnification 200X. **B:** Magnified images of the region indicated by dashed boxes.

Figure 7.

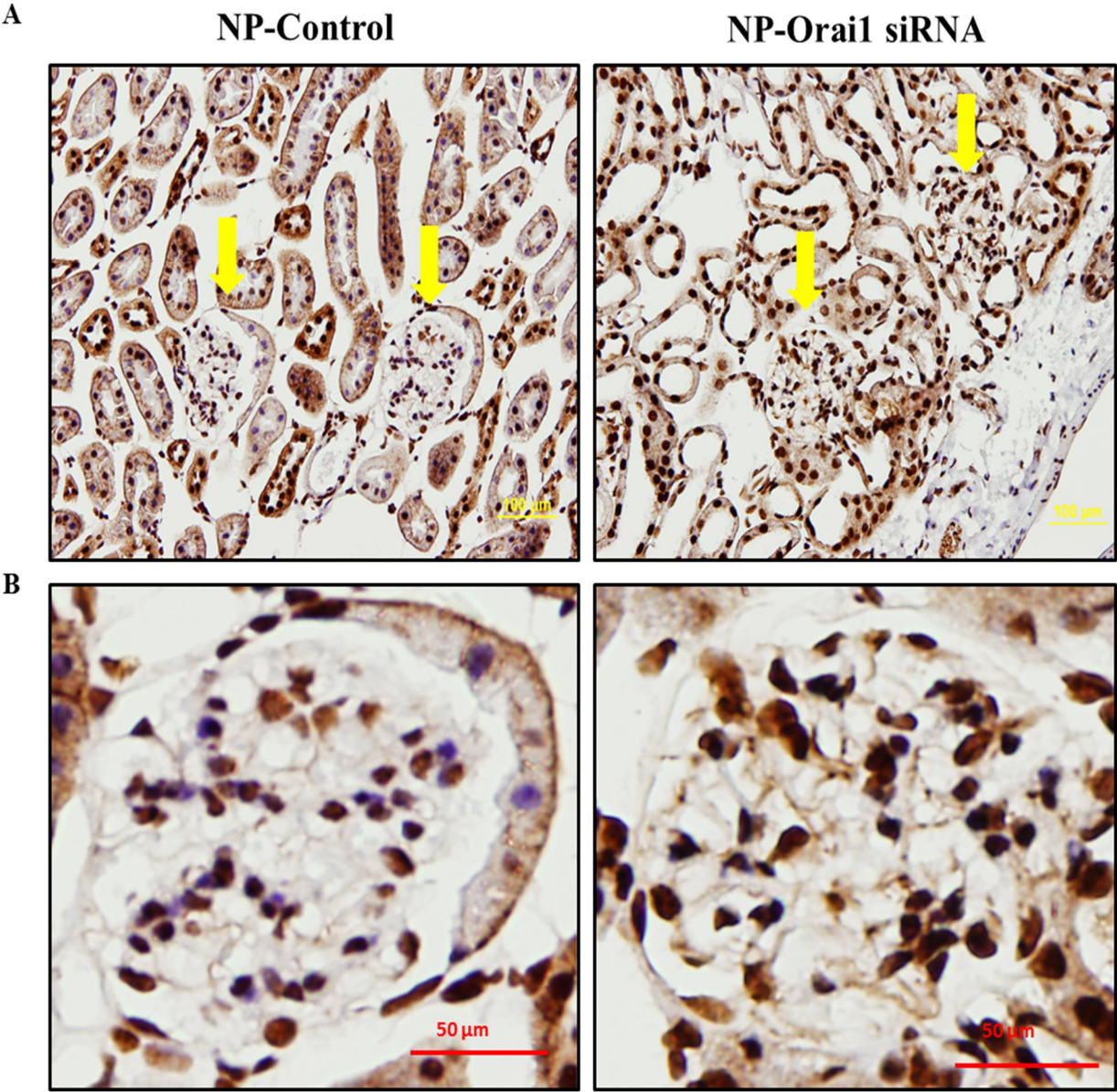
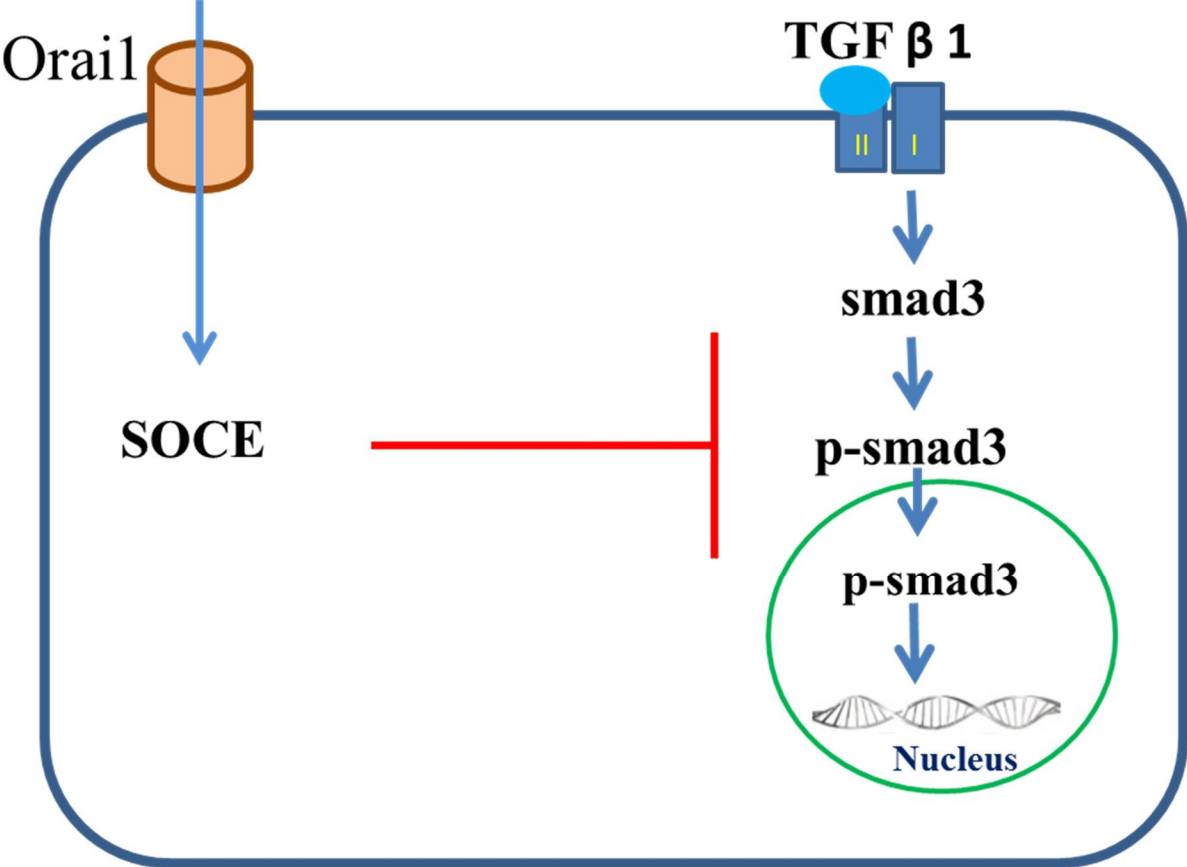


Figure 8. Simplified summary diagram demonstrating the pathway involved in negative regulation of TGFβ1-Smad3 signaling by Orai1-mediated SOCE in MCs.

Red line indicates inhibition and blue arrows indicate promotion of the pathway.

Figure 8.



Abbreviations

CDKs: cyclin dependent kinases

DN: diabetic nephropathy

ECM: extracellular matrix

FBS: fetal bovine serum

HCl: 4 mM HCl with 0.1% BSA at 1:4000 as the vehicle control for TGF β 1

HMCs: human mesangial cells

IDV: integrated density value

La³⁺: Lanthanum

MAPKs: mitogen associated protein kinases

MCs: mesangial cells

NP: nanoparticles

NP-Cy3- siOrai1: nanoparticles containing Cy3- tagged siRNA against mouse Orai1

p-Smad3: phosphorylated Smad3

R-Smads: receptor operated smads

siRNA: small interfering RNA

SOC: store-operated channels

SOCE: store operated calcium entry

TBP: TATA binding protein

TG: thapsigargin

TGF β : transforming growth factor beta

YFP: yellow fluorescent protein

References

- (1) Schena FP, Gesualdo L. Pathogenetic mechanisms of diabetic nephropathy. *Journal of the American Society of Nephrology* 2005;16(3 suppl 1):S30-S33.
- (2) Kanwar YS, Wada J, Sun L, Xie P, Wallner EI, Chen S, et al. Diabetic nephropathy: mechanisms of renal disease progression. *Exp Biol Med* 2008;233(1):4-11.
- (3) Lane PH, Steffes MW, Fioretto P, Mauer SM. Renal interstitial expansion in insulin-dependent diabetes mellitus. *Kidney Int* 1993;43(3):661-667.
- (4) Steffes MW, Østerby R, Chavers B, Mauer SM. Mesangial expansion as a central mechanism for loss of kidney function in diabetic patients. *Diabetes* 1989;38(9):1077-1081.
- (5) Collins AJ, Foley RN, Chavers B, Gilbertson D, Herzog C, Ishani A, et al. US Renal Data System 2013 Annual Data Report. *Am J Kidney Dis* 2014 Jan;63(1 Suppl):A7.
- (6) Foley RN, Collins AJ. End-stage renal disease in the United States: an update from the United States Renal Data System. *J Am Soc Nephrol* 2007 Oct;18(10):2644-2648.
- (7) Coresh J, Selvin E, Stevens LA, Manzi J, Kusek JW, Eggers P, et al. Prevalence of chronic kidney disease in the United States. *JAMA: the journal of the American Medical Association* 2007;298(17):2038-2047.
- (8) Pyram R, Kansara A, Banerji MA, Loney-Hutchinson L. Chronic kidney disease and diabetes. *Maturitas* 2012;71(2):94-103.

- (9) Heilig CW, Liu Y, England RL, Freytag SO, Gilbert JD, Heilig KO, et al. D-Glucose Stimulates Mesangial Cell GLUT1 Expression and Basal and IGF-I-Sensitive Glucose Uptake in Rat Mesangial Cells: Implications for Diabetic Nephropathy. *Diabetes* 1997;46(6):1030-1039.
- (10) Abboud HE. Mesangial cell biology. *Exp Cell Res* 2012;318(9):979-985.
- (11) Schlondorff D, Banas B. The mesangial cell revisited: no cell is an island. *J Am Soc Nephrol* 2009 Jun;20(6):1179-1187.
- (12) Amcheslavsky A, Yeromin AV, Penna A, Cahalan MD. Store-Operated Calcium Channels. In: Editors-in-Chief: William J. Lennarz, M. Daniel Lane, editors. *Encyclopedia of Biological Chemistry* Waltham: Academic Press; 2013. p. 314-320.
- (13) Lewis RS. The molecular choreography of a store-operated calcium channel. *Nature* 2007;446(7133):284-287.
- (14) Parekh AB, Putney JW. Store-operated calcium channels. *Physiol Rev* 2005;85(2):757-810.
- (15) Wu P, Wang Y, Davis ME, Zuckerman JE, Chaudhari S, Begg M, et al. Store-Operated Ca²⁺ Channels in Mesangial Cells Inhibit Matrix Protein Expression. *Journal of the American Society of Nephrology* 2015;26(11):2691-2702.
- (16) Hoffman BB, Sharma K, Zhu Y, Ziyadeh FN. Transcriptional activation of transforming growth factor- β 1 in mesangial cell culture by high glucose concentration. *Kidney Int* 1998;54(4):1107-1116.

- (17) Hayashida T, Schnaper HW. High ambient glucose enhances sensitivity to TGF-beta1 via extracellular signal--regulated kinase and protein kinase Cdelta activities in human mesangial cells. *J Am Soc Nephrol* 2004 Aug;15(8):2032-2041.
- (18) Metwally SS, Mosaad YM, Nassr AA, Zaki OM. Transforming growth factor-beta 1 in diabetic nephropathy. *Egypt J Immunol* 2005;12(1):103-112.
- (19) Mason RM, Wahab NA. Extracellular matrix metabolism in diabetic nephropathy. *Journal of the American Society of Nephrology* 2003;14(5):1358-1373.
- (20) Wang A, Ziyadeh FN, Lee EY, Pyagay PE, Sung SH, Sheardown SA, et al. Interference with TGF-beta signaling by Smad3-knockout in mice limits diabetic glomerulosclerosis without affecting albuminuria. *Am J Physiol Renal Physiol* 2007 Nov;293(5):F1657-65.
- (21) Wang W, Koka V, Lan HY. Transforming growth factor- β and Smad signalling in kidney diseases. *Nephrology* 2005;10(1):48-56.
- (22) Lan HY. Transforming growth factor- β /Smad signalling in diabetic nephropathy. *Clinical and Experimental Pharmacology and Physiology* 2012;39(8):731-738.
- (23) Poncelet A, De Caestecker MP, Schnaper HW. The transforming growth factor- β /SMAD signaling pathway is present and functional in human mesangial cells. *Kidney Int* 1999;56(4):1354-1365.
- (24) Runyan CE, Schnaper HW, Poncelet AC. Smad3 and PKCdelta mediate TGF-beta1-induced collagen I expression in human mesangial cells. *Am J Physiol Renal Physiol* 2003 Sep;285(3):F413-22.

- (25) Isono M, Chen S, Hong SW, Iglesias-de la Cruz, M Carmen, Ziyadeh FN. Smad pathway is activated in the diabetic mouse kidney and Smad3 mediates TGF- β -induced fibronectin in mesangial cells. *Biochem Biophys Res Commun* 2002;296(5):1356-1365.
- (26) Attisano L, Wrana JL. Smads as transcriptional co-modulators. *Curr Opin Cell Biol* 2000;12(2):235-243.
- (27) Feng X, Derynck R. Specificity and versatility in TGF- β signaling through Smads. *Annu Rev Cell Dev Biol* 2005;21:659-693.
- (28) Lan HY. Diverse roles of TGF-beta/Smads in renal fibrosis and inflammation. *Int J Biol Sci* 2011;7(7):1056-1067.
- (29) Chaudhari S, Wu P, Wang Y, Ding Y, Yuan J, Begg M, et al. High glucose and diabetes enhanced store-operated Ca(2+) entry and increased expression of its signaling proteins in mesangial cells. *Am J Physiol Renal Physiol* 2014 May 1;306(9):F1069-80.
- (30) Bartlett DW, Davis ME. Physicochemical and biological characterization of targeted, nucleic acid-containing nanoparticles. *Bioconjug Chem* 2007;18(2):456-468.
- (31) Kaname S, Uchida S, Ogata E, Kurokawa K. Autocrine secretion of transforming growth factor- β in cultured rat mesangial cells. *Kidney Int* 1992;42(6):1319-1327.
- (32) Wolf G, Sharma K, Chen Y, Ericksen M, Ziyadeh FN. High glucose-induced proliferation in mesangial cells is reversed by autocrine TGF- β . *Kidney Int* 1992;42(3):647-656.

- (33) Xia L, Wang H, Munk S, Kwan J, Goldberg HJ, Fantus IG, et al. High glucose activates PKC-zeta and NADPH oxidase through autocrine TGF-beta1 signaling in mesangial cells. *Am J Physiol Renal Physiol* 2008 Dec;295(6):F1705-14.
- (34) Kagami S, Border WA, Miller DE, Noble NA. Angiotensin II stimulates extracellular matrix protein synthesis through induction of transforming growth factor-beta expression in rat glomerular mesangial cells. *J Clin Invest* 1994 Jun;93(6):2431-2437.
- (35) Throckmorton DC, Brogden AP, Min B, Rasmussen H, Kashgarian M. PDGF and TGF- β mediate collagen production by mesangial cells exposed to advanced glycosylation end products. *Kidney Int* 1995;48(1):111-117.
- (36) Ha H, Lee HB. Reactive oxygen species as glucose signaling molecules in mesangial cells cultured under high glucose. *Kidney Int* 2000;58:S19-S25.
- (37) Fujimoto M, Maezawa Y, Yokote K, Joh K, Kobayashi K, Kawamura H, et al. Mice lacking Smad3 are protected against streptozotocin-induced diabetic glomerulopathy. *Biochem Biophys Res Commun* 2003;305(4):1002-1007.
- (38) Leask A, Abraham DJ. TGF-beta signaling and the fibrotic response. *FASEB J* 2004 May;18(7):816-827.
- (39) Li JH, Huang XR, Zhu H, Johnson R, Lan HY. Role of TGF- β signaling in extracellular matrix production under high glucose conditions. *Kidney Int* 2003;63(6):2010-2019.

- (40) Li J, Qu X, Ricardo SD, Bertram JF, Nikolic-Paterson DJ. Resveratrol inhibits renal fibrosis in the obstructed kidney: potential role in deacetylation of Smad3. *The American journal of pathology* 2010;177(3):1065-1071.
- (41) Schnaper HW, Hayashida T, Hubchak SC, Poncelet AC. TGF-beta signal transduction and mesangial cell fibrogenesis. *Am J Physiol Renal Physiol* 2003 Feb;284(2):F243-52.
- (42) Zuckerman JE, Davis ME. Targeting therapeutics to the glomerulus with nanoparticles. *Advances in chronic kidney disease* 2013;20(6):500-507.
- (43) Zuckerman JE, Gale A, Wu P, Ma R, Davis ME. siRNA Delivery to the Glomerular Mesangium Using Polycationic Cyclodextrin Nanoparticles Containing siRNA. *nucleic acid therapeutics* 2015;25(2):53-64.
- (44) Choi CHJ, Zuckerman JE, Webster P, Davis ME. Targeting kidney mesangium by nanoparticles of defined size. *Proceedings of the National Academy of Sciences* 2011;108(16):6656-6661.
- (45) Gruszczynska-Biegala J, Pomorski P, Wisniewska MB, Kuznicki J. Differential roles for STIM1 and STIM2 in store-operated calcium entry in rat neurons. *PloS one* 2011;6(4):e19285.
- (46) Leung F, Yung L, Yao X, Laher I, Huang Y. Store-operated calcium entry in vascular smooth muscle. *Br J Pharmacol* 2008;153(5):846-857.
- (47) Pan Z, Brotto M, Ma J. Store-operated Ca²⁺ entry in muscle physiology and diseases. *BMB Rep* 2014 Feb;47(2):69-79.

- (48) Targos B, Baranska J, Pomorski P. Store-operated calcium entry in physiology and pathology of mammalian cells. *Acta Biochim Pol* 2005;52(2):397-409.
- (49) Uehara A, Yasukochi M, Imanaga I, Nishi M, Takeshima H. Store-operated Ca^{2+} entry uncoupled with ryanodine receptor and junctional membrane complex in heart muscle cells. *Cell Calcium* 2002;31(2):89-96.
- (50) Ma R, Smith S, Child A, Carmines PK, Sansom SC. Store-operated Ca^{2+} channels in human glomerular mesangial cells. *Am J Physiol Renal Physiol* 2000 Jun;278(6):F954-61.
- (51) Chaudhari S, Ma R. Store-operated calcium entry and diabetic complications. *Exp Biol Med* (Maywood) 2016 Feb;241(4):343-352.
- (52) Eddy AA. Molecular basis of renal fibrosis. *Pediatric nephrology* 2000;15(3-4):290-301.
- (53) Liu Y. Renal fibrosis: new insights into the pathogenesis and therapeutics. *Kidney Int* 2006;69(2):213-217.
- (54) Xu L, Chen Y, Massagué J. The nuclear import function of Smad2 is masked by SARA and unmasked by TGF β -dependent phosphorylation. *Nat Cell Biol* 2000;2(8):559-562.
- (55) Shi Y, Massagué J. Mechanisms of TGF- β signaling from cell membrane to the nucleus. *Cell* 2003;113(6):685-700.
- (56) Mai X, Shang J, Liang S, Yu B, Yuan J, Lin Y, et al. Blockade of Orai1 Store-Operated Calcium Entry Protects against Renal Fibrosis. *J Am Soc Nephrol* 2016 Mar 3.

- (57) Duan W, Yu X, Huang X, Yu J, Lan HY. Opposing roles for Smad2 and Smad3 in peritoneal fibrosis in vivo and in vitro. *The American journal of pathology* 2014;184(8):2275-2284.
- (58) Meng XM, Huang XR, Chung AC, Qin W, Shao X, Igarashi P, et al. Smad2 protects against TGF-beta/Smad3-mediated renal fibrosis. *J Am Soc Nephrol* 2010 Sep;21(9):1477-1487.
- (59) Bennett D, Alphey L. PP1 binds Sara and negatively regulates Dpp signaling in *Drosophila melanogaster*. *Nat Genet* 2002;31(4):419-423.
- (60) Wrighton KH, Feng X. To (TGF) β or not to (TGF) β : Fine-tuning of Smad signaling via post-translational modifications. *Cell Signal* 2008;20(9):1579-1591.
- (61) Liu T, Feng XH. Regulation of TGF-beta signalling by protein phosphatases. *Biochem J* 2010 Sep 1;430(2):191-198.
- (62) Chen X, Xu L. Mechanism and regulation of nucleocytoplasmic trafficking of smad. *Cell & bioscience* 2011;1(1):1.
- (63) Lin X, Duan X, Liang Y, Su Y, Wrighton KH, Long J, et al. PPM1A functions as a Smad phosphatase to terminate TGF β signaling. *Cell* 2006;125(5):915-928.

CHAPTER V

SUMMARY, GENERAL DISCUSSION AND FUTURE DIRECTION

Summary and General Discussion

Glomerular mesangial cells (MCs) form one of the major cell population in the glomerulus (1). The function of MCs predominantly depend on their intracellular Ca^{2+} signaling. The various Ca^{2+} channels that contribute to Ca^{2+} homeostasis in these cells are comprised of voltage operated Ca^{2+} channels (VOCC), receptor operated channels (ROC) and store operated channels (SOC) (2). Ca^{2+} entry through SOC known as store-operated calcium entry (SOCE), is responsible for multiple physiological functions ranging from intracellular Ca^{2+} concentration maintenance to cell growth. Disturbances of SOCE have been observed in numerous pathological conditions, including diabetes in a variety of cells (3). However, whether SOCE in MCs is altered in diabetes and what its significance is are not known.

The first study presented here aimed to determine the effect of high glucose (HG)/diabetes on SOCE. Exposure to HG for 7 days or more increased cyclopiazonic acid (CPA)-induced SOCE in cultured human MCs. Consistently, the whole cell patch clamp experiments demonstrated that the IP_3 -stimulated SOC current was significantly augmented by 7

days of HG treatment. The increase in SOC current response and SOCE to prolonged HG treatment were abolished by selective SOC blocker GSK7975A. We next studied the molecular mechanisms for this HG-enhanced SOCE. STIM1 and Orai1 are known key components of SOC (4,5). We found that abundance of both STIM1 and Orai1 was significantly increased with different concentrations of HG (10, 20 and 30 mM) as well as after 7 days of HG treatment. Consistently, glomeruli from streptozotocin (STZ)-induced diabetic rats (Type 1 diabetic model) exhibited upregulation of both STIM1 and Orai1 proteins at 4 weeks after STZ injection. Similar findings were observed in renal cortices of the rats with high fat diet followed by STZ treatment (type II diabetes model) for 20 weeks. Increase in protein abundance can be due to either increased production or decreased degradation. Our further study showed that HG treatment significantly increased mRNA expression level of STIM1, but not that of Orai1. These results suggest that a transcriptional mechanism was involved in STIM1 elevations while a post-transcriptional mechanism(s) was involved in increased Orai1 protein expression in response to a prolonged HG treatment.

The findings that SOCE in MCs was altered by diabetes led to the next study investigating its relevance to diabetic kidney disease. SOCE has discrete effects on cellular processes in different types of cells. It stimulates cell growth in cardiac myocytes while it suppresses cell growth in mouse embryonic fibroblasts and rat uterine leiomyoma cells (6,7). Since MCs are one of major sources for production of extracellular matrix proteins (ECM), and over production of ECM proteins is a hallmark of early stage of diabetic nephropathy (DN), we next studied whether SOCE regulated ECM protein expression. We found that activation of SOCE by thapsigargin (TG), a classical activator of SOC, significantly reduced abundance of fibronectin and this response was significantly attenuated by a SOC blocker, GSK-7975A.

Consistently, inhibition of SOCE using 2-aminoethyl diphenylborinate (2-APB) (50 μ M), increased contents of fibronectin and collagen IV. Both ECM proteins were also increased by HG and the HG response was abolished by TG. Knockdown of Orai1, the pore forming unit of SOC, increased fibronectin protein abundance in human MCs. In agreement with the *in vitro* study, specific knockdown of Orai1 in MCs *in vivo* using the targeted nanoparticle siRNA (NP-siRNA) delivery system also increased the abundance of glomerular fibronectin and Collagen IV and mesangial index in mice. These results suggest that SOCE in MCs negatively regulates ECM protein expression in kidney.

The third study focused on the mechanism by which SOCE suppresses ECM protein expression. TGF β 1-Smad3 pathway is a well-known fibrotic pathway in kidney cells, including MCs (8,9). We then studied if inhibition of TGF β 1-Smad3 pathway contributed to the inhibitory effect of SOCE on ECM protein expression. We showed that treatment of human MCs with TG did not significantly change the content of TGF β 1 protein in the cell culture media and the cell lysates, suggesting that SOCE did not affect the secretion or production of TGF β 1 by human MCs. Recombinant human TGF β 1 increased the phosphorylation of Smad3 and translocation of Smad3 to the nucleus in MCs. TG inhibited the TGF β 1-induced activation and nuclear translocation of Smad3. Knockdown of Orai1 increased phosphorylated Smad3 while overexpression of orai1 further decreased the TG-abrogated phosphorylated Smad3 expression after TGF β 1 treatment. Immunohistological examination of kidney sections from mice with *in vivo* Orai1 knockdown in MCs also exhibited increased phosphorylation and nuclear translocation of Smad3 in glomeruli. The findings from this study suggest that inhibition of TGF β 1-Smad3 pathway is a downstream mechanism for SOCE inhibiting ECM protein expression in MCs.

There are a few limitations in these studies. The changes in STIM1 and Orai1 protein expression seen *in vivo* in renal cortices or glomeruli from diabetic animals may not be fully attributed to MCs. Other glomerular cells might also be involved. However, considering that MCs are a major population of cells in glomerulus, the results from the specific region of kidney may still be used as an indication of MC response. Another limitation is that the NP-siRNA delivery system used in our study transfects siRNA to MCs transiently because of fast degradation of siRNA. Considering the progressive and chronic nature of DN it would be appropriate to study the effect of long-term knockdown of Orai1 in these animals.

Taking together, our findings in the present study suggest that prolonged hyperglycemia enhances SOCE in MCs through upregulation of STIM1 and Orai1 protein abundance, and SOCE suppresses ECM protein expression and glomerular mesangial expansion by inhibiting TGF β 1-Smad3 pathway. Figure 1 summarized these findings and illustrates the beneficial pathway of SOCE. Since accumulation of ECM proteins/mesangial expansion is one of major pathological changes in DN, our findings may provide an alternative therapeutic option for patients with DN.

Future directions:

Enhancing SOCE *in vivo*

Our study showed that SOCE in MCs downregulated abundance of ECM proteins and hence is beneficial for diabetic kidneys. Therefore, enhancement of SOCE in MCs in kidney diseases with ECM accumulation may be of therapeutic importance. This can be achieved either by activating SOCE in MCs pharmacologically or upregulating expression level of its channel proteins (STIM1 and Orai1). Although a delivery system delivering expression plasmids or drugs

selectively to MCs is not available currently, developing such an approach has high pharmaceutical and clinical significance. Alternatively, we could downregulate activity or amount of endogenous inhibitors of SOC to upregulate SOC function. The α -isoform of the inhibitor of the myogenic family (I-mfa) is a cytosolic protein and has been demonstrated to suppress SOC activity(10). Theoretically, knocking down I-mfa using our targeted NP/siRNA-delivery system can release SOC signaling from its inhibition and, in turn decrease ECM protein expression by activating SOCE pathway.

NP-siRNA delivery system as the therapeutic tool in human subjects

The targeted NP-siRNA delivery system used in the present study may be used as a therapeutic option in human subjects as this delivery system has already been tested in humans (11). It would be interesting to know if the findings in animals studies can be extended to human subjects. Also, other proteins in MCs that play a detrimental role in kidney diseases can be targeted through this approach.

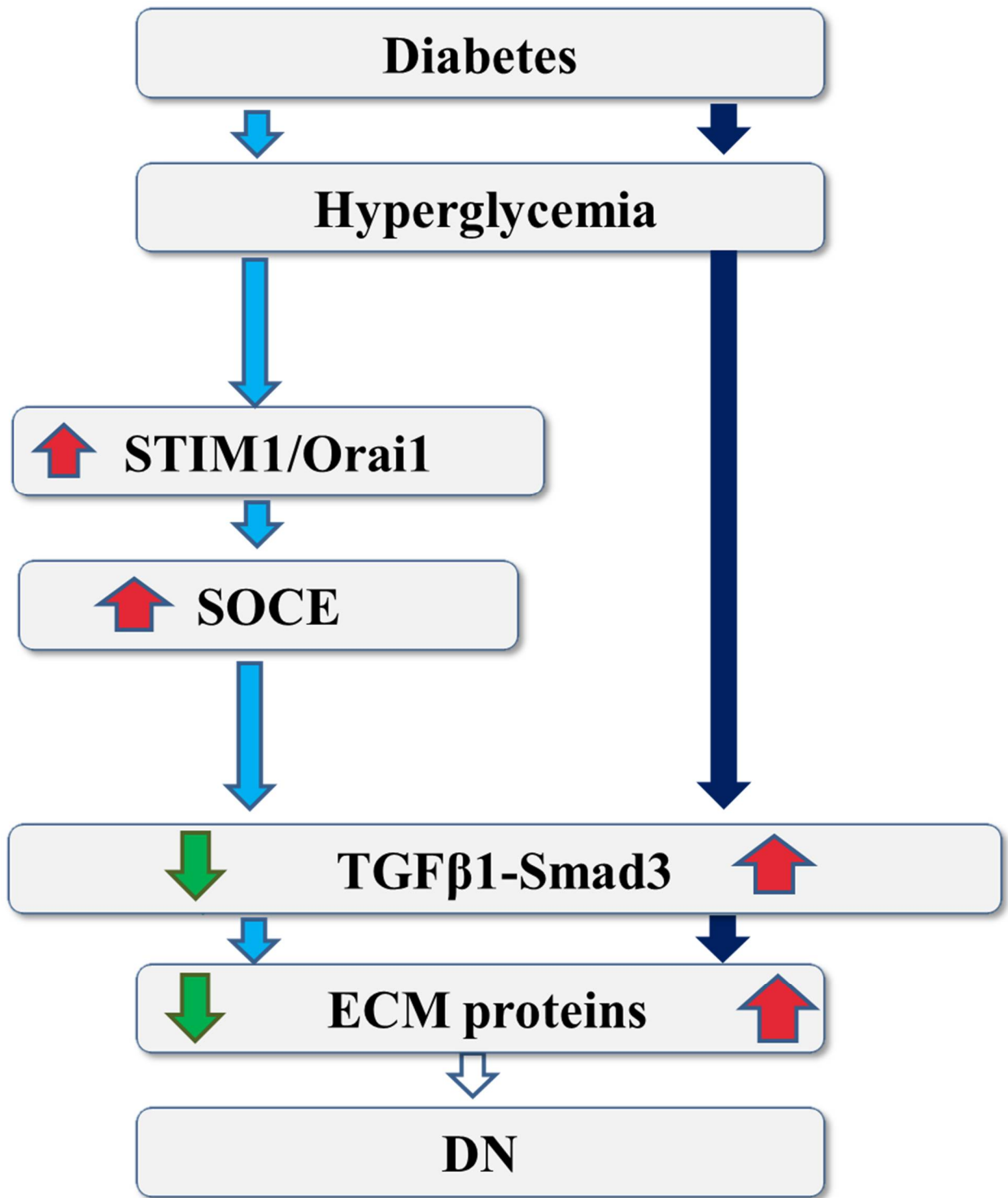
Mechanism of TGF β 1-Smad3 pathway inhibition by SOCE

SOCE inhibited TGF β 1-induced phosphorylation of Smad3. Since TGF β receptors are serine-threonine kinases, a major possibility is that the members of protein Serine-Threonine phosphatases are playing a role in de-phosphorylation of Smad3. Some of the important phosphatases to consider are a receptor specific phosphatase PP1c or Ca²⁺ dependent phosphatase, calcineurin. Also the possible role of nuclear localized Smad2/3 SXS-motif specific phosphatase, PP1MA/PP2C α in dephosphorylation of activated Smad3 and enhancing its export out of the nucleus would be interesting to determine. Additional experiments studying the effect of SOCE on TGF β 1-mediated phosphorylation of Smad3 in presence of the inhibitors of these phosphatases will provide valuable information for these speculations. Other possibilities

include suppression of the receptor activation or Smad3 activation by inhibiting the type II or type I receptor kinases respectively. SOCE may also interact with another known parallel pathway that regulates the TGF β 1-Smad3 pathway (12). Further experiments are needed to evaluate the role of SOCE on those pathways and its ultimate role in the complex network of cross talk between these multiple pathways.

Figure 1. Summary diagram depicting the pathways known in diabetes (dark blue arrows) and the compensatory pathway derived from this study (light blue arrows). Red arrow indicates an increase while green arrow indicates a reduction.

Figure 1.



Abbreviations:

2-APB: 2-aminoethyl diphenylborinate

CPA: Cyclopiazonic acid

DN: diabetic nephropathy

ECM: extracellular matrix

HG: high glucose

I-mfa: inhibitor of the myogenic family

IP3: inositol-triphosphate

MCs: mesangial cells

NP-siRNA: nanoparticle siRNA

ROC: receptor operated channels

SOC: store operated channels

SOCE: store-operated calcium entry

STZ: Streptozotocin

TG: thapsigargin

VOCC: Voltage operated Ca²⁺ channels

References

- (1) Mene P, Simonson MS, Dunn MJ. Physiology of the mesangial cell. *Physiol Rev* 1989 Oct;69(4):1347-1424.
- (2) Ma R, Pluznick JL, Sansom SC. Ion channels in mesangial cells: function, malfunction, or fiction. *Physiology* 2005;20(2):102-111.
- (3) Roberts-Thomson SJ, Peters AA, Grice DM, Monteith GR. ORAI-mediated calcium entry: mechanism and roles, diseases and pharmacology. *Pharmacol Ther* 2010;127(2):121-130.
- (4) Zhang SL, Yeromin AV, Zhang XH, Yu Y, Safrina O, Penna A, et al. Genome-wide RNAi screen of Ca²⁺ influx identifies genes that regulate Ca²⁺ release-activated Ca²⁺ channel activity. *Proceedings of the National Academy of Sciences* 2006;103(24):9357-9362.
- (5) Soboloff J, Spassova MA, Tang XD, Hewavitharana T, Xu W, Gill DL. Orai1 and STIM reconstitute store-operated calcium channel function. *J Biol Chem* 2006;281(30):20661-20665.
- (6) Voelkers M, Salz M, Herzog N, Frank D, Dolatabadi N, Frey N, et al. Orai1 and Stim1 regulate normal and hypertrophic growth in cardiomyocytes. *J Mol Cell Cardiol* 2010;48(6):1329-1334.
- (7) Peng H, Liu J, Sun Q, Chen R, Wang Y, Duan J, et al. mTORC1 enhancement of STIM1-mediated store-operated Ca²⁺ entry constrains tuberous sclerosis complex-related tumor development. *Oncogene* 2012.
- (8) Lan HY. Transforming growth factor β /Smad signalling in diabetic nephropathy. *Clinical and Experimental Pharmacology and Physiology* 2012;39(8):731-738.

- (9) Poncelet A, De Caestecker MP, Schnaper HW. The transforming growth factor- β /SMAD signaling pathway is present and functional in human mesangial cells. *Kidney Int* 1999;56(4):1354-1365.
- (10) Ma R, Rundle D, Jacks J, Koch M, Downs T, Tsiokas L. Inhibitor of myogenic family, a novel suppressor of store-operated currents through an interaction with TRPC1. *J Biol Chem* 2003 Dec 26;278(52):52763-52772.
- (11) Davis ME, Zuckerman JE, Choi CHJ, Seligson D, Tolcher A, Alabi CA, et al. Evidence of RNAi in humans from systemically administered siRNA via targeted nanoparticles. *Nature* 2010;464(7291):1067-1070.
- (12) Derynck R, Zhang YE. Smad-dependent and Smad-independent pathways in TGF- β family signalling. *Nature* 2003;425(6958):577-584.